

STUDIES ON CHIRAL SPIROPYRAN DERIVATIVES

A THESIS SUBMITTED TO
THE GRADUATE SCHOOL OF NATURAL AND APPLIED SCIENCES
OF
MIDDLE EAST TECHNICAL UNIVERSITY

BY
BENĞİ ŐENTÜRK

IN PARTIAL FULFILLMENT OF THE REQUIREMENTS
FOR
THE DEGREE OF MASTER OF SCIENCE
IN
CHEMISTRY

AUGUST 2021

Approval of the thesis:

STUDIES ON CHIRAL SPIROPYRAN DERIVATIVES

submitted by **BENĐİ ŐENTÜRĐ** in partial fulfillment of the requirements for the degree of **Master of Science in Chemistry, Middle East Technical University** by,

Prof. Dr. Halil Kalıpçılar
Dean, Graduate School of **Natural and Applied Sciences**

Prof. Dr. Özdemir Dođan
Head of the Department, **Chemistry**

Prof. Dr. Akın Akdađ
Supervisor, **Chemistry, METU**

Examining Committee Members:

Prof. Dr. Özdemir Dođan
Chemistry Department, METU

Prof. Dr. Akın Akdađ
Chemistry Department, METU

Prof. Dr. Ali Çırpan
Chemistry Department, METU

Assoc. Prof. Dr. Serhan Türkyılmaz
Chemistry Department, METU

Assoc. Prof. Dr. Bilge Baytekin
Chemistry Department, İ.D. Bilkent University

Date: 13.08.2021

I hereby declare that all information in this document has been obtained and presented in accordance with academic rules and ethical conduct. I also declare that, as required by these rules and conduct, I have fully cited and referenced all material and results that are not original to this work.

Name Last name : Bengi Şentürk

Signature :

ABSTRACT

STUDIES ON CHIRAL SPIROPYRAN DERIVATIVES

Şentürk, Bengi
Master of Science, Chemistry
Supervisor: Prof. Dr. Akın Akdağ

August 2021, 134 pages

Spiropyran are a class of organic molecules that possess photochromic characteristics. Their isomerization to the merocyanine form can be induced by light, heat, polarity, and pH of the environment. The merocyanine form is obtained from the heterolytic cleavage of the bond between spiro carbon and the oxygen, which results in a transformation of the optically active spiropyran into an achiral form. The back conversion of the achiral merocyanine to the spiropyran leads to racemization. In this study, *D* and *L* forms of alanine and phenylalanine derivatives were incorporated into a spiropyran with alcohol functionality to obtain optically active spiropyran. Their photochemical and photophysical properties were studied in methanol, isopropanol, dichloromethane and hexane. The results showed that these spiropyran display different characteristics in their spectroscopic analyses. The effect of the benzyl and methyl units on the ring closure rate of the merocyanines was also investigated. For this purpose, ring closure kinetics of different merocyanines containing hydroxy group as well as *D*-alanine and *D*-phenylalanine derivatives were compared. The results reveal that the ring closure rate of the merocyanine with benzyl group attached is faster than the rate of the structures with methyl or hydroxy groups.

Keywords: Spiropyran, Merocyanine, Chirality, Photoisomerization

ÖZ

KİRAL SPIROPİRAN TÜREVLERİ ÜZERİNE ÇALIŞMALAR

Şentürk, Bengi
Yüksek Lisans, Kimya
Tez Yöneticisi: Prof. Dr. Akın Akdağ

Ağustos 2021, 134 sayfa

Spiropiranlar fotokromizm gösteren madde türlerinden biridir. Isı, ışık, pH ve polaritenin etkisiyle merosiyanine dönüşürler. Spiro karbon ve oksijen arasındaki bağın heterolitik olarak kırılması sonucunda merosiyanin formu elde edilir ve bu da optik olarak aktif spiropiranları akiral forma dönüştürür. Uygun koşullar sağlandığında ve merosiyanin formunun spiropirana dönüşü tetiklendiğinde rasemizasyon meydana gelir. Bu çalışmada, bünyesinde alkol grubu bulduran bir spiropirana, *D* ve *L* alanin ve fenilalaninden türevlendirilmiş gruplar eklenmiştir. Böylece optik olarak aktif spiropiranlar elde edilmiştir. Sonrasında, bu maddelerin fotokimyasal ve fotofiziksel özellikleri metanol, isopropanol, diklorometan ve hekzan gibi çözücülerin içerisinde incelenmiştir. Sonuçlar, maddelerin spektroskopik özelliklerinin farklı olduğunu göstermiştir. Bunlara ek olarak bu çalışmada benzil ve metil gruplarının, merosiyaninlerin halka kapanması üzerindeki etkisi incelenmiştir. Bu amaçla, *D*-alanin, *D*-fenilalanin türevleri ve hidroksi içeren merosiyaninler karşılaştırılmıştır. Bu çalışma benzil grubu içeren merosiyaninin halka kapanma hızının metil ve hidroksi içerenlerden daha yüksek olduğunu ortaya çıkarmıştır.

Anahtar Kelimeler: Spiropiran, Merosiyanin, Kiralite, Fotoisomerizasyon

To my beloved family

ACKNOWLEDGMENTS

As with many research that results in the production of a thesis, this study also has challenging times. Although only two names are written on the cover of this thesis, there are many unsung heroes provided me assistance, guidance, and encouragement throughout this study. I feel fortunate to have all those people who have given me much of their time and energy.

There are so many people I would like to thank. First and foremost, I am deeply indebted to my supervisor Prof. Dr. Akın Akdağ, whose sincerity, encouragement, and guidance I will never forget. I am thankful for the experiences and opportunities he arranged for me to grow professionally. He gave me a chance to work in his laboratory when I was an undergraduate student and continued to have faith in me over the years.

Besides my supervisor, I would like to thank the rest of the committee members: Prof. Dr. Özdemir Doğan, Prof. Dr. Ali Çırpan, Assoc. Prof. Dr. Serhan Türkyılmaz and Assoc. Prof. Dr. Bilge Baytekin for assisting me with their insightful comments in shaping the final draft of this study.

In the third year of my bachelor's degree, I had a chance to work with Assoc. Prof. Dr. Stelios Arseniyadis at the Queen Mary University of London as an intern student. It was a great experience. So, I must also thank Assoc. Prof. Dr. Stelios Arseniyadis for giving me this opportunity.

Getting through my study required not just academic support but also moral support. Therefore, I must express my gratitude and appreciation to Gizem Ünay and Perihan Öztürk Düzenli for providing me both. They gave me inspiration, encouragement, and advice to accomplish my goals. They so generously took time out of their schedules to motivate me with love and patience. I will always be thankful for their endless support.

I would like to extend my sincere thanks to my group members: Ece Ayça Erdoğan, Ege Hoşgör, Berçin Asya, Umut Aydemir, Oğuzhan Albayrak, Bulem Çakmak, Fatmanur Aydemir, Doruk Baykal, Ozan Ünver, Nihat Aksoy, Sadia Tul Munna, and our former group members: Dr. Duygu Tan and Sevban Doğan Ekici for providing such a rich source of conversation, education, and entertainment. There are so many memorable moments that we shared. I would not imagine that there could be such a workplace where people can be truly themselves. I am very proud to be a part of this excellent working environment.

Some special words of gratitude go to my friend Neslihan Tüzün, who has always been one of the major sources of support when things would get a bit discouraging.

Last but not least, my warm and heartfelt thanks go to my family: Hava Şentürk, Selçuk Şentürk, and Berk Şentürk, for their tremendous support and hope they had given me. Thank you for all the strength you gave me. I love you so muc

TABLE OF CONTENTS

ABSTRACT	v
ÖZ.....	vi
ACKNOWLEDGMENTS	viii
TABLE OF CONTENTS	x
LIST OF SCHEMES	xiv
SCHEMES.....	xiv
LIST OF FIGURES	xvi
CHAPTERS	
1 INTRODUCTION	1
1.1 Photoswitchable Compounds	1
1.1.1 Azobenzenes.....	3
1.1.2 Diarylethenes.....	4
1.1.3 Spiropyrans.....	7
1.1.3.1 Structure	7
1.1.3.2 Synthesis.....	10
1.1.3.3 Properties.....	12
1.1.3.3.1 Photochromism.....	12
1.1.3.3.2 Solvatochromism.....	14
1.1.3.3.3 Acidochromism	18
1.1.3.3.4 Thermochromism	19
1.1.3.4 Applications.....	22
2 AIM OF THE STUDY	25

3	RESULTS AND DISCUSSION	27
3.1	Preliminary Studies on Spiropyrans.....	27
3.2	Synthesis of the Spiropyrans Containing a Chiral Moiety.....	30
3.3	Photophysical and Photochemical Studies.....	39
3.3.1	UV-Vis Spectroscopy Studies.....	39
3.3.1.1	UV-Vis Spectroscopy Studies of SPA-I	41
3.3.1.2	UV-Vis Spectroscopy Studies of SPA-II	43
3.3.1.3	UV-Vis Studies of SPA-III	44
3.3.1.4	UV-Vis Studies of SPA-IV	46
3.3.2	Kinetics of Ring Closure.....	47
3.3.3	CD Measurements.....	51
3.3.4	Fluorescence Studies.....	51
3.4	HPLC Studies.....	52
4	CONCLUSION.....	55
5	EXPERIMENTAL	57
5.1	Methods and Materials.....	57
5.2	Synthesis of the Chiral Unit Attached Spiropyrans	59
5.2.1	Synthesis of 2,3,3-trimethyl-3 <i>H</i> -indole	59
5.2.2	Synthesis of 1,2,3,3-tetrimethyl-3 <i>H</i> -indolium iodide	59
5.2.3	Synthesis of 1,3,3-trimethyl-2-methyleneindoline	60
5.2.4	Synthesis of (<i>R/S</i>)- 1',3',3'-trimethylspiro[chromene-2,2'-indoline]	60
5.2.5	Synthesis of 2-hydroxy-5-nitrobenzaldehyde	61
5.2.6	Synthesis of 1',3',3'-trimethyl-6-nitrospiro[chromene-2,2'-indoline].....	61
5.2.7	Synthesis of (2 <i>R</i> ,3 <i>R</i>) dimethyl 2,3-dihydroxysuccinate	62

5.2.8	Synthesis of (4 <i>R</i> ,5 <i>R</i>) dimethyl 2,2-dimethyl-1,3-dioxolane-4,5-di carboxylate	62
5.2.9	Synthesis of ((4 <i>S</i> ,5 <i>S</i>)-2,2-dimethyl-1,3-dioxolane-4,5 diyl)di methanol	63
5.2.10	Synthesis of ((4 <i>S</i> ,5 <i>S</i>)-2,2-dimethyl-1,3-dioxolane-4,5-diyl)bis (methylene)bis(4-methylbenzenesulfonate)	64
5.2.11	Synthesis of Methyl 2,3-O-isopropylidene- β - <i>D</i> -ribofuranoside	64
5.2.12	Synthesis of ((3 <i>aR</i> ,4 <i>R</i> ,6 <i>aR</i>)-6-methoxy-2,2-dimethyltetrahydro furo[3,4- d][1,3]dioxol-4-yl)methyl 4-methylbenzenesulfonate	65
5.2.13	Synthesis of (3 <i>aS</i> ,4 <i>S</i> ,6 <i>S</i> ,6 <i>aR</i>)-4-(iodomethyl)-6-methoxy-2,2-di methyltetrahydrofuro[3,4- <i>d</i>][1,3]dioxole	66
5.2.14	Synthesis of (<i>R/S</i>)-9,9,9 <i>a</i> -Trimethyl-2,3,9,9 <i>a</i> -tetrahydrooxazolo[3,2 <i>a</i>] indole.....	66
5.2.15	Synthesis of (<i>R/S</i>)-2-(3',3'-dimethyl-6-nitrospiro[chromene-2,2'-indolin]- 1'-yl)ethan-1-ol	67
5.2.16	Synthesis of (<i>S</i>)-2-(1,3-dioxoisindolin-2-yl)propanoic acid.....	68
5.2.17	Synthesis of (<i>R</i>)-2-(1,3-dioxoisindolin-2-yl)propanoic acid	68
5.2.18	Synthesis of (<i>S</i>)-2-(1,3-dioxoisindolin-2-yl)propanoic acid.....	69
5.2.19	Synthesis of (<i>R</i>)-2-(1,3-dioxoisindolin-2-yl)-3-phenylpropanoic acid...69	
5.2.20	Synthesis of SPA-I	70
5.2.21	Synthesis of SPA-II	71
5.2.22	Synthesis of SPA-III	72
5.2.23	Synthesis of SPA-IV	73
	REFERENCES	75
	APPENDICES	
A.	NMR Spectra	85

B. IR Spectra	125
C. HRMS Spectra	128
D. FLUORESCENCE Spectra.....	130
E. UV-Vis Spectra.....	133

LIST OF SCHEMES

SCHEMES

Scheme 1. a) Photochromism of tetracene solution b) Change in the structure of the solid-state dinitroethane c) Structure of β -TCDHN	2
Scheme 2. Photoisomerization of azobenzenes	3
Scheme 3. Photoisomerization of stillebenes and its irreversible oxidation to phenanthrene.....	5
Scheme 4. The conversion between spiropyran and merocyanine.....	9
Scheme 5. Racemization during photoisomerization of the spiropyran.....	10
Scheme 6. The first method for the synthesis of a spiropyran	10
Scheme 7. A modification of the first method	11
Scheme 8. The mechanism of the spiropyran synthesis	11
Scheme 9. The second method for the synthesis of a spiropyran.....	12
Scheme 10. Photoisomerization of SP-A	14
Scheme 11. Isomerization of SP-B	17
Scheme 12. Acidochromism of an indolino-spiropyran	19
Scheme 13. Thermochromism of spiropyrans with different substituents	21
Scheme 14. Schematic illustration of controlled release of coumarin 102	23
Scheme 15. Synthesis of compound 4	27
Scheme 16. The conversion of compound 4 into the corresponding merocyanine.	28
Scheme 17. The synthesis of compound 6	29
Scheme 18. Synthesis of compound 11	31
Scheme 19. Synthetic pathway for compound 7	32
Scheme 20. Synthetic route for compound 13	33
Scheme 21. Alternative way for the synthesis of compound 16	34
Scheme 22. Synthesis of Compound 19	35
Scheme 23. Synthesis of compound 21	36

Scheme 24. Amino protection of both enantiomers of alanine and phenylalanine.	36
Scheme 25. Synthesis of SPA-I through acyl chloride esterification procedure....	37
Scheme 26. Synthesis of SPA-III through CDI coupling procedure	37
Scheme 27. Synthesis of SPA-III through EDC coupling procedure	38
Scheme 28. Synthesis of SPA-I , SPA-II , SPA-III , and SPA-IV	39
Scheme 29. Photoisomerization of SPA-I to MCA-I	41
Scheme 30. Photoisomerization of SPA-II to MCA-II	43
Scheme 31. Photoisomerization of SPA-III to MCA-III	44
Scheme 32. Photoisomerization of SPA-IV to MCA-IV	46

LIST OF FIGURES

FIGURES

Figure 1. Azobenzene derivatives synthesized by Blege (compound AB-1) and Samanta (compound AB-2).....	4
Figure 2. Examples of dithienylethenes with different linkers.....	5
Figure 3. a) Photoisomerization between compounds ODE and CDE b) Absorption spectra of the two photoisomers	6
Figure 4. The dithienylethenes with unsaturated ethyl benzoate moiety and tetraalkene derivatives	7
Figure 5. The first record of spiropyrans.....	7
Figure 6. The basic structure of a spiropyran	8
Figure 7. The spiropyrans reported by Fischer and Hirshberg	8
Figure 8. Numbering of an indolino-benzospiryran	13
Figure 9. Isomers of the merocyanine form	16
Figure 10. Potential energy diagram displaying solvatochromism of merocyanines redrawn inspired from reference 41	17
Figure 11. Spiropyrans derivatives exhibiting thermochromism	20
Figure 12. a) ¹ H NMR of Compound 4 b) UV-Vis spectrum of Compound 4	28
Figure 13. ¹ H NMR spectrum of compound 6	29
Figure 14. HPLC chromatogram of compound 6.....	30
Figure 15. UV-Vis spectrum of compound 6	30
Figure 16. The designed spiropyran containing chiral moiety derived from tartaric acid	31
Figure 17. The spiropyran containing chiral moiety derived from <i>D</i> -ribose	32
Figure 18. The target compounds; SPA-I , SPA-II , SPA-III , and SPA-IV	35
Figure 19. UV-Vis spectra of a) SPA-I b) SPA-II c) SPA-III d) SPA-IV in different solvents prior to 365 nm illumination	40
Figure 20. UV-Vis spectra of SPA-I in a) methanol b) isopropanol.....	41
Figure 21. UV-Vis spectra of SPA-I in a) dichloromethane b) hexane	42
Figure 22. UV-Vis spectra of SPA-II in a) methanol b) isopropanol.....	43

Figure 23. UV-Vis spectra of SPA-II in a) dichloromethane b) hexane	44
Figure 24. UV-Vis spectra of SPA-III a) methanol b) isopropanol	45
Figure 25. UV-Vis spectra SPA-III a) dichloromethane b) hexane	45
Figure 26. UV-Vis spectra of SPA-IV a) methanol b) isopropanol	46
Figure 27. UV-Vis spectra of SPA-IV a) dichloromethane b) hexane.....	47
Figure 28. Studies on ring-closure of a) Compound 21 b) SPA-II and c) SPA-IV	48
Figure 29. Ring closure kinetics of a) Compound 21 b) SPA-II c) SPA-IV	50
Figure 30. CD spectra of SPA-I , SPA-II , SPA-III , SPA-IV	51
Figure 31. HPLC chromatogram of compound 21	52
Figure 32. HPLC chromatogram of SPA-II	53
Figure 33. HPLC Chromatogram of SPA-II	53
Figure 34. ¹ H NMR spectrum of Compound 1	86
Figure 35. ¹ H NMR spectrum of Compound 2	87
Figure 36. ¹ H NMR spectrum of Compound 3	88
Figure 37. ¹ H NMR spectrum of Compound 4	89
Figure 38. ¹ H NMR spectrum of 2-hydroxy-5-nitrobenzaldehyde.....	90
Figure 39. ¹ H NMR spectrum of Compound 6	91
Figure 40. ¹ H NMR spectrum of Compound 8	92
Figure 41. ¹ H NMR spectrum of Compound 9	93
Figure 42. ¹³ C NMR spectrum of compound 9	94
Figure 43. ¹ H NMR spectrum of Compound 10	95
Figure 44. ¹ H NMR spectrum of Compound 11	96
Figure 45. ¹³ C NMR spectrum of Compound 11	97
Figure 46. ¹ H NMR spectrum of Compound 14	98
Figure 47. ¹ H NMR spectrum of Compound 15	99
Figure 48. ¹ H NMR spectrum of Compound 17	100
Figure 49. ¹ H NMR spectrum of Compound 19	101
Figure 50. ¹ H NMR spectrum of Compound 21	102
Figure 51. ¹ H NMR spectrum of Compound 22a-S	103

Figure 52. ¹ H NMR spectrum of Compound 22a-R	104
Figure 53. ¹ H NMR spectrum of Compound 22b-S	105
Figure 54. ¹ H NMR spectrum of Compound 22b-R	106
Figure 55. ¹ H NMR spectrum of SPA-I	107
Figure 56. ¹³ C NMR spectrum of SPA-I	108
Figure 57. DEPT90 NMR spectrum of SPA-I	109
Figure 58. DEPT135 NMR spectrum of SPA-I	110
Figure 59. ¹ H NMR spectrum of SPA-II	111
Figure 60. ¹³ C NMR spectrum of SPA-II	112
Figure 61. COSY NMR spectrum of SPA-II	113
Figure 62. DEPT90 NMR spectrum of SPA-II	114
Figure 63. DEPT135 NMR spectrum of SPA-II	115
Figure 64. ¹ H NMR spectrum of SPA-III	116
Figure 65. ¹³ C NMR spectrum of SPA-III	117
Figure 66. DEPT90 NMR spectrum of SPA-III	118
Figure 67. DEPT135 NMR spectrum of SPA-III	119
Figure 68. ¹ H NMR spectrum of SPA-IV	120
Figure 69. ¹³ C NMR spectrum of SPA-IV	121
Figure 70. COSY NMR spectrum of SPA-IV	122
Figure 71. DEPT90 NMR spectrum of SPA-IV	123
Figure 72. DEPT135 NMR spectrum of SPA-IV	124
Figure 73. IR spectrum of SPA-I	126
Figure 74. IR spectrum of SPA-II	126
Figure 75. IR spectrum of SPA-III	127
Figure 76. IR spectrum of SPA-IV	127
Figure 78. HRMS spectra of SPA-I , SPA-II , SPA-III , and SPA-IV	129
Figure 79. Fluorescence absorption and emission spectra of SPA-I	131
Figure 80. Fluorescence absorption and emission spectra SPA-II	131
Figure 81. Fluorescence absorption and emission spectra of SPA-III	131
Figure 82. Fluorescence absorption and emission spectra of SPA-IV	132

Figure 83. Acidochromism of Compound **6** 134

LIST OF ABBREVIATIONS

ABBREVIATIONS

CD	Circular Dichromism
CDI	1-1'-Carbonyldiimidazole
DBU	1,8-Diazabicyclo(5.4.0)undec-7-ene
DCU	1,3-Dicyclohexyl urea
DCC	N,N'-Dicyclohexylcarbodiimide
DMAP	4-Dimethylaminopyridine
MEK	Methyl Ethyl Ketone
MC	Merocyanine
SP	Spiropyran

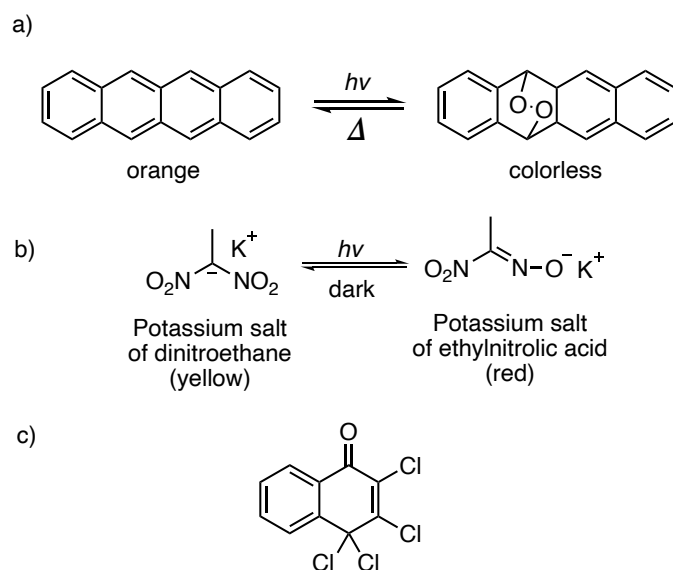
CHAPTER 1

INTRODUCTION

1.1 Photoswitchable Compounds

Photochromism is one of the most studied concepts in recent years. Hirshberg first declared the term photochromism in the middle of the twentieth century and explained it as the reversible and photo-induced transformation of a compound between two isomers.¹ The isomers have not only different geometrical structures but also distinctive absorption spectra, refractive index, and dielectric constant as a result of the conversion triggered by illumination of specific wavelengths. Photochromic action can act towards both products and reactants sides. The intense color can be observed upon exposure to irradiation, or an initial colorless state can be accessed after subjected to heat or light.¹

In the 1860s, Fritsche pointed out that a tetracene solution with orange color bleached under sunlight and turned back to its initial state color in the dark (Scheme 1a). It was the first report of the photochromic phenomena. Afterwards, it was reported by E. ter Meer in 1876 that the color of the potassium salt of the solid-state dinitroethane altered from red in the daylight to yellow in the dark (Scheme 1b). In 1899, Markwald published the reversible color change of 2,3,4,4-tetrachloronaphthalen-1(4H)-one (β -TCDHN) (Scheme 1c).¹



Scheme 1. a) Photochromism of tetracene solution b) Change in the structure of the solid-state dinitroethane c) Structure of β -TCDHN

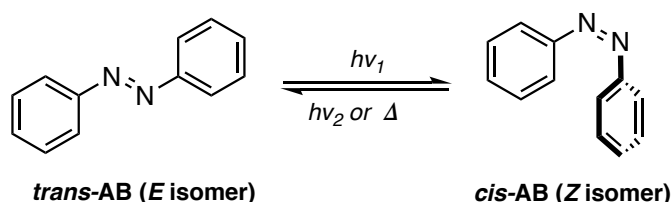
Studies on photochromism were scarce between the 1940s and 1960s, while synthetic studies were still being developed by the research groups of Fischer and Hirshberg, who first referred to the term photochromism in 1950.² During the 1960s, the advancement of organic synthesis and characterization techniques such as X-ray, IR, and NMR pushed photochromism research forward. Along with these lines, various applications such as photochromic micro image (PCMI) and glasses were developed.² Nonetheless, photodegradation of present organic compounds exhibiting photochromism restricted their applications until the 1980s. Then, chromenes and spirooxazine derivatives, resistant to photo fatigue, were synthesized.² Accomplishment in photochromic studies rendered the manufacture of ophthalmic lenses possible.²

The compounds possessing photochromism are known as photochromic or photoswitchable compounds.³ Such compounds are widely reported and extensively explored in the literature.⁴ This brings a broad range of applications across various research disciplines such as material science, biological science and physics. Today, photoswitchable compounds are mainly utilized in photopharmacology, optical data

storage, and fabrication of smart materials.⁵ Azobenzenes, diarylethenes, and spiropyrans are the most prevalent examples of this group of compounds.⁴

1.1.1 Azobenzenes

Azobenzenes consist of two aryl rings attached to each other with an azo group (—N=N—). They have inherently two isomers, *E* and *Z*. The *trans*-form (*E* isomer) is planar, whereas their *cis* isomer (*Z* form) is nonplanar. Azobenzenes undergo photoisomerization when exposed to irradiation. In other words, the conversion between *E* and *Z* forms takes place as shown in Scheme 2, and this renders such compounds photochromic. Their simplest member is an azobenzene containing two unsubstituted phenyl rings. When azobenzene is subjected to the 365 nm irradiation, $\pi\text{-}\pi^*$ transition occurs, which results in the transformation of the *E* isomer into *Z*.⁶ Although 450 nm irradiation stimulates photoisomerization, the *Z* form is not entirely converted into *E* isomer. Therefore, *E* isomer cannot be obtained in 100% yield at 450 nm. The reason for that is the proximity and overlapping of the wavelengths required to produce the $n\text{-}\pi^*$ transitions present in the *cis* and *trans* isomers.⁷



Scheme 2. Photoisomerization of azobenzenes

The recent studies on photoisomerization have shown that the absorbance maxima of *E* and *Z* forms of azobenzenes can differ substantially with respect to the nature of substituents introduced to the phenyl ring.⁶ In the case that the substituent on phenyl rings has the electron-withdrawing nature such as fluorine, the electron density on the azo group (—N=N—) decreases.⁷ Provided that substituent with electron-donating ability exists on the rings, the relative energy of the highest

occupied molecular orbital (HOMO) in *trans* isomer increases, resulting in a red-shift.⁸ In case that substituents generate steric hindrance, the sp^2 character of the N=N bond is reduced. Correspondingly, a red-shift occurs owing to the resultant increase in the energy of HOMO.⁷ In other words, $n-\pi^*$ bands of *E* and *Z* isomers can differ considering the types of substituents. When the appropriate difference is acquired in the structure of the azobenzene, *cis* and *trans* isomers are selectively obtained by exploiting the visible light. As reported by Bleger *et al.*, it is possible to obtain the *Z* isomer in 90% yield when an azobenzene derivative accommodating fluorine at its *para*-position and an ester at *ortho*-position (compound **AB-1**, Figure 1) is synthesized. Subsequently, the photoisomerization is induced by green light ($\lambda > 500\text{nm}$) in order to obtain the *Z* isomer. The fact that the *E* isomer of that azobenzene derivative is recovered in 97% yield as a result of exploiting blue light ($\lambda=410\text{ nm}$) was also noted.⁷ Likewise, Samanta and coworker have reported that for the *cis* isomer in 98% yield to be obtained, red light ($\lambda=635\text{nm}$) could be facilitated for an azobenzene derivative with crosslinked peptide and tetra-*ortho*-methoxy substituents (compound **AB-2**, Figure 1). Upon irradiation of 450 nm (blue light), the *trans* isomer in 85% yield could be obtained.⁹

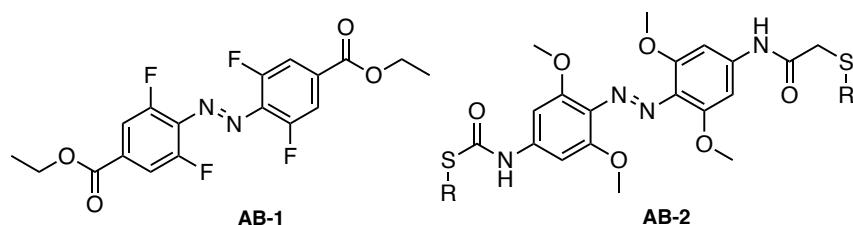
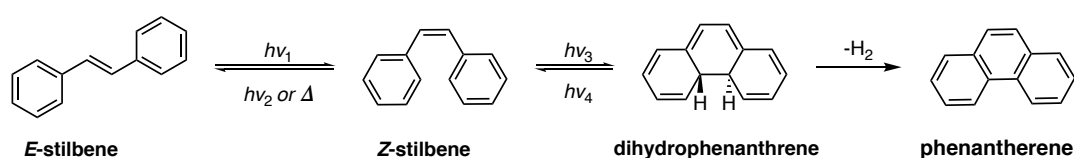


Figure 1. Azobenzene derivatives synthesized by Bleger (compound **AB-1**) and Samanta (compound **AB-2**)

1.1.2 Diarylethenes

Diarylethenes consist of a C=C double bond with appended aryl groups at 1 and 2 positions. Their simplest example is a stilbene, including two unsubstituted phenyl groups.¹⁰ Stilbenes undergo the *E* to *Z* isomerization under the UV light illumination

as depicted in Scheme 3. Subsequent 6π electrocyclization is followed by the formation of dihydrophenanthrene. Then, phenanthrene can be obtained, accompanying an irreversible hydrogen elimination step.⁶ Apart from the last step, the other steps are reversible, and thus photochromic.



Scheme 3. Photoisomerization of stilbenes and its irreversible oxidation to phenanthrene

Dithienylethenes with improved stability can be formed by the replacement of the phenyl rings of stilbenes with thiophene. They are the most popular members of the diarylethenes owing to their enhanced stability. Also, another modification can be acquired by replacing the C=C double bond with a six-membered ring such as benzoquinone **DE-1**, or a five-membered ring such as cyclopentene **DE-2**, fluorocyclopentene **DE-3** and maleic anhydride moiety **DE-4** (Figure 2). Malononitrile unit **DE-5** can also be used for the modification.¹⁰

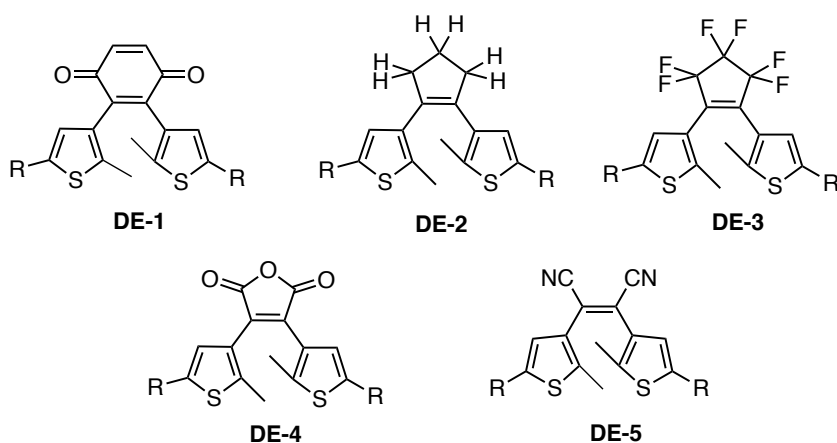


Figure 2. Examples of dithienylethenes with different linkers

Apart from the other photochromic compounds, the reverse isomerization of diarylethenes is not triggered thermally.¹¹ As an example of the changes in

geometrical and electronic structures, 1,2-bis(5-dimethyl-3-thienyl)perfluorocyclopentene can be examined (Figure 3a). Considering the ring open form of that compound (**ODE**), its UV-Vis absorption spectrum is in accordance with the substituted thiophene since π -conjugation does not extend all over the molecule. On the other hand, the delocalization of π -conjugation throughout the molecule is induced by ring closing (**CDE**). Hence the decrease in the gap between HOMO and LUMO leads to a shift of the absorbance band to a longer wavelength (red shift or bathochromic). The red color on the spectrum given in Figure 3b represents the delocalization of π -conjugation, which demonstrates the change in the compound's electronic and geometrical structure.¹¹

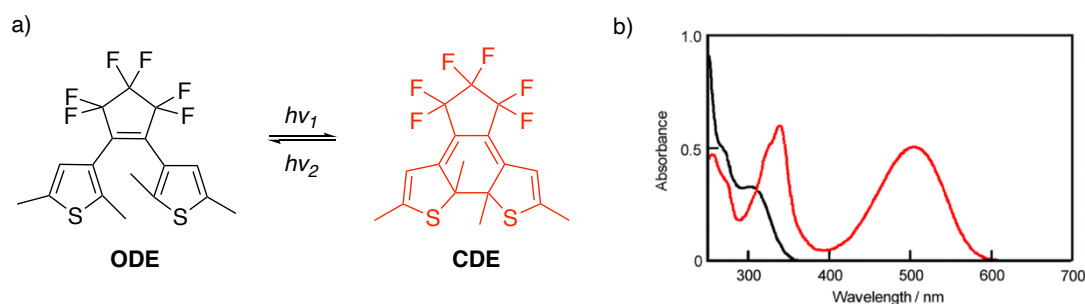


Figure 3. a) Photoisomerization between compounds **ODE** and **CDE** b) Absorption spectra of the two photoisomers

In addition, another approach to acquire a shift in the absorbance maximum to the longer wavelengths is to extend the length of π -conjugation. In the work of Tasic *et al.*, a bathochromic shift was attained by incorporating unsaturated ethyl benzoate moiety **DE-6** or a tetraalkene derivative **DE-7** into the dithienylethene (Figure. 4). Prior to 420 nm (blue light) illumination, these compounds primarily adopted a ring-open form whose absorption wavelength is approximately 340 nm. After the irradiation, the ring-closed form was obtained, and the absorbance maximum shifted to a longer wavelength than 630 nm.¹¹

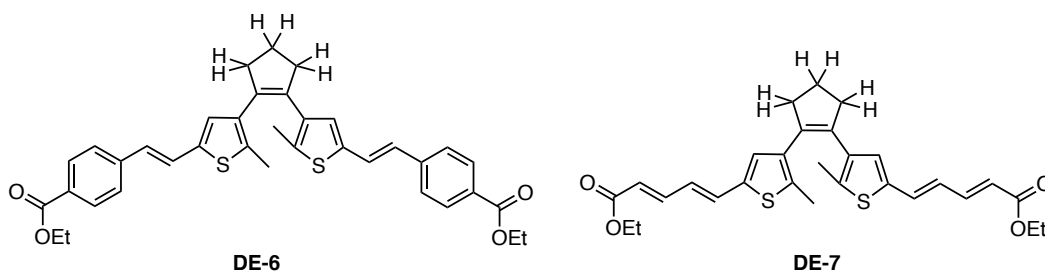


Figure 4. The dithienylethenes with unsaturated ethyl benzoate moiety and tetraalkene derivatives

1.1.3 Spiropyrans

The word “spiropyran” is the combination of two words, which are spiro and pyran. In chemistry, the two words have meaning. Spiro stands for at least two rings connected to each other through one atom,^{12,13} while pyran is a heterocyclic compound. Spiropyran, as a word, could indicate the existence of two pyran rings approximately orthogonal to each other, as shown in figure 6.^{14,15}

1.1.3.1 Structure

At the beginning of the twentieth century, Decker *et al.* had reported the synthesis of a compound (Figure 5) coincidentally while trying to synthesize a coumarin derivative. The compound had two benzopyran hybrid rings attached through a chiral center and displayed no photochromism (Figure 5). He then named this compound “spiropyran”.¹⁶

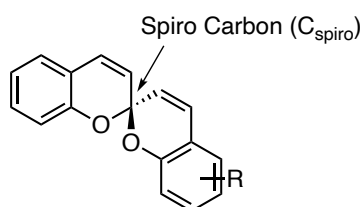


Figure 5. The first record of spiropyrans

From this date forward, the word spiropyran has been accepted as a general term for such compounds that usually have two heterocyclic aromatic rings provided that one of the rings is pyran. The two rings are attached with a spiro carbon (C_{spiro}) with sp^3 hybridization. The basic structure of a spiropyran is illustrated in Figure 6.¹⁷

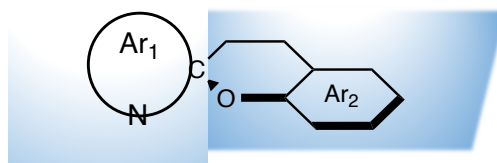


Figure 6. The basic structure of a spiropyran

The Ar_1 and Ar_2 ring shown in Figure 6 can be functionalized such as thiophenol, anthracene, benzene, indoline, and naphthalene. However, they should be aromatic rings.¹⁸

Over the following decades, various non-photochromic spiropyrans have been reported. In the middle of the twentieth century, Fischer and Hirshberg managed to synthesize spiropyrans exhibiting photochromism (Figure 7).¹⁹ Photochromic indolino-benzospiropyrans, on the other hand, have been broadly studied owing to facile synthesis and their potential to have applications in many areas of technology, including optical switching and data storage (Figure 7).^{20,21,1,22}

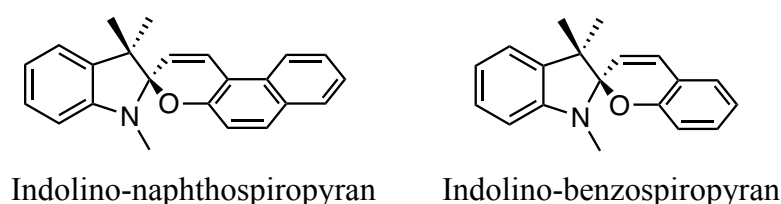
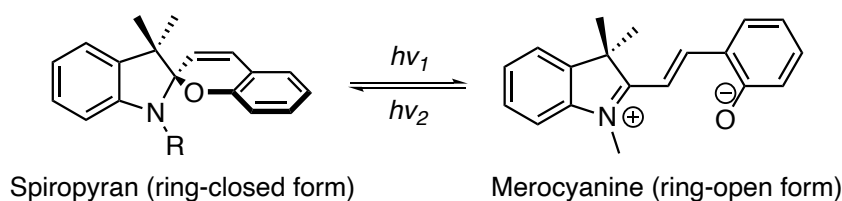


Figure 7. The spiropyrans reported by Fischer and Hirshberg

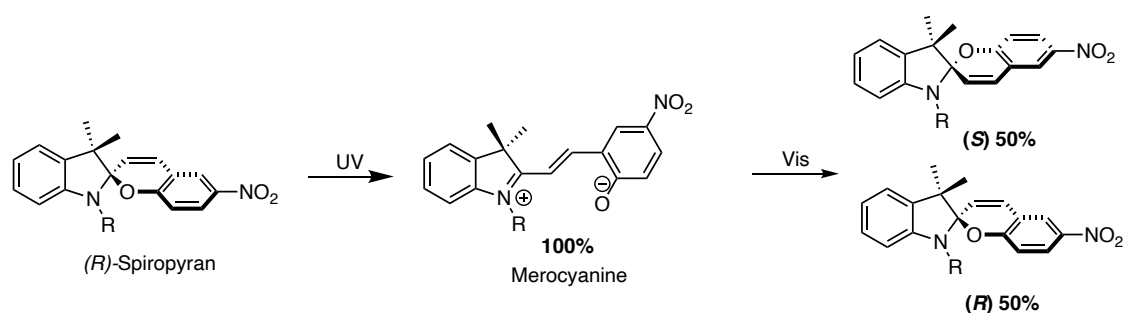
Considering the structure of spiropyrans, due to the orthogonality of two rings connected through C_{spiro} , the absence of the conjugation can be easily deduced. Accordingly, prior to UV illumination, the absorption peaks of spiropyrans show up within 200-400 nm in the UV region of the electromagnetic spectrum.²³ Upon

exposure to UV irradiation, their structure changes since the cleavage of the bond between the oxygen and C_{spiro} occurs, which induces planarity (Scheme 4). The non-conjugated ring-closed form turns into a fully conjugated system. The compound having a different structure and properties than spiropyrans is called merocyanine.²⁴ The transformation of spiropyrans (SP) into merocyanine (MC) leads to a red shift in the absorption spectrum. The absorption peaks of merocyanines appear in the visible spectral region, generally within 500-600 nm.^{25,26,27}



Scheme 4. The conversion between spiropyran and merocyanine

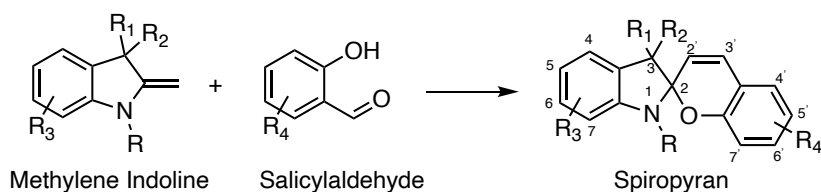
In a solution of spiropyrans, the ring-open form tends to be in equilibrium with the ring-closed form. External stimulants such as light, pH, temperature, and polarity of the environment can trigger a shift in the equilibrium, resulting in a change in the color of the solution. A solution containing predominantly spiropyrans is colorless, whereas it becomes colored due to the conversion of spiropyrans into merocyanines.²⁸ These two forms have remarkably different properties, i.e., dipole moment, dielectric constant, and absorption spectra, as well as geometrical structure and color.²⁹ Another difference between these two forms is their stereochemistry. Spiropyrans are chiral molecules due to the stereogenic center on the spiro carbon. However, their synthesis generally leads to a racemic mixture. When the enantiomers are separated and individually undergo photoisomerization to the corresponding merocyanine form, the loss of the chirality is observed (Scheme 5). The back conversion of the merocyanine into the spiropyran leads to racemization. In other words, an optically active spiropyran solution will be inactive after isomerization.¹⁸



Scheme 5. Racemization during photoisomerization of the spiropyran

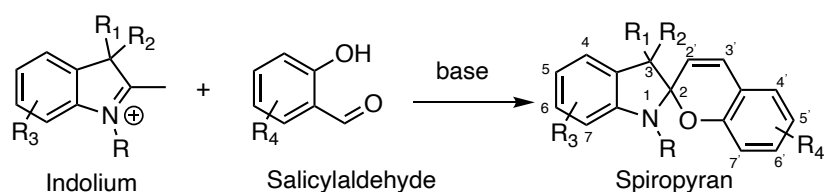
1.1.3.2 Synthesis

The preparation of an indolino-benzospirogyran can be examined into two parts.³⁰ The first method includes the reaction of an ortho-hydroxy aromatic aldehyde with a methylene base, especially the Fischer base, in a proper solvent (Scheme 6). The solvent of choice is generally ethanol.¹⁸



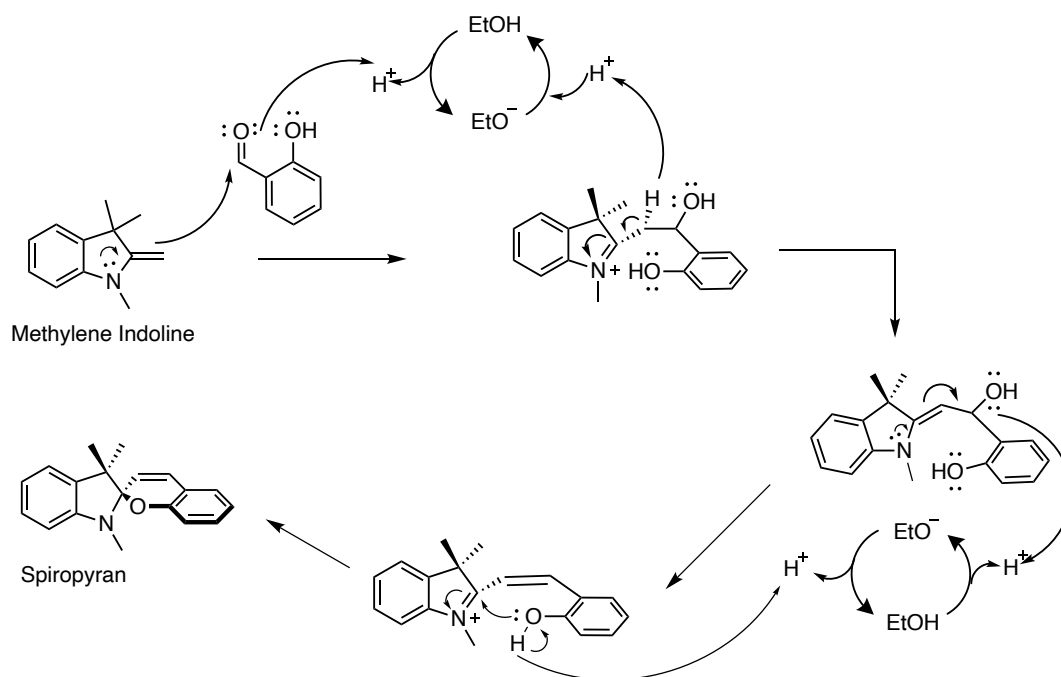
Scheme 6. The first method for the synthesis of a spiropyran

The alternative way includes the reaction between the salt form of the methylene base (indolium) and aromatic ortho-hydroxy aldehyde (Scheme 7). The reaction proceeds in the presence of a base such as piperidine and pyridine. This procedure is a modification of the first method described in this thesis. The alternative way facilitates the formation of the Fischer base (methylene indoline) *in situ* rather than isolating.



Scheme 7. A modification of the first method

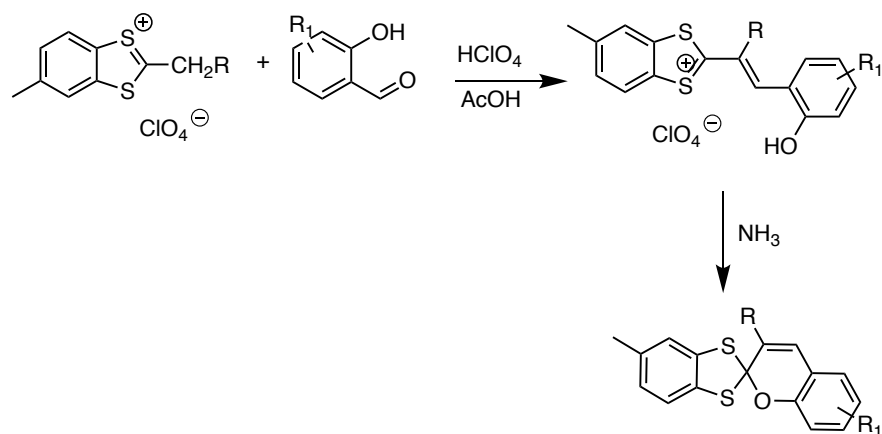
The proposed mechanism for the synthesis of an indolino-benzospiryran is depicted in Scheme 8.¹⁶ The reaction starts with the nucleophilic attack of the methylene indoline to the salicylaldehyde and is followed by the attack of the hydroxy oxygen to the spiro carbon to afford a spiropyran (Scheme 8).



Scheme 8. The mechanism of the spiropyran synthesis

In the second method, the thermodynamically or kinetically stable merocyanine form rather than the spiropyran form is isolated due to the reaction between the heterocyclic cations having an active methylene group and an aromatic ortho-hydroxy aldehyde (Scheme 9). The reaction takes place in acidic conditions, and a catalytic amount of perchloric acid is used. After removing perchlorate with an organic base such as ammonia and amines, the spiropyran form is obtained. To attain

higher yields in this reaction, benzene or ether solution of dry ammonia should be used.³⁰



Scheme 9. The second method for the synthesis of a spiropyran

1.1.3.3 Properties

The direction of equilibrium between spiropyran and merocyanine can shift towards either the ring-open form (MC) or ring-closed form (SP). The aforementioned external stimulants, which are electromagnetic radiation, solvent, pH, and temperature, can trigger this shift, and thus the color of the initial spiropyran solution changes. Accordingly, spiropyrans and merocyanines exhibit photochromism, solvatochromism, acidochromism, and thermochromism, depending on the condition.²⁹

1.1.3.3.1 Photochromism

Photochromism is described as a reversible transformation of a compound into a chemical species with different physical properties, induced by the absorption of electromagnetic radiation. As a result of this process, the absorption spectrum and the color of the solution change necessarily.³¹ With this approach, when a colorless compound is converted into an intensely colored one by means of irradiation, the

process is considered positive photochromism. The exact opposite case is referred to as negative photochromism.³² A spiropyran solution, either colored or colorless, contains both the spiropyran and the merocyanine forms but in different proportions. The amount of spiropyran and merocyanine forms in a solution determines the type of photochromism.²⁹

All colorless spiropyran solutions, upon exposure to the UV light, transform into the merocyanine form and become colored regardless of solvent polarity. The colored solutions, i.e., solutions containing the merocyanine form dominantly, become intensely colored, and their absorption intensity increases after the UV irradiation. These two situations are the example of positive photochromism.²⁶

Since the environment in which spiropyrans and merocyanines are present can alter the type of photochromism, it might be inappropriate that the classification is done without considering the environmental factors.²⁹ Correspondingly, it was reported in the literature that spiropyran bearing carboxyl, free hydroxyl or nitro groups are dissolved in a polar solvent and then irradiated with visible light. Negative photochromism is observed since polar solvents can stabilize the merocyanine form superior to non-polar solvent.³³ In this regard, the study conducted by Barachevsky and his coworkers revealed the effects of substituents attached to the pyran ring of the spiropyrans on photochromism (Figure 8).³¹ According to this study, increasing the acidity of pyran fragment by the electron-withdrawing groups, especially at 5' and 7' positions, raises merocyanine's stability and hence, leads to an increment in the intensity of the absorption band. Besides, replacing the nitro group at position-7' by bromide brings about a shift of the equilibrium to the ring-closed form accompanied by a decrease in the absorption band intensity.³¹

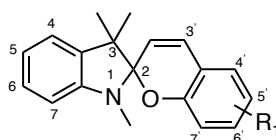
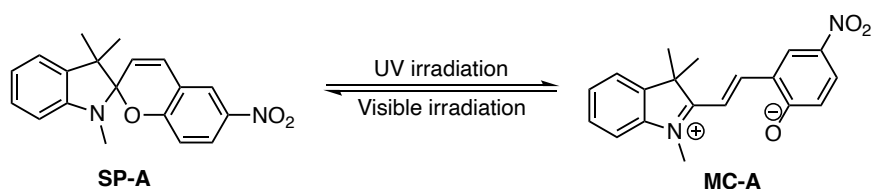


Figure 8. Numbering of an indolino-benzospiropyran

In literature, there are many reports that focus on the photochemistry and photophysics of **SP-A** (Scheme 10). Kyu *et al.* studied this spiropyran in hexane. They observed that the solution was initially colorless and, there was no discernable UV-Vis absorption peak in its spectrum. Afterwards, **SP-A** solution became dark blue upon exposure to the UV irradiation (Scheme 10). While the initial solution contains the spiropyran form predominantly, the solution consists of mainly the merocyanine form after 4 minutes UV illumination. The absorption band around 590 nm can be attributed to the predominance of the ring open form. When UV light is removed, the solution turns back to its colorless state, which confirms the reversible nature of SP-MC photoisomerization.³⁴



Scheme 10. Photoisomerization of **SP-A**

When the same spiropyran is dissolved in ethanol, the color of the initial solution is pale pink.³⁵ After UV irradiation, it becomes intensely colored. In the same manner, the major component of the solution is initially the ring-closed form, accompanying the ring-open form. The absorption band around 550 nm shows the existence of the merocyanine form. The increase in the intensity at this wavelength demonstrates the shifting of the equilibrium towards **MC-A**.³⁵ The results also highlight the importance of solvents and reveal the necessity to discuss the term solvatochromism.

1.1.3.3.2 Solvatochromism

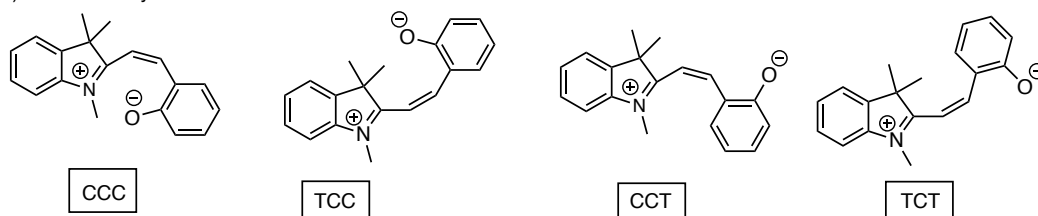
Solvatochromism refers to a change in position of the absorption band and/or an alteration in its intensity and shape. It mainly depends on the nature of solvents, particularly the polarity.³⁶ The effect of solvents during a chemical reaction has been inspected extensively. Also, whether changing polarity of solvents induces any difference in an absorption band and equilibrium constant has been studied.³⁷ The

idea of correlating the polarity with some parameters such as dipole moment and dielectric constant has not been very successful because of the excessive simplifications. Accordingly, the polarity of a solvent can be associated with its solvating behavior. Therefore, the influence of intermolecular forces such as hydrogen bonding and dispersion force comes into prominence in the comprehension of solvent effect on the spectral properties of a solute. Solute-solvent interactions can be categorized into two groups, which are general and specific.³⁷

Induced dipole-induced dipole, dipole-dipole, and dipole-induced dipole are the types of electrostatic forces and can be examined under the category of general solute-solvent interactions. In the case that the dipole moment of solute molecules increases during their excitation, for example π - π^* transitions, the excited state is better stabilized by a polar solvent in comparison with the ground state. Consequently, since the difference between excited and ground state decreases, the absorption takes place at a longer wavelength; that is, red shift occurs. This effect is known as positive solvatochromism or bathochromic shift.²⁹ On the other hand, a blue shift is observed if the dipole moment decreases upon the excitation process. This shift arises from the polar solvents stabilizing the ground state. n - π^* transitions are the example of this situation, which is also known as negative solvatochromism.²⁹ Besides, as the second group, specific solute-solvent interactions can bring about a considerable change in the spectral properties of solutes. Charge transfer interactions, hydrogen bonding, and complexation are example of this type of interaction. It takes place between the chromophore part of the solute and the solvent. In the case of hydrogen bonding formed, the energy of the electronic state is decreased by virtue of the attraction between the positively polarized hydrogen atom of the solute and the lone pair electrons of the atom, connected to the solute and having a basic character, regardless of excited state or ground state. The formation of hydrogen bonds prevents the migration of charge density from the basic atom during excitation, leading to a blue shift. On the contrary, a red-shift is observed when hydrogen bond formation opposes the migration of electron density towards basic atom during the excitation process.³⁷

It is also known that solvatochromism is the property related to the molecules having π -electron conjugated system. Accordingly, the merocyanine form rather than the spiropyran form possesses this property.³⁸ At that point, examining the merocyanine form can be helpful. There are eight isomers of it as shown in Figure 9. These isomers are primarily classified as *cisoid* (*E*) and *transoid* (*Z*) with respect to the double bond positioned in the middle of the molecule. Then, the position of α , β , and γ bonds between spiro carbon and the phenolate part is considered while classifying.¹⁶ Although there are several isomers of a merocyanine form, their energies are similar.³⁹ This phenomenon is confirmed by monitoring their spectroscopic properties.¹⁶ The identification of its four *transoid* isomers was performed through Raman and multiple dimensional NMR spectroscopies.¹⁸ Additionally, Ernsting *et al.* worked on the unsubstituted indolino-benzospiropyran. They demonstrated by theoretical calculations and time-resolved studies that the TTC isomer of the corresponding merocyanine form was the most stable among other *transoid* isomers considering their relative energies.³⁹

a) *cisoid*-merocyanines



b) *transoid*-merocyanines

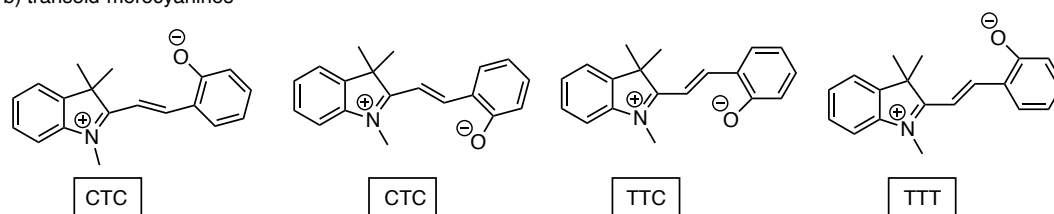


Figure 9. Isomers of the merocyanine form

Solvatochromism of merocyanines is observed when there is a gradual coloration in accordance with the increase in solvent polarity. It is the indication of the merocyanine form being predominant in the solution.⁴⁰ Accordingly, the polar

merocyanine forms are better stabilized by polar solvents, which results from the ability of these solvents to lower the energy of the ring-open form in consideration of the information mentioned earlier.⁴¹ The decrease in the energy required to convert a spiropyran into the corresponding merocyanine form is observed. Also, it leads to a maximum 40 nm shift in the absorption of the merocyanine. Sometimes the existence of a shoulder in its absorption band can be observed. The shoulder indicates the presence of other *transoid* isomers.¹⁶

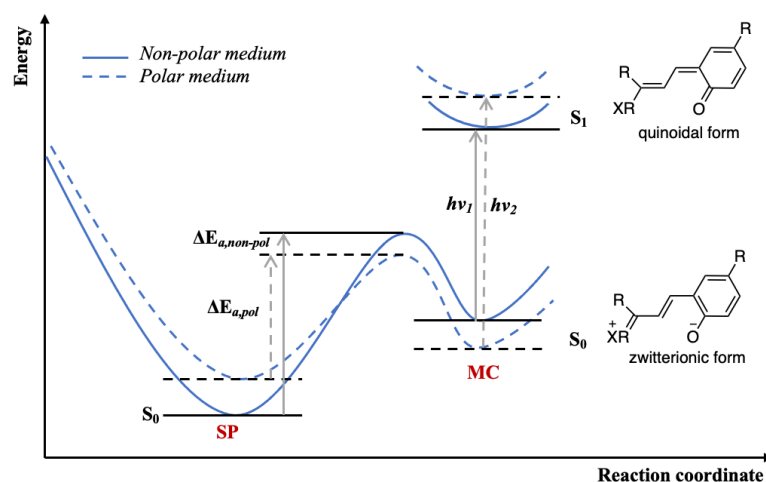
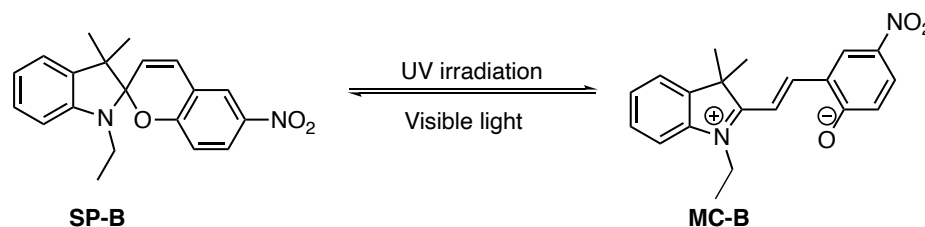


Figure 10. Potential energy diagram displaying solvatochromism of merocyanines redrawn inspired from reference 41

When the merocyanine form of indolino-benzospiropyrans is considered, the ground state is better represented by a zwitterionic structure while the excited state resembles a quinoidal form primarily (Figure 10). As a result of the decrease in the dipole moment during the excitation process, the ground state is stabilized by polar solvents. Thus the gap between S_0 and S_1 increases, which produces a blue-shift.⁴²



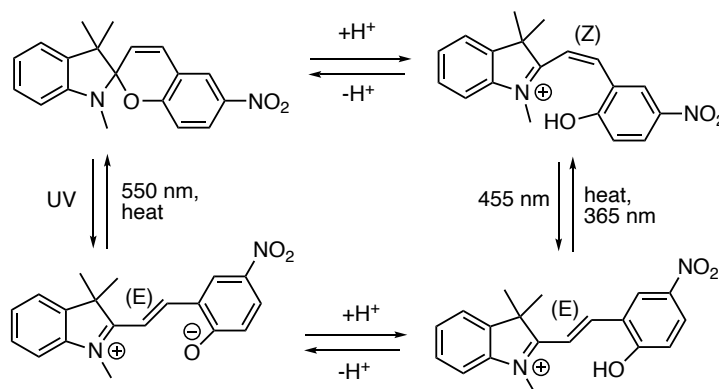
Scheme 11. Isomerization of SP-B

Tian and coworker investigated the photochromic and solvatochromic properties of **SP-B** (Scheme 11).²⁹ They reported that the **SP-B** in non-polar solvents, such as petroleum ether and hexane, displays positive photochromism. Their solutions are initially colorless when they are kept in the dark place. Then, they become colored with UV illumination. According to this report, a red shift is observed in the **SP-B** solutions starting from polar solvents to non-polar solvents. They showed that the merocyanine's charge distribution is altered considerably by the alcohols owing to their ability to make hydrogen bonds. Moreover, it was reported that the absorption intensity of the merocyanine continuously declines with the decrease in solvent polarity.²⁹

1.1.3.3 Acidochromism

Acidochromism is a phenomenon in which the treatment of a compound with acid induces a change in the absorption spectrum.¹⁶ Nowadays, it is known that the merocyanines are better stabilized compared to the spiropyrans in the presence of protons owing to their charged structure. Prior to photochromism of spiropyrans, the alteration in the color of non-photochromic spiro compounds in the presence of acids was a general phenomenon. However, whether or not acids possess sufficient strength to protonate the ring-closed form and induce the ring-opening was an important concern.^{16,43} In 1995, Sammes and Roxburgh reported that spiropyrans exhibit acidochromism upon addition of trifluoroacetic acid, whereas that was not the case in the presence of acetic acid. They also confirmed the existence of an intermediate *cisoid* species, whose lifetime is limited, by utilizing ¹H NMR spectroscopy.⁴⁴ Besides, Zhou *et al.* indicated that the intermediate form is such a protonated structure whose bond between the spiro carbon and the oxygen atom has been broken. However, the planarization has not yet been achieved (Scheme 12).⁴⁵ Then, the planar structure was supported by Shiozaki's research on the treatment of spiropyrans with sulfuric acid, trifluoroacetic acid, and hydrochloric acid.⁴⁶ The results are essential to show the existence of protonated or unprotonated *cisoid* and

transoid structures of merocyanines. Moreover, the change in the response of indolino-benzospiropyran derivatives to acid strength and the fact that acids stronger than phenolate stimulate the ring-opening render the pH-gated photochromism possible. It is noted that the absorption of the protonated *E*-merocyanine can be seen somewhere about 400 nm in a UV-Vis spectrum, whereas that of *Z*-merocyanine is absent when pH is between 2 and 8. The fact that *Z*-merocyanines have lower pK_a than that of *E*-merocyanines renders the usage of spiropyrans as a photoacid possible.⁴⁷ In order for spiropyrans to be exploited as a photoacid, pK_a of the acid employed is required to be lower than those of the *cisoid* merocyanine and ring-closed form. In such systems, the proton uptake does not occur since the pK_a of acid employed is larger than that of spiropyrans. Upon exposed to the UV irradiation, the *E*-merocyanine, which tends to be protonated since its affinity to the proton is higher than the acid, is obtained, causing the increase in pH. The isomerization of the *E*-merocyanine to *Z*-merocyanine is induced by exposing the visible light irradiation, and consequently, pK_a of the molecule decreases the accompanying release of the proton. The ring-closure takes place concurrently.⁴⁸



Scheme 12. Acidochromism of an indolino-spiropyran

1.1.3.3.4 Thermochromism

It was not noted until 1926 that the color of spiropyrans changes while heated and returns to their original state upon cooling. At the beginning of the 1960s,

spiropyrans could be the most studied among the compounds exhibiting thermochromism since they can be examined without using an optical device.⁴⁹ Nonetheless, the fact that the color of dibenzospiropyrans does not change upon heating and thermochromism is possessed mainly by naphtho- and indolinospiryran were reported.⁵⁰ The work of Wizinger showed that polarization of the spiro center by incorporating indolino group as shown in Figure 11 renders benzospiropyran thermochromic.¹⁶

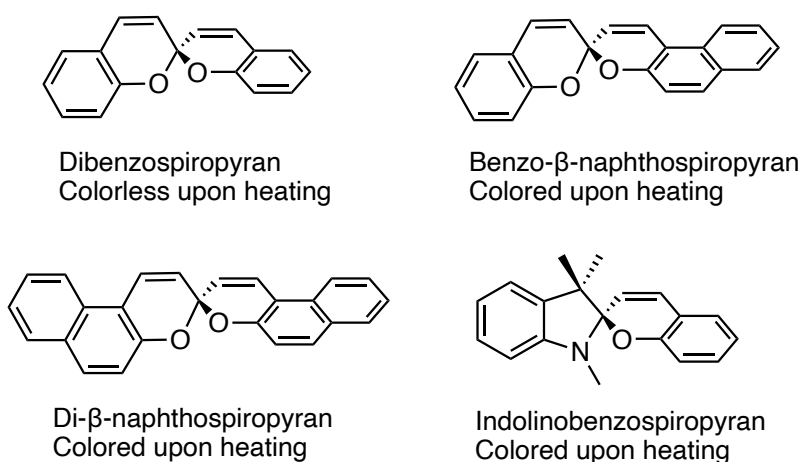
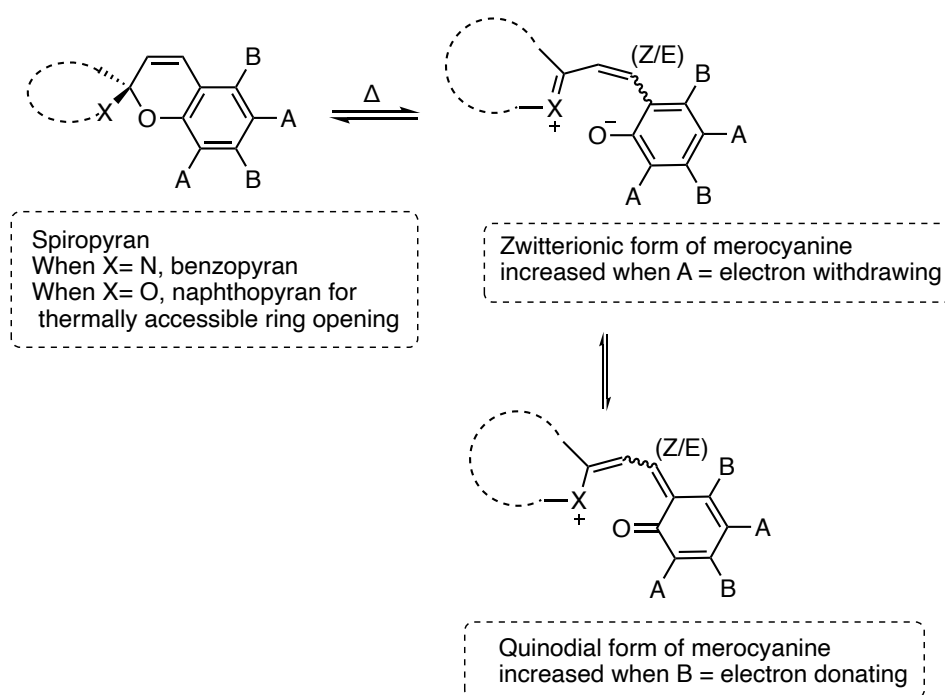


Figure 11. Spiropyran derivatives exhibiting thermochromism

The ring-opening that occurred at elevated temperatures was anticipated due to the heterolytic cleavage of the bond between the spiro-carbon and the oxygen atom. Even though Heller *et al.* announced a weak signal in EPR for the ring-open form, the assessment that the conversion of spiropyran into merocyanine takes place through free radical mechanism was abandoned.⁵¹ Even if the experimental results mainly designate the zwitterionic form as an accurate structure, either quinoidal or zwitterionic forms can be the most plausible description for the ring-open form depending on the nature of solvents, substituents on the pyran ring, and the type of heterocycle.⁴⁹ Accordingly, since the stability of merocyanine form greatly results from the delocalization of charge, substituents on the compound have a significant effect. In order for the quinoidal form to be obtained, aromaticity is required to be lost. Therefore, the tendency of benzospiropyran to be transformed into merocyanines is lower compared to that of naphthospiropyran.⁵² In

naphthospiroprans, the heterocyclic ring contributes to the stabilization owing to its ability of charge delocalization. In order for benzospiroprans to possess thermochromism, at least one of their pyran rings needs to be naphthopyran. Another aspect contributing to stabilization of the ring-open form at elevated temperatures is the substituents on the pyran ring stabilizing the phenolate along with the electron-donating ability of the heterocyclic ring (Scheme 13).¹⁶

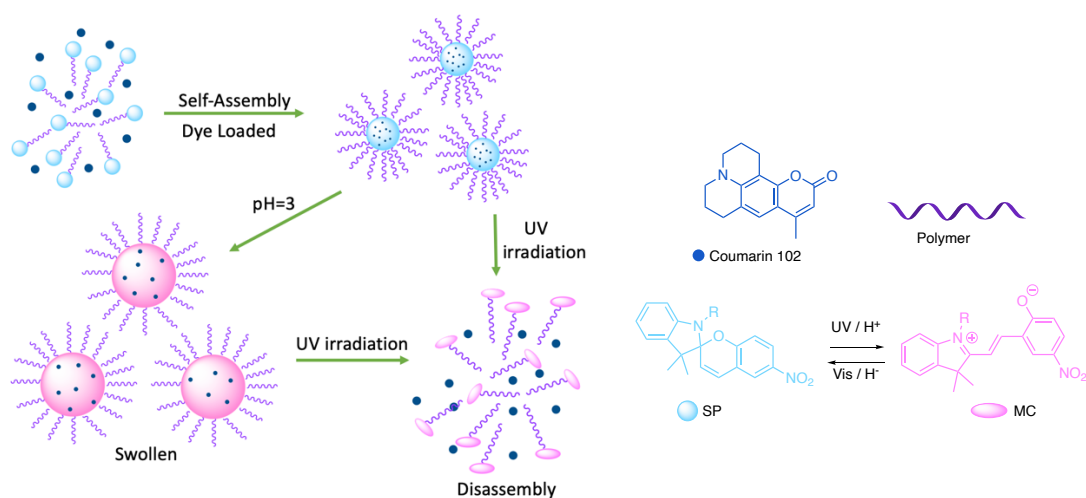


Scheme 13. Thermochromism of spiropyrans with different substituents

In 1953, Hirshberg and Fischer identified the merocyanine's isomers having different colors at elevated temperatures starting from 105 K. When the temperature increased progressively, solutions with distinct colors were observed at 123 K and 165 K. These solutions became colorless at ambient temperature.⁵³ The findings support the idea of existing energetically different *cisoid* and *transoid* structures at different temperatures. Besides, the number of accessible isomers increases while approaching the boiling point of solvents. As it is mentioned before, there are energetically distinct eight isomers for merocyanine form.¹⁶

1.1.3.4 Applications

Parallel with the features mentioned before, spiropyrans have some distinctive characteristics such as high sensitivity, high photo fatigue resistance, reversibility, ease of synthesis, and showing fast response to multiple stimuli.⁵⁴ Since the two isomers manifest significantly different chemical and physical properties, spiropyrans have been used in the fabrication of many smart polymers. In the literature, there are numerous reports referring to their attachment to polymers. As a result of the isomerization between spiropyrans and merocyanines, the physico-chemical properties of polymer matrices are altered. Thus, especially photo- and thermochromism of spiropyrans can extend the utilization of the polymers to drug-delivery systems, bioimaging, and chemosensors.⁵⁴ For example, Chen *et al.* have synthesized a block copolymer bearing *N*-isopropylacrylamide (NIPAM) and spiropyran, providing responsiveness to pH, light, and temperature changes. The polymers can self-assemble into micellar nanoparticles in an aqueous medium. The hydrophobic core is formed by spiropyrans, and there is a hydrophilic shell due to the existence of the NIPAM block. In this study, the encapsulated coumarin-102 loaded into these micellar nanoparticles. When they were subjected to UV illumination, or the medium was acidic, coumarin 102 was released with the dissociation or swelling of the micellar nanoparticles (Scheme 14).⁵⁵



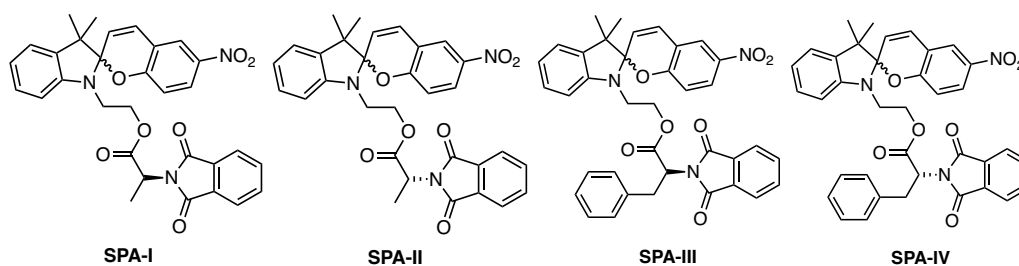
Scheme 14. Schematic illustration of controlled release of coumarin 102

Temperature, pH, and polarity of the environment can induce the isomerization of spiropyrans and alter the spectral properties of these compounds as well. Also, some organic and inorganic molecules contributing to the resonance form of merocyanines can lead to a reversible change in fluorescence or absorbance spectra of merocyanines. Observation of their spectral properties makes the detection of these molecules, metal ions, anions, and even biomolecules possible.⁵⁶ Furthermore, by utilizing the photochromism of spiropyrans, materials used for optical data storage, photoreceptors, and photochromic lenses have been fabricated.³⁰

CHAPTER 2

AIM OF THE STUDY

Spiropyrans are a class of well-known compounds with photoswitching ability. Several studies in literature focus on the synthesis and the photochemistry of indolino-spiropyran derivatives. These compounds possess point chirality with the stereogenic center on the spiro-carbon. However, when external stimuli trigger the isomerization to the corresponding merocyanine form, the optical activity is lost due to the heterolytic cleavage of the bond between spiro-carbon and the oxygen on the pyran ring. Hence, the conversion of the merocyanine back to the spiropyran results in racemization. Although spiropyrans are widely studied in literature, studies on the spiropyrans containing a chiral moiety are limited. With this in mind, in this study, the aim is to incorporate a chiral unit into a spiropyran and to investigate the effect of the chiral center on the configuration of the spiro-carbon after photoisomerization. Towards this goal, spiropyrans containing *D* and *L* enantiomers of alanine and phenylalanine (**SPA-I**, **SPA-II**, **SPA-III**, and **SPA-IV**) derivatives will be synthesized, and their photoisomerization will be studied. Furthermore, ring closing kinetics of these compounds will be investigated to determine the effects of alanine and phenylalanine derived units on the ring-closure.

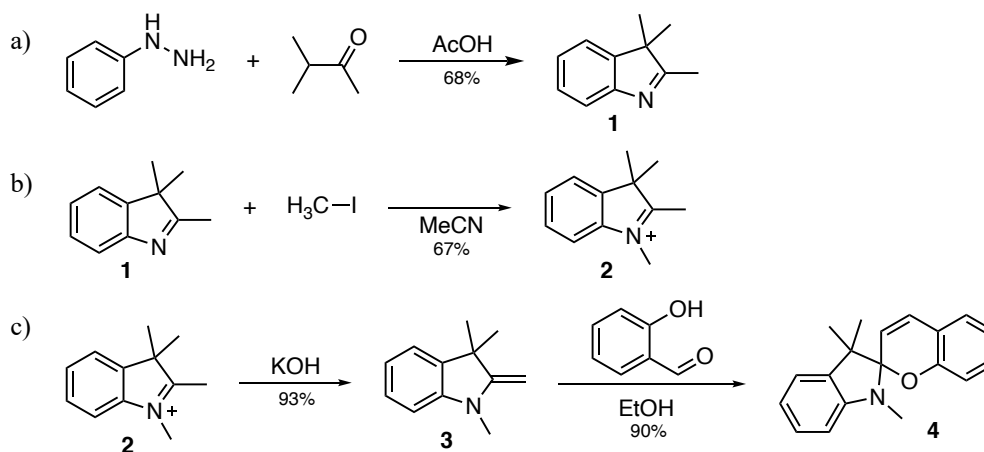


CHAPTER 3

RESULTS AND DISCUSSION

3.1 Preliminary Studies on Spiropyrans

In this study, our goal was to synthesize spiropyrans bearing chiral moieties, and to analyze the effect of this chiral unit on the configuration of spiro carbon after the ring opening and closure. For this purpose, we have studied synthesis of the simplest spiropyran and its spectroscopic properties. Firstly, 2,3,3-trimethyl-3*H*-indole (**1**) was synthesized from phenyl hydrazine and isopropyl methyl ketone (Scheme 15a). The synthesis furnished 2,3,3-trimethyl-3*H*-indole (**1**) in 68% yield. According to ¹H NMR spectrum, the obtained indole derivative was found to be pure enough to be used in the next step without any further purification. Next, compound **1** was treated with iodomethane in acetonitrile to yield Compound **2** in 67% (Scheme 15b). Lastly, compound **3** was obtained as a result of the treatment of compound **2** with the 2 M NaOH solution. Subsequently, compound **3** was reacted with salicylaldehyde in ethanol in order to obtain the target spiropyran in 90% yield (Scheme 15c).



Scheme 15. Synthesis of compound **4**

The characterization of compound **4** was done with ^1H NMR and UV-Vis spectroscopy (Figure 12a-b). The spectroscopic data were consistent with the literature.^{57,58} In ^1H NMR spectrum, the two doublets at 5.6 ppm and 6.8 ppm showed the formation of the spiroopyran form with the coupling constants of 10.4 Hz and 10.5 Hz.

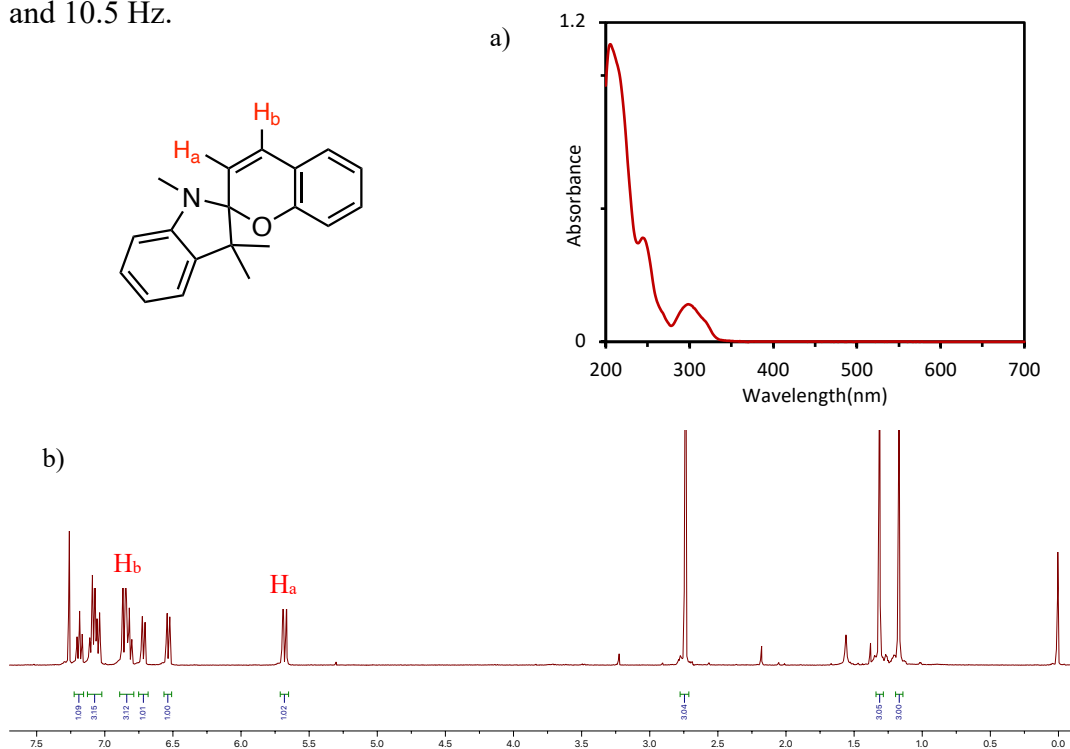
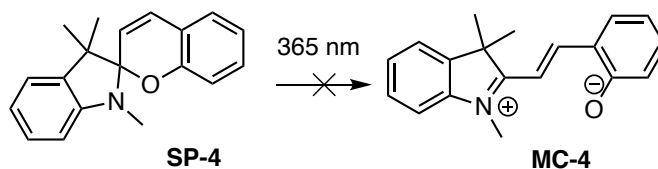


Figure 12. a) ^1H NMR of Compound **4** b) UV-Vis spectrum of Compound **4** (10^{-5} M in acetonitrile)

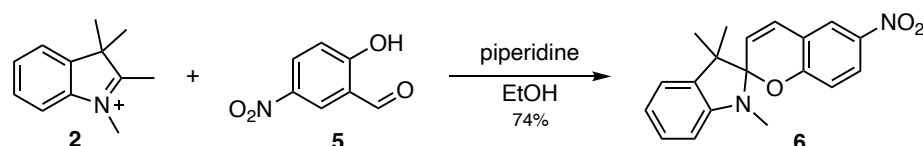
To further expand our experience, we decided to irradiate compound **4** at 365 nm. However, the spiroopyran could not be converted into the corresponding merocyanine form under these conditions (Scheme 16).



Scheme 16. The conversion of compound **4** into the corresponding merocyanine

With the failed result, we decided that the synthesis of the nitro-substituted spiroopyran should be done. The reason for that is the dipole moment in the latter

compound would be better than that of compound **4**, which helps the conversion of nitro-substituted spiropyran into the merocyanine form. Therefore, to synthesize nitro-substituted spiropyran, salicylaldehyde was nitrated with nitric acid to get 2-hydroxy-5-nitrobenzaldehyde (**5**) followed by the treatment with compound **2** in the presence of piperidine and methanol to yield compound **6** in 74% yield (Scheme 17).



Scheme 17. The synthesis of compound **6**

The compound was characterized with ^1H NMR (Figure 13) and UV-Vis spectroscopy. The results were in accordance with those described in literature.⁵⁹

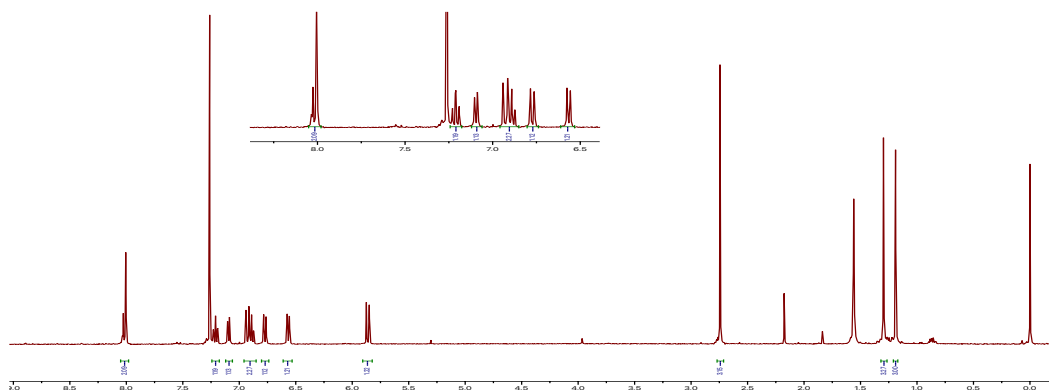


Figure 13. ^1H NMR spectrum of compound **6**

Compound **6** was loaded to chiral HPLC. As expected, two peaks on the chromatogram (fifty-fifty to each other) appeared, which are the enantiomers of each other (Figure 14). This result showed us the HPLC could be a good method to monitor stereoselectivity of such compounds.

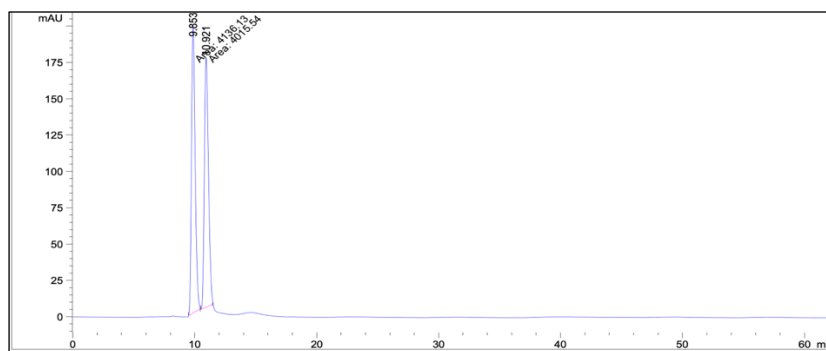


Figure 14. HPLC chromatogram of compound **6** (Chiralcel OD-H, eluent 90:10 n-Hexane:*i*PrOH, flow rate 1.0 ml/min, t_R : 9.8, 10.9 min)

The photoisomerization of compound **6** to the merocyanine form was studied. First, UV-Vis spectrum of compound **6** was measured (Figure 15). It was found that irradiating compound **6** at 365 nm will convert it into the merocyanine form. Compound **6** was exposed to 365 nm light. Then, UV-Vis measurement on the resulting solution showed a new absorption band at λ_{\max} 556 nm which is due to the merocyanine form. Furthermore, such observation was seen upon addition of nitric acid which shows that the compound is acidochromic as well (Appendix E).⁴⁸

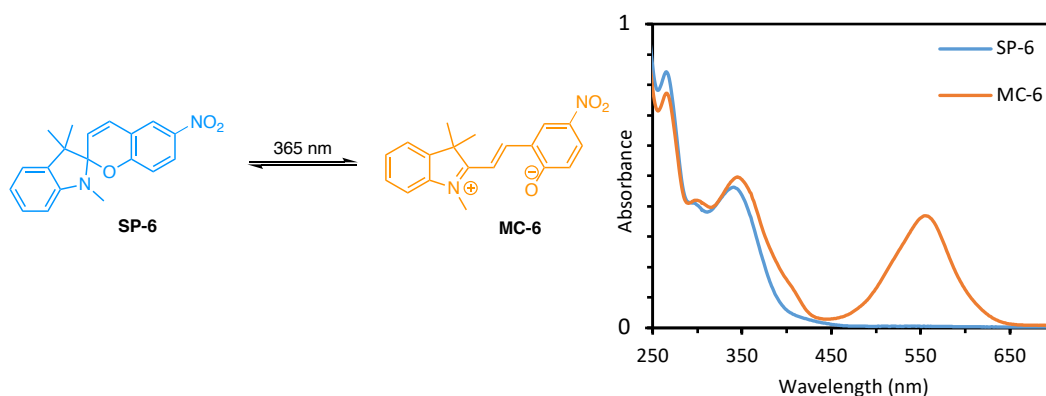


Figure 15. UV-Vis spectrum of compound **6** (10^{-5} M) in acetone and after irradiating with 365 nm light for 2.5 min

3.2 Synthesis of the Spiropyrans Containing a Chiral Moiety

With the experience on spiropyran synthesis and photochemical studies, we decided to synthesize a spiropyran dimer linked through a moiety derived from tartaric acid

(Figure 16). The moiety will provide a chiral environment. Therefore, when the racemic spiropyran unit opens to the merocyanine which closes back to the spiropyran would be stereoselective.

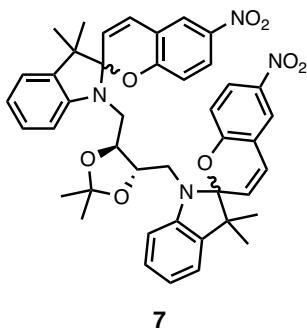
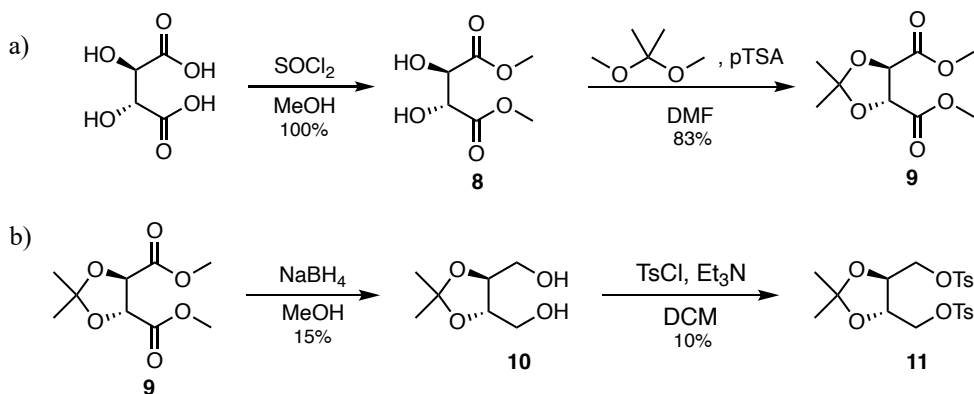


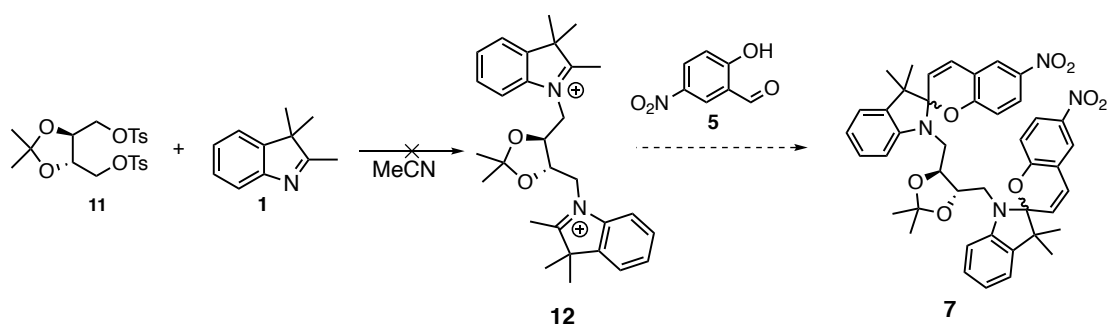
Figure 16. The designed spiropyran containing chiral moiety derived from tartaric acid

The linker unit synthesis started with *L*-tartaric acid esterification. Diol unit on compound **8** was then protected with 2,2-dimethoxypropane in DMF (Scheme 18a). Compound **9** was reduced to diol **10** with sodium borohydride in methanol. Afterwards, compound **10** was tosylated to get ditosyl **11** as depicted in Scheme 18b.



Scheme 18. Synthesis of compound **11**

Previously, it was shown that indoline **1** reacted with iodomethane through S_N2 reaction. With this in mind, ditosyl **11** was treated with compound **1** in acetonitrile as shown in the Scheme 19. The expected product (**12**) was not observed. The reaction was monitored with TLC for 2 days and did not proceed as we expected. Then, the synthesis of the target compound **7** was abandoned.



Scheme 19. Synthetic pathway for compound **7**

The failure of the synthesis of compound **7** led us to think that the dimer formation would be problematic. Therefore, we turned our attention to monotosylated *D*-ribose unit and designed compound **13** as shown in the Figure 14.

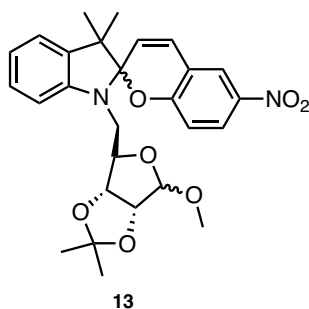
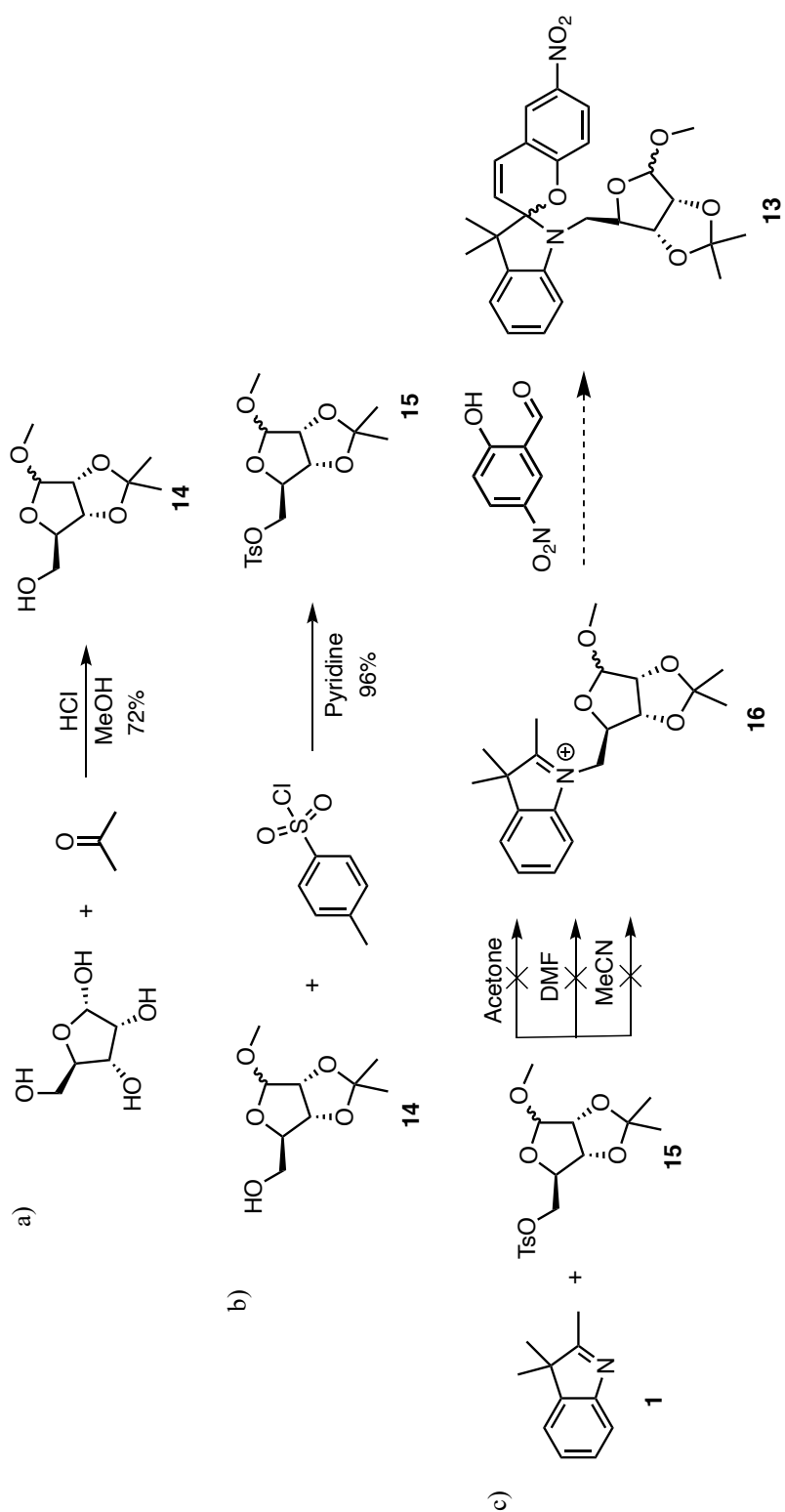


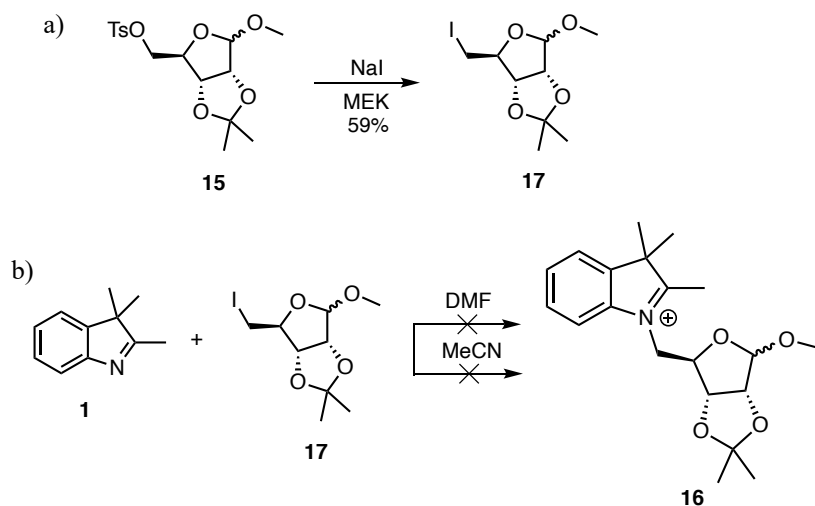
Figure 17. The spirocyclic containing chiral moiety derived from *D*-ribose

The synthesis of the chiral moiety started with the diol protection of *D*-ribose and methyl glycoside of it. *D*-ribose was treated with acetone and methanol mixture in the presence of HCl solution to get methyl 2,3-O-isopropylidene- β -*D*-ribofuranoside (**14**) in 72% yield (Scheme 20a). The hydroxy at position 5 was then tosylated in pyridine (Scheme 20b). The tosylated compound **15** was treated with compound **1** in acetonitrile. The desired product formation was not observed (Scheme 20c). Then, the same reaction was carried out in DMF and acetone. In these solvents, the product **13** did not form either. With these results, it was thought that tosyl group is not that active to drive the reaction forward.



Scheme 20. Synthetic route for compound **13**

The iodinated compound **17** synthesized from the tosylated compound **15** as shown in Scheme 21a. Iodinated compound **17** was then treated with the compound **1**. Both in DMF and MeCN, the reaction did not proceed to furnish desired compound **16**. The reason that the reaction did not work might be due to the steric hindrance of the neighboring carbon.⁶⁰



Scheme 21. Alternative way for the synthesis of compound **16**

With the failed results accounted for the steric hindrance attributed to the groups next to the reactive carbon, we decided to attach a group having functional group, that will be suitable for further modification, to indoline (**1**). Bromoethanol was found to be perfect fit for this purpose. Therefore, four new compounds were designed as seen in Figure 18. The designed compounds will have the chirality due to the two amino acids. Both enantiomers of the amino acids will be attached. Alanine and phenylalanine are distinct from each other by a phenyl group. With these target compounds, we will not only study the effect of chirality on the spiro carbon configuration, but also ring opening and ring closure kinetics of alanine and phenyl alanine attached spiropyrans will be compared in order to investigate the effect of benzyl and methyl groups on these processes.

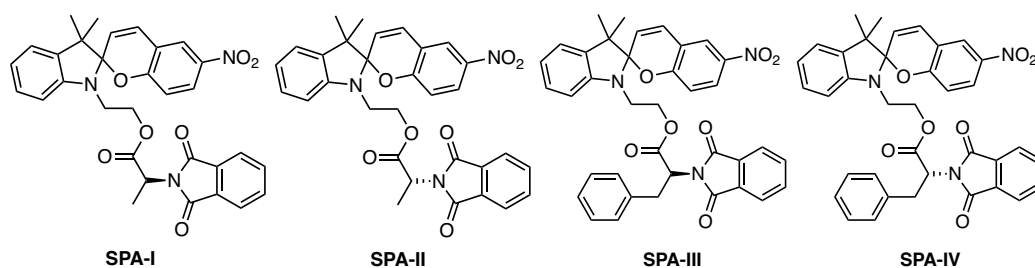
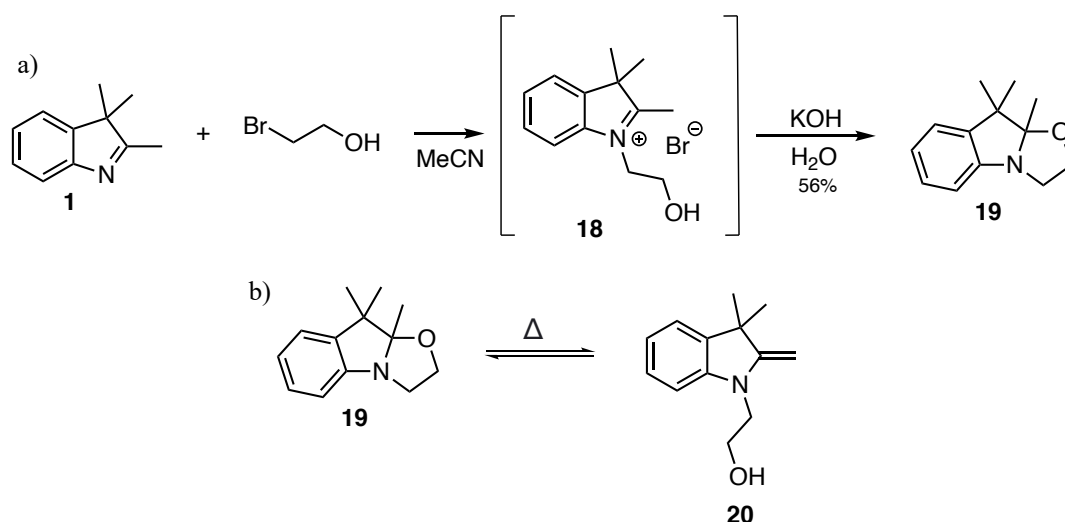


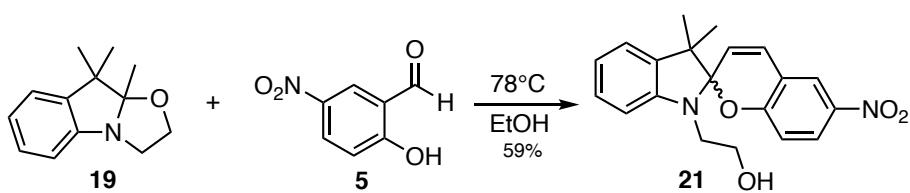
Figure 18. The target compounds; **SPA-I**, **SPA-II**, **SPA-III**, and **SPA-IV**

Towards the synthesis of the new targets, indoline was treated with bromoethanol (Scheme 22a). In this reaction, we expected compound **20**. However, it was not isolated. Upon addition of potassium hydroxide solution, compound **19** was isolated in 56% yield. Hemiaminal ethers can undergo a transformation into enamine as shown in Scheme 22b.



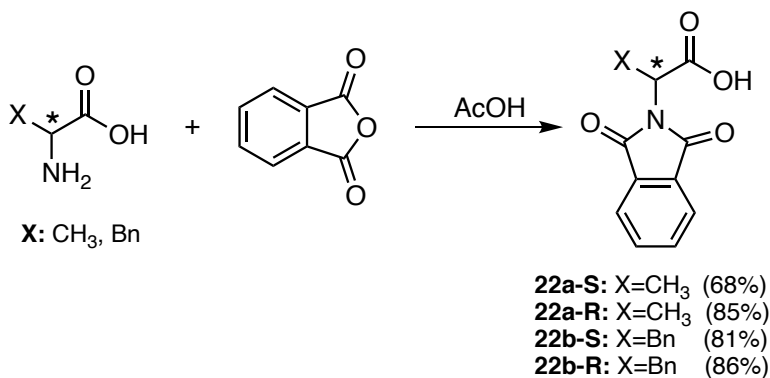
Scheme 22. Synthesis of Compound **19**

Afterwards, compound **19** was treated with 5-nitrosalicylaldehyde (**5**) in ethanol at 78°C. The reaction yielded compound **21** in 59% yield (Scheme 23). This compound would be further modified through alcohol functionality.



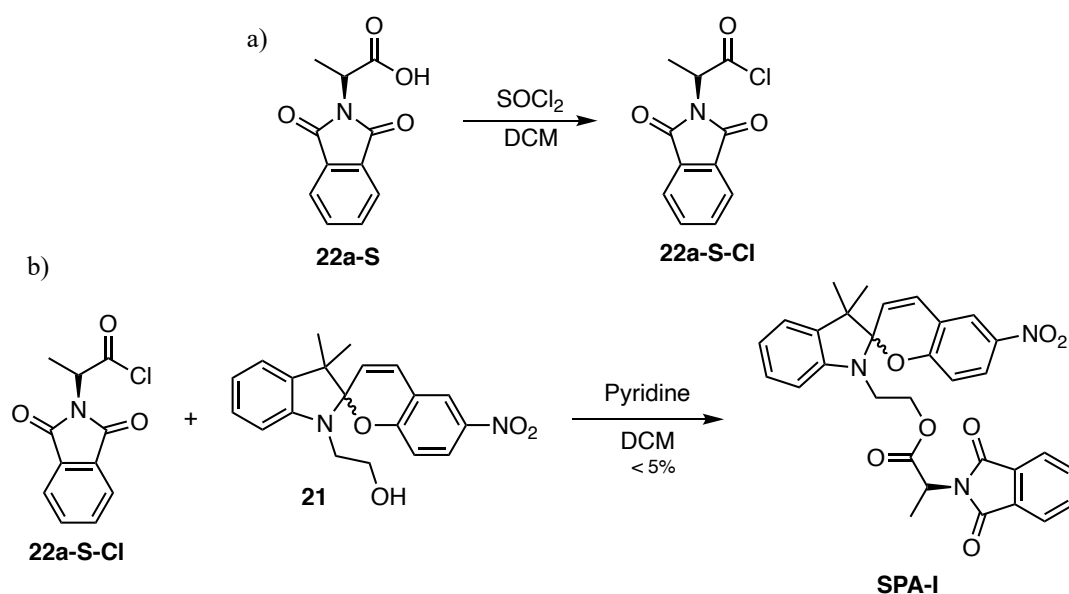
Scheme 23. Synthesis of compound **21**

Both enantiomers of phenylalanine and alanine were treated with phthalic anhydride to protect the amino group (Scheme 24). Phthalimides will contribute to the steric hindrance, which would affect the chiral center on spiropyrans. Furthermore, ease of procedure without racemization could be another reason for choosing phthalic anhydride.



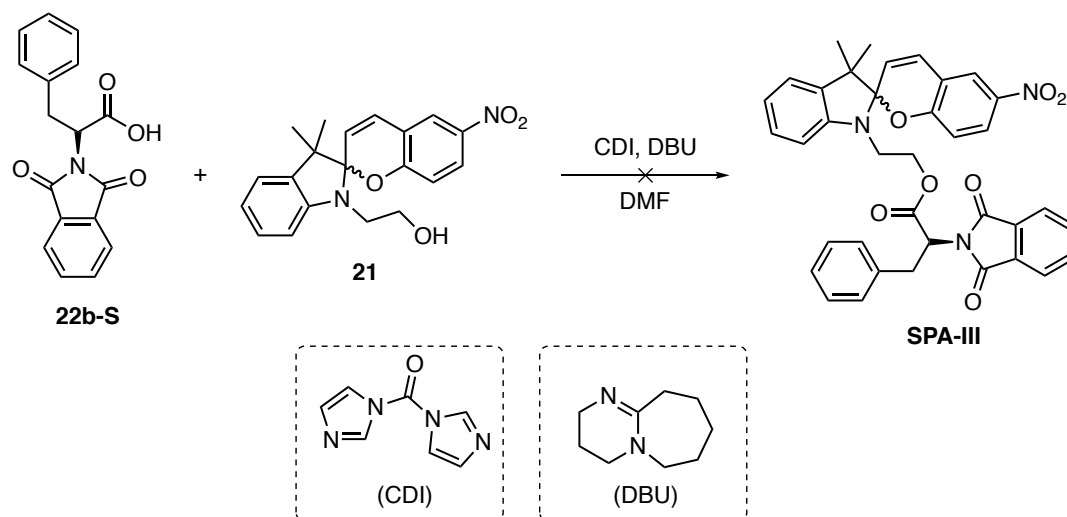
Scheme 24. Amino protection of both enantiomers of alanine and phenylalanine

The amino protected *L*-alanine was modified to the corresponding acyl chloride with the action of thionyl chloride as shown in Scheme 25a. Then, compound **22a-S-Cl** was treated with compound **21** to get esterification product **SPA-I** (Scheme 25b). Even though **SPA-I** was obtained from the reaction, the yield was less than 5%. The low yield is accounted for the high reactivity of the corresponding acyl chloride. The coupling reactions are alternative to the acyl chloride esterification procedure.



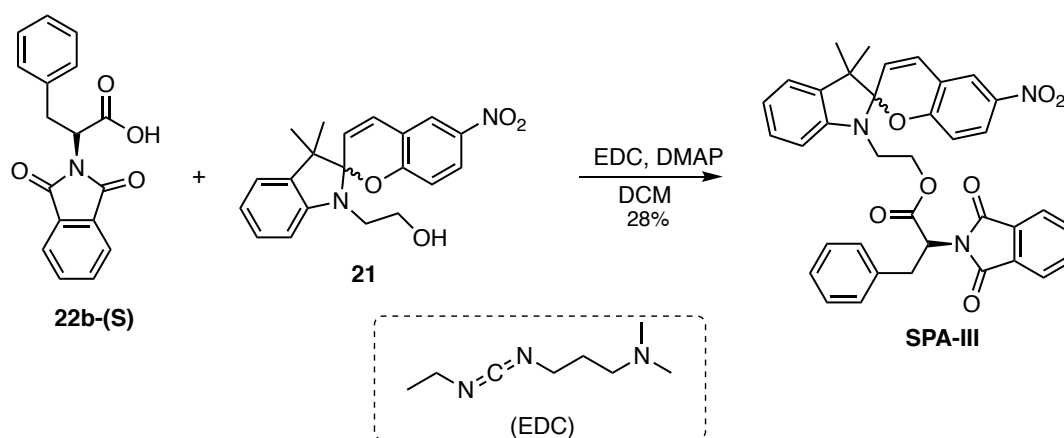
Scheme 25. Synthesis of **SPA-I** through acyl chloride esterification procedure

The first coupling reaction employed in our study was to esterification reaction with CDI due to its relatively simple work-up conditions. Compound **21** and **22b-S** were dissolved in DMF and subsequently CDI and DBU were added (Scheme 26). The reaction was stirred at 85°C for approximately 24 hours, which was monitored with TLC. After 24 hours, the product formation was not observed.



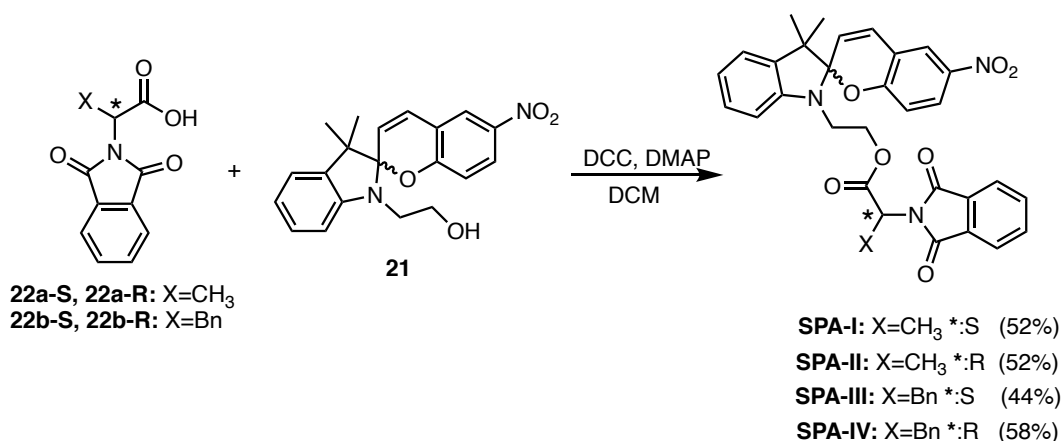
Scheme 26. Synthesis of **SPA-III** through CDI coupling procedure

The same reaction was carried out by adopting EDC coupling procedure to the synthesis of **SPA-III** as seen in Scheme 27. Amino protected *L*-phenylalanine **22b-S** was treated with compound **21** in the presence of EDC (free base form) in DCM. DMAP was used as a base in this reaction. After 24 hours, TLC showed the product formation. However, the starting materials were not consumed fully. Nevertheless, the desired compound was isolated in 28% yield.



Scheme 27. Synthesis of **SPA-III** through EDC coupling procedure

Even though DCC coupling is cumbersome, its cost efficiency was attractive. Therefore, we decided to synthesize the target compounds implementing DCC coupling procedure. Amino protected amino acids **22a-S**, **22a-R**, **22b-S**, and **22-R** with compound **21** in the presence of DCC and DMAP in DCM to get the desired compounds (Scheme 28). The final compounds were isolated after performing column chromatography several times. This was due to the difficulty of separating *N*-*N'*-dicyclohexylurea from the products. Nevertheless, all the desired compounds were in hand characterized with ^1H , ^{13}C NMR and HRMS successfully (Appendices A and C).



Scheme 28. Synthesis of SPA-I, SPA-II, SPA-III, and SPA-IV

3.3 Photophysical and Photochemical Studies

3.3.1 UV-Vis Spectroscopy Studies

UV-Vis spectra of all spiropyrans were measured in methanol, isopropanol, dichloromethane and hexane. These solvents were chosen due to their different dielectric constants, which will affect the transformation of the spiropyrans into the corresponding merocyanine forms.²⁹ The ground state of the merocyanine includes its zwitterionic form, and thus, it is expected to be stabilized in polar solvents. All compounds showed similar features on their spectra.

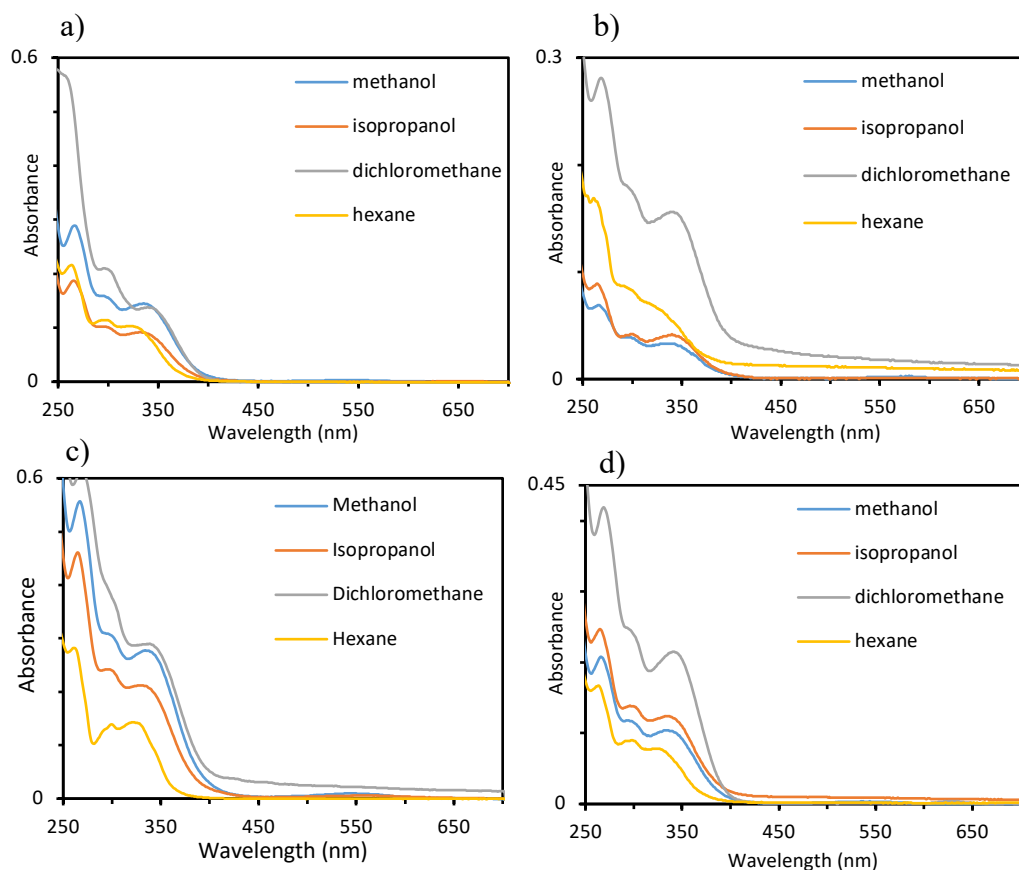
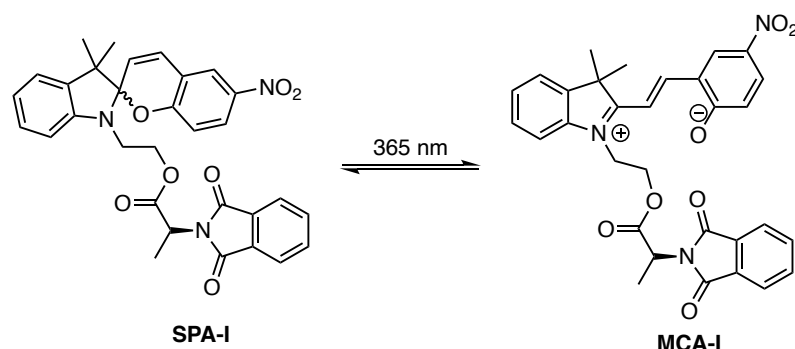


Figure 19. UV-Vis spectra of a) SPA-I b) SPA-II c) SPA-III d) SPA-IV (10^{-5} M) in different solvents prior to 365 nm illumination

As seen in the Figure 19, the spiropyrans containing both enantiomers of alanine and phenylalanine derivatives showed a λ_{max} around 340 nm. This band extended to 400 nm, which is due to the spiropyran form. According to the first law of photochemistry, any light with wavelength less than 400 nm will convert the spiropyrans into the merocyanic form. With the availability of the 365 nm light source, we conducted the studies on the photoisomerizations of SPA-I, SPA-II, SPA-III and SPA-IV in different solvents. The concentrations of all spiropyrans in methanol, isopropanol, dichloromethane, and hexane were set to 10^{-5} M, and irradiated for 2, 6, 12, 20, and 30 minutes with 365 nm light.

3.3.1.1 UV-Vis Spectroscopy Studies of SPA-I



Scheme 29. Photoisomerization of SPA-I to MCA-I

For SPA-I in methanol, it was shown that there is no significant increase in the intensity of the merocyanine absorption band around 550 nm after 20 minutes illumination (Figure 20a). In isopropanol, λ_{max} of merocyanine form shifted to *ca.* 570 nm. With the irradiation, MCA-I concentration in the solution increased (Figure 20b).

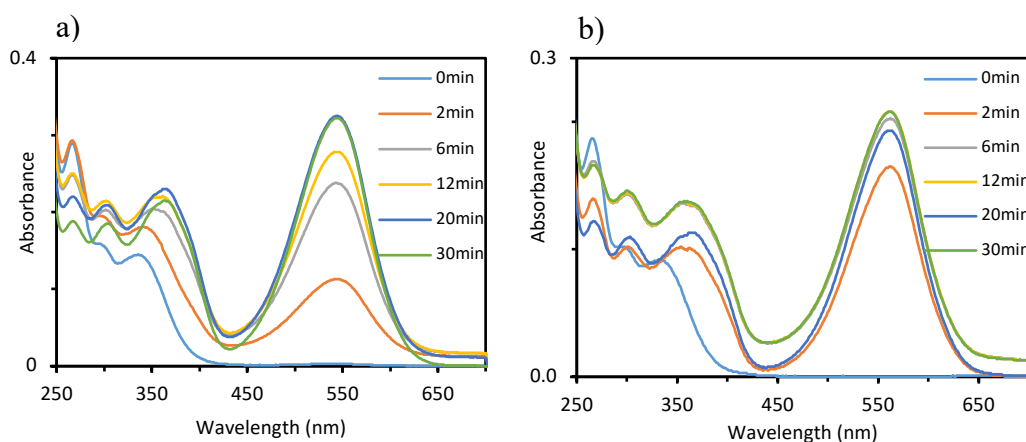


Figure 20. UV-Vis spectra of SPA-I (10^{-5} M) in a) methanol b) isopropanol

Upon 365 nm illumination in dichloromethane, it was observed that there is no significant increase in the merocyanine concentration after 6 minutes, and it started to decrease after 12 minutes irradiation (Figure 21a). Besides, with the illumination, a new absorption band in *ca.* 430 nm appeared. The intensity of this absorption band increased as the time of the irradiation increases. The possible explanation may be

the presence of the excited state isomers of **MCA-I**. In hexane, contrary to expectations, the merocyanine form of the **SPA-I** was observed (Figure 21b). After 6 minutes illumination, it was seen that the intensity of merocyanine absorption band around 580 nm started to decrease. This could be due to both the spiropyran and merocyanine forms not having great solubility in hexane. Therefore, spiropyran molecules in hexane were close to the interface between hexane and the walls of the quartz cell. When they were irradiated, the merocyanine was formed and stuck to the walls of the quartz cell. This observation was further seen when we transferred the solution from the cells to another container. The quartz cell was purple colored after the analysis.

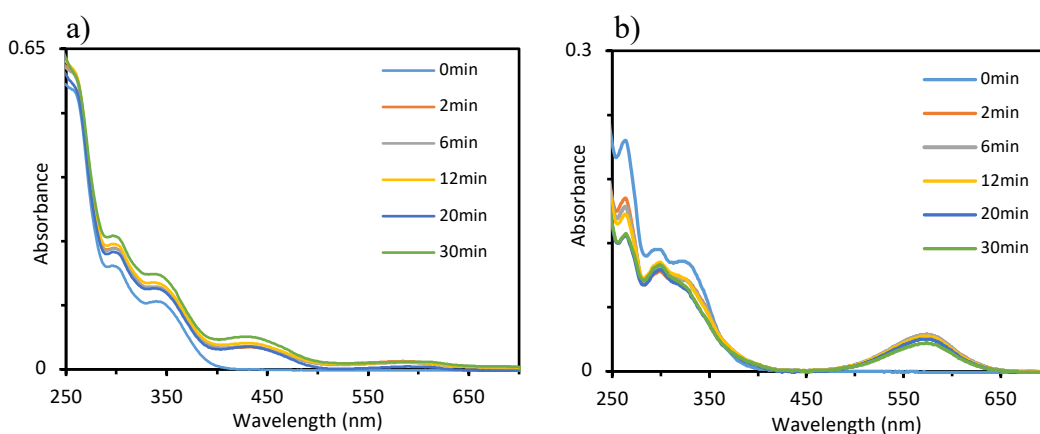
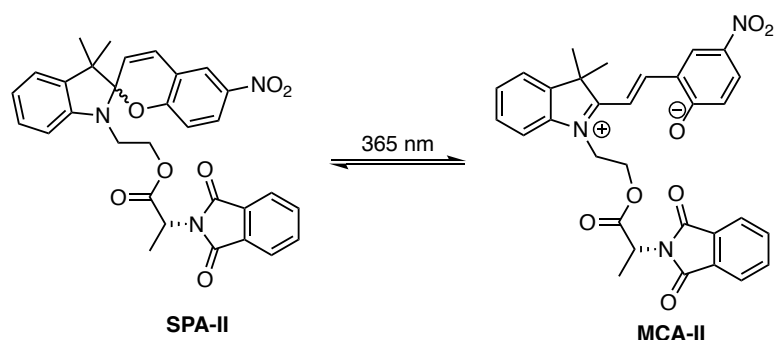


Figure 21. UV-Vis spectra of **SPA-I** in (10^{-5} M) a) dichloromethane b) hexane

It can be concluded that the conversion of **SPA-I** into the merocyanine was smooth in methanol and isopropanol. However, in aprotic solvents such as dichloromethane and hexane, the conversion of this compound was not smooth. This could be explained by the stabilization of the merocyanine by the polar protic solvents. In addition, it was observed that polarity of the solvent increases, the absorption band of the merocyanine form shifts to the longer wavelengths.

3.3.1.2 UV-Vis Spectroscopy Studies of SPA-II



Scheme 30. Photoisomerization of SPA-II to MCA-II

SPA-II solution in methanol showed similar features with SPA-I (Figure 22a). As the solution was irradiated with 365 nm light (Scheme 30), the merocyanine concentration (MCA-II) in the solution increased. However, there was no significant increase in the merocyanine absorption intensity after 20 minutes irradiation. In isopropanol, MCA-II concentration reached its maximum with 12 minutes irradiation and then started to decrease (Figure 22b).

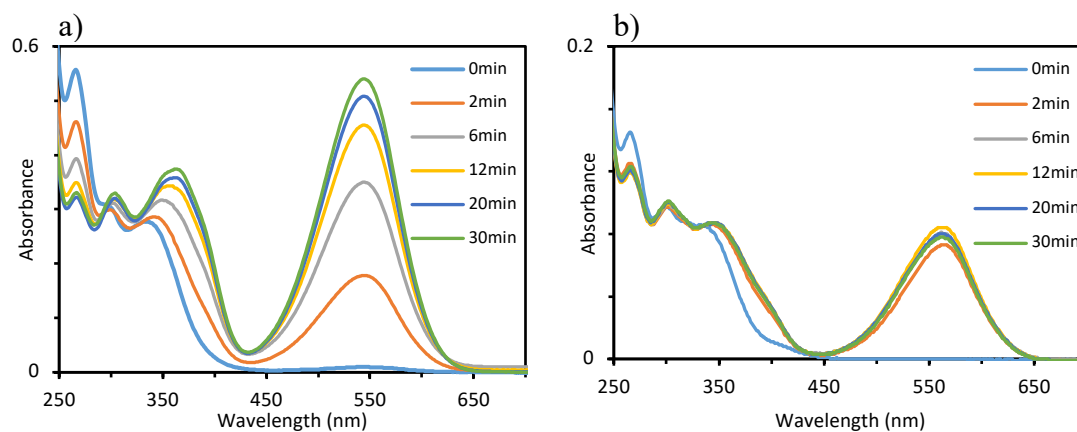


Figure 22. UV-Vis spectra of SPA-II (10⁻⁵ M) in a) methanol b) isopropanol

Similar with SPA-I, a shoulder around 440 nm was observed in dichloromethane and there was no significant increase in the concentration of MCA-II after 2 minutes irradiation. When SPA-II was subjected to 365 nm illumination, the concentration

of **MCA-II** in the solution reached its maximum and started to decline after 2 minutes.

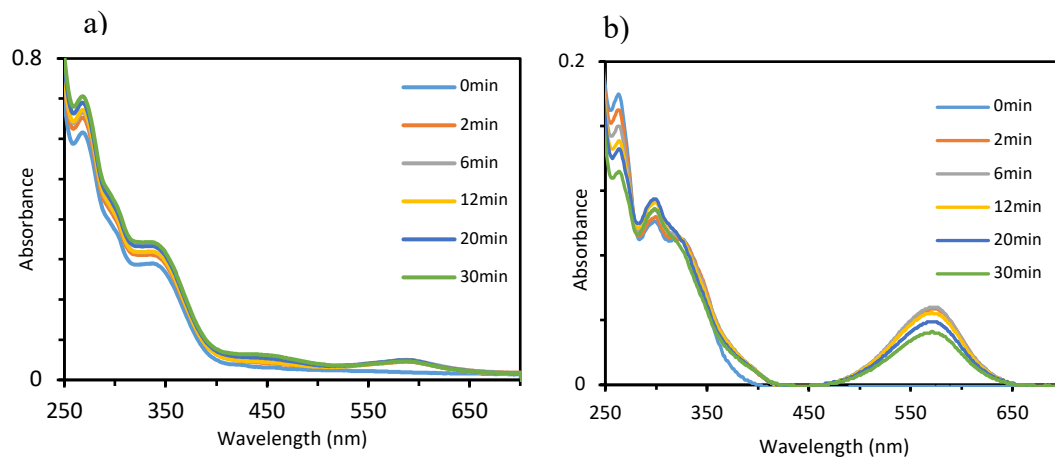
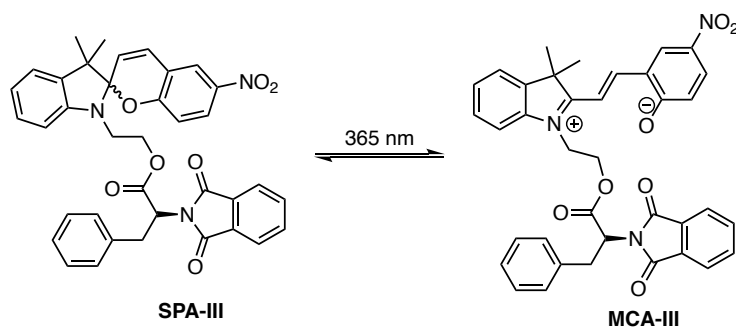


Figure 23. UV-Vis spectra of **SPA-II** in (10^{-5} M) a) dichloromethane b) hexane

3.3.1.3 UV-Vis Studies of SPA-III



Scheme 31. Photoisomerization of **SPA-III** to **MCA-III**

In methanol, the absorption intensity of the merocyanine form increased with the increased irradiation time (Figure 24a). Unlike methanol, the concentration of **MCA-III** in isopropanol started to decrease after 12 minutes illumination as shown in Figure 24b.

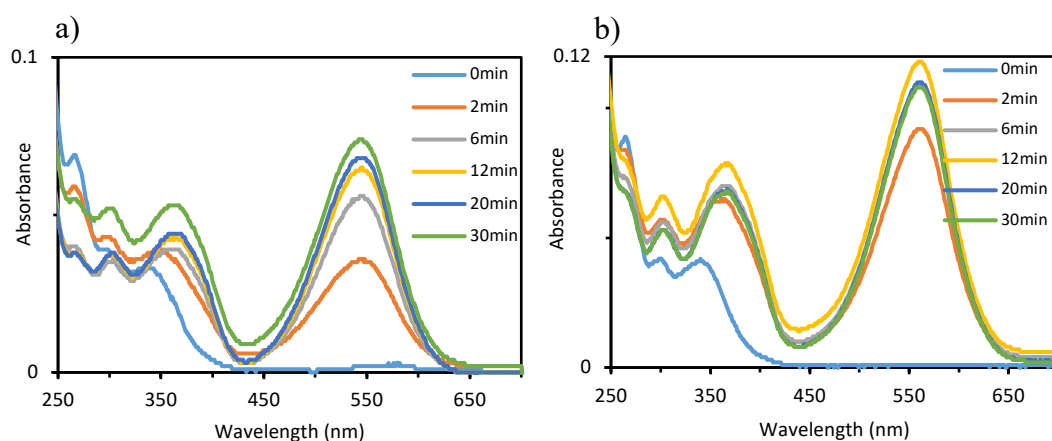


Figure 24. UV-Vis spectra of SPA-III (10^{-5} M) a) methanol b) isopropanol

In dichloromethane, the absorption of the excited state MCA-III isomers is more apparent around 460 nm (Figure 25a). When the exposure time increased, the merocyanine absorption intensity *ca.* 600 nm decreased, which was accompanied by the increase in absorption around 460 nm (Figure 25b). In hexane, there was no significant increase in the concentration of the merocyanine form after 12 minutes as in the case of MCA-II.

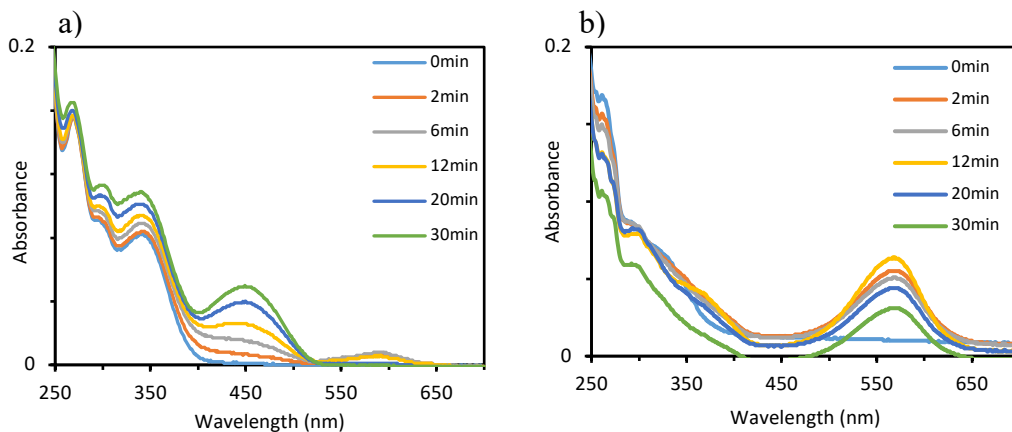
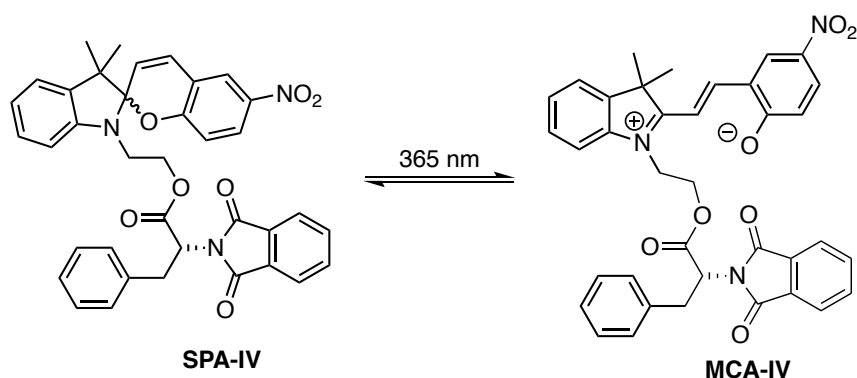


Figure 25. UV-Vis spectra SPA-III (10^{-5} M) a) dichloromethane b) hexane

3.3.1.4 UV-Vis Studies of SPA-IV



Scheme 32. Photoisomerization of SPA-IV to MCA-IV

In methanol and isopropanol, contrary to the expectations, the MCA-IV absorption intensity decreased after 20 minutes illumination (Figure 26a-b). The decrease in intensity was more pronounced in methanol.

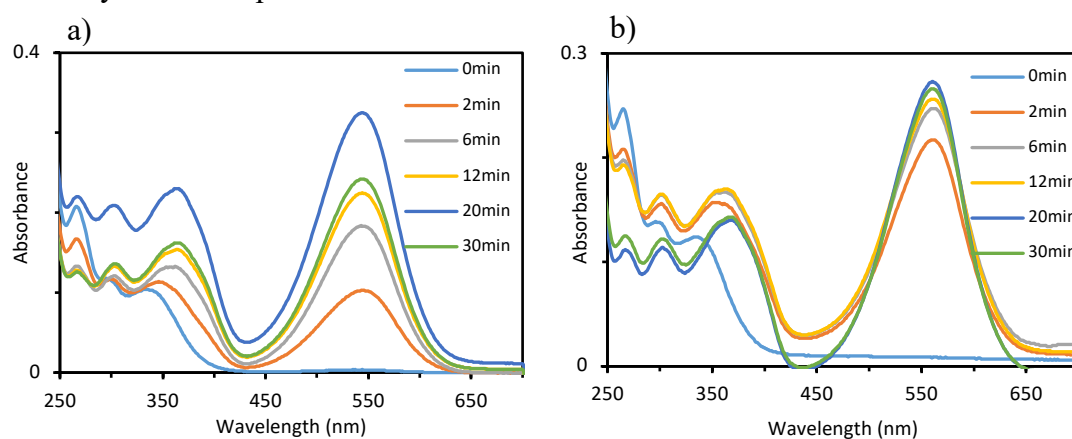


Figure 26. UV-Vis spectra of SPA-IV (10⁻⁵ M) a) methanol b) isopropanol

In dichloromethane and hexane, SPA-IV solutions showed similar feature with SPA-III (Figure 27a-b).

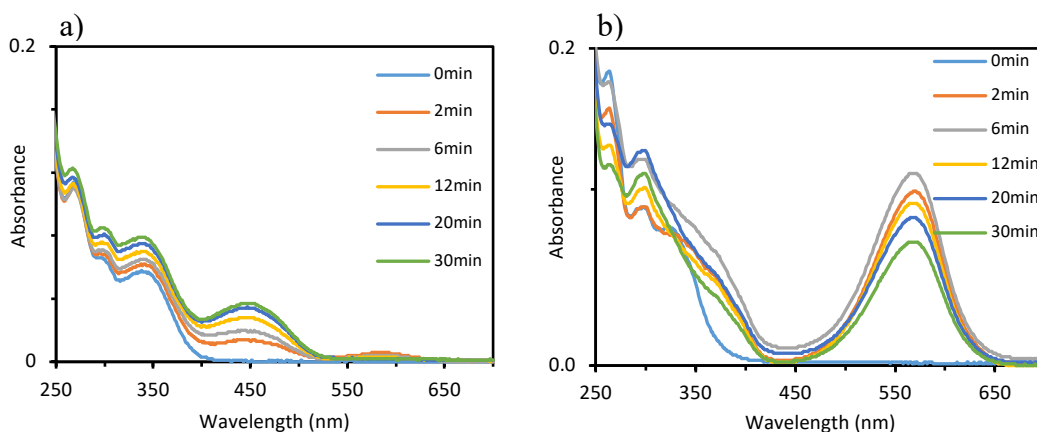


Figure 27. UV-Vis spectra of SPA-IV (10^{-5} M) a) dichloromethane b) hexane

3.3.2 Kinetics of Ring Closure

With studies on photoisomerization of the spiropyrans in hand, we investigated the transformation of the merocyanines into spiropyrans. The focus of this study is to examine whether attached alanine and phenylalanine derivatives alter the spectroscopic properties and switching behavior of compound **21**. We chose to conduct this experiment in isopropanol due to the fast kinetics of ring opening. Furthermore, the solubilities of the compounds in isopropanol are better compared to dichloromethane and hexane and toxicity of methanol led us consider isopropanol as the solvent of choice.

Both *D*-phenylalanine and *L*-phenylalanine derived compounds were considered to behave similarly. Therefore, we chose one of the compounds for the survey. Likewise, the same was applied to the spiropyrans containing alanine derivative.

Compound **21**, SPA-II and SPA-IV were subjected to 365 nm for 15 minutes and then UV-Vis spectra were taken to observe the corresponding merocyanine forms. Afterwards, MCA-21 was kept in dark for 15 minutes and MCA-II and MCA-IV were kept in dark for 10 minutes. UV-Vis spectra were recorded in one minute intervals, as shown in Figure 28. It was observed that the concentrations of the corresponding merocyanine forms decrease with the time (Figure 28). After 10 minutes, MCA-II and MCA-IV turned back to the spiropyran forms completely. On

the other hand, **MC-21** was not fully converted into compound **21**. The difference between their ring closure kinetics is more pronounced in 6 minutes.

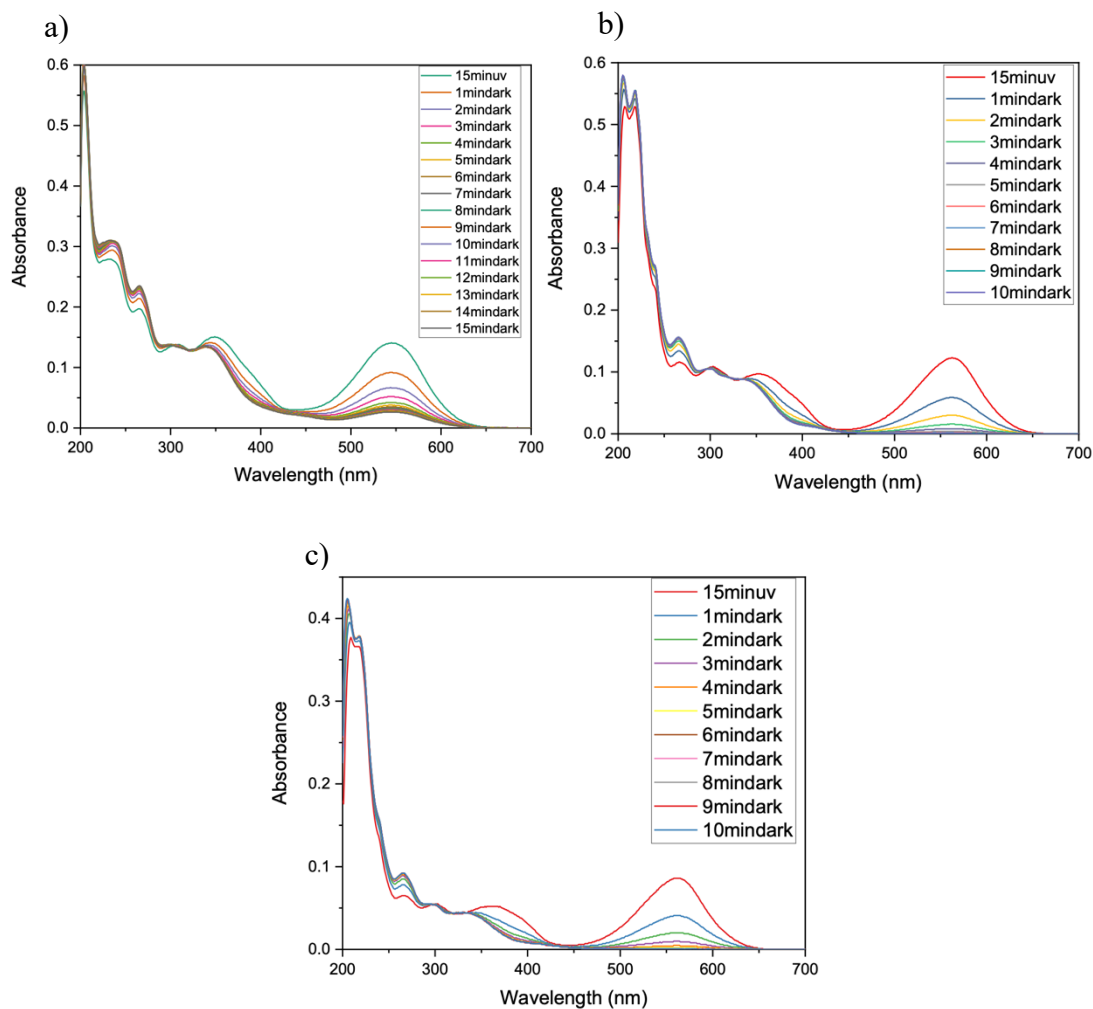
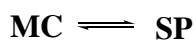


Figure 28. Studies on ring-closure of a) Compound **21** b) SPA-II and c) SPA-IV

All compounds showed first order kinetics in the conversion of the merocyanines into the spiropyrans.



$$-\frac{d[\text{MC}]}{dt} = \frac{d[\text{SP}]}{dt} = k[\text{MC}]$$

$$\frac{d[\text{MC}]}{dt} = -k[\text{MC}]$$

$$\int_{[MC]_0}^{[MC]_t} \frac{d[MC]}{[MC]} = -k \int_0^t dt$$

$$[\ln[MC]_t - \ln[MC]_0 = -k [t - 0]$$

$$\ln \frac{[MC]_t}{[MC]_0} = -kt$$

$$\frac{[MC]_t}{[MC]_0} = e^{-kt}$$

$$[MC]_t = [MC]_0 e^{-kt}$$

Concentration is directly proportional to absorbance as stated in Beer's Law. Accordingly, the absorbance versus time graphs for the compounds were drawn by fitting the absorbance values at $\lambda_{\max}=561$ nm to the equation 1. In this equation, **a** is the absorbance value at t=0, **k** is the rate constant, **t** is the time and **b** is the baseline offset (Figure 29).

$$y = ae^{-kt} + b$$

Equation 1

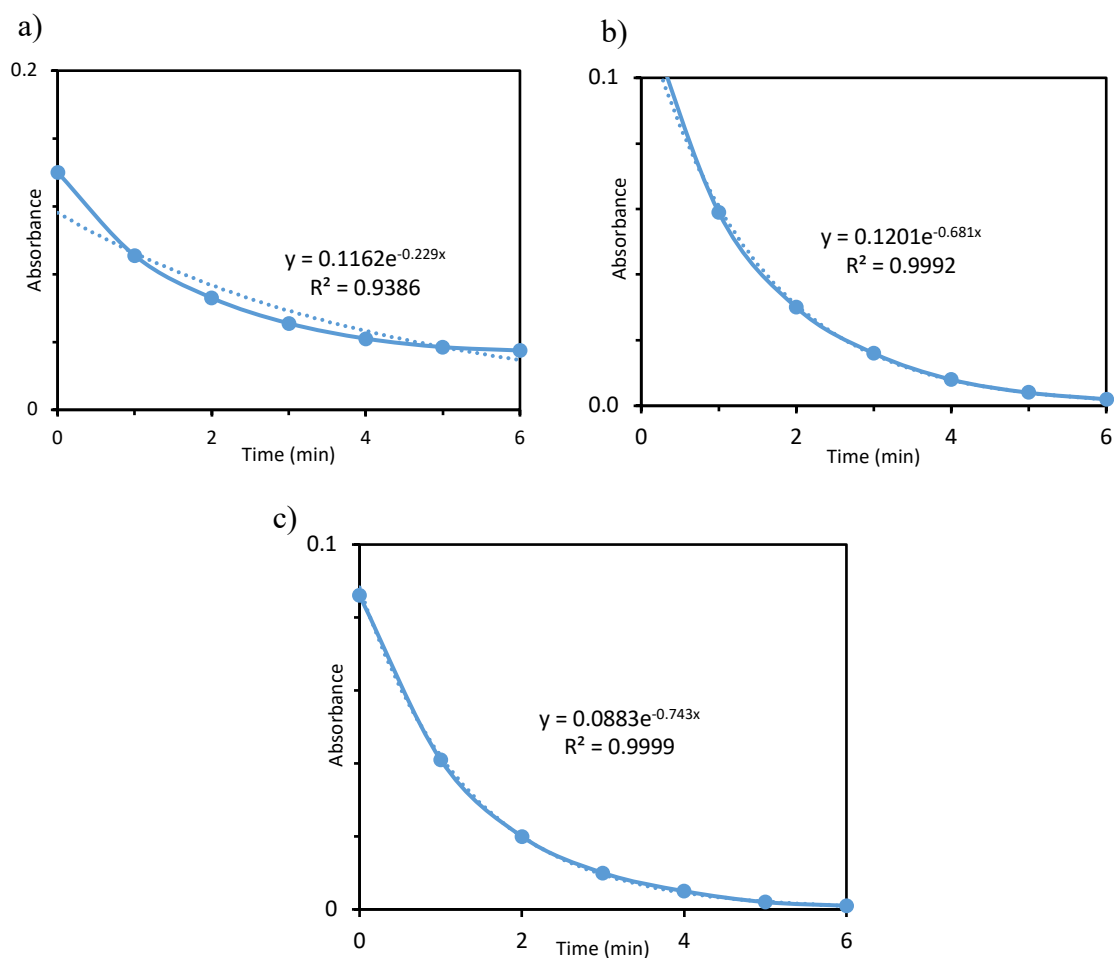


Figure 29. Ring closure kinetics of a) Compound **21** b) SPA-II c) SPA-IV with the exponential fitting

According to the first order rate constants ($k_{MC-21}=0.229 \text{ s}^{-1}$, $k_{MCA-II}=0.681 \text{ s}^{-1}$ and $k_{MCA-IV}=0.743 \text{ s}^{-1}$), it was shown that the merocyanines form of both alanine and phenylalanine derived spiropyrans are converted into their initial state (the spiropyran form) faster at room temperature. It was further seen that among those alanine and phenylalanine attached merocyanines, the one with phenylalanine closes faster. This may arise from due to the fact that benzyl group contributes the hydrophobicity compared to the methyl group. Hydrophobic groups on charged molecules probably create a micro hydrophobic environment, which destabilizes the charge formation. Therefore, chargeless spiropyran forms were favored.

3.3.3 CD Measurements

CD measurements of **SPA-I**, **SPA-II**, **SPA-III**, and **SPA-IV** were performed. CD spectra of these compounds in isopropanol (10^{-3} M) are shown in Figure 30a. The CD spectra of the spiropyrans with *L* and *D*-alanine derivatives are symmetric, as expected, to each other. The CD activity was observed in the region of UV absorption band. Similarly, the CD spectra of *L* and *D*-phenylalanine derived spiropyrans were also measured. Again, the CD spectra are symmetric with respect to each other (Figure 30b).

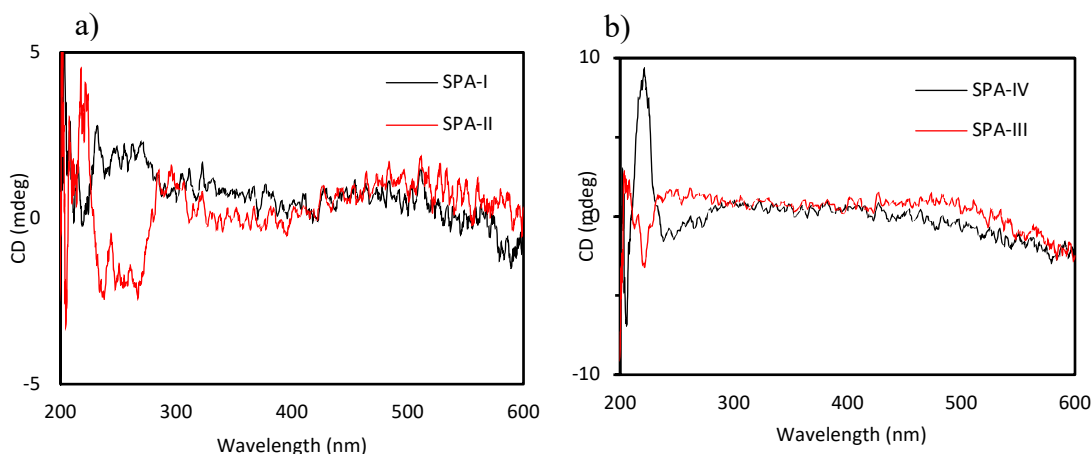


Figure 30. CD spectra of **SPA-I**, **SPA-II**, **SPA-III**, **SPA-IV** in isopropanol

To determine if the chiral unit on the molecule has an effect on the merocyanine form, we subjected the spiropyrans **III** and **IV**, which have *L* and *D* phenylalanine derivatives, to 365 nm light. Both compounds showed similar pattern at around 500 nm. Specifically, they had positive CD signal *ca.* 500 nm. In the region below 300 nm, their CD spectra are symmetric to each other. It can be concluded that the chirality transfer to the chromophore (merocyanine form) was not observed.

3.3.4 Fluorescence Studies

Fluorescence measurements of the spiropyrans (**SPA-I**, **II**, **III**, and **IV**) were attempted. The problem observed was that when we excite the spiropyrans, they are

converted into the merocyanine form, and thus, we observed fluorescence due to the the *transoid* merocyanine forms of these compounds in isopropanol. The fluorescence spectra are given in Appendix D.

3.4 HPLC Studies

HPLC studies were conducted to observe the ratio between diastereomers of the spiropyrans after photoisomerization. Firstly, compound **21** as a reference compound was loaded to HPLC equipped with a chiral column. The ratio between the enantiomers of Compound **21** was observed to be fifty-fifty (Figure 31).

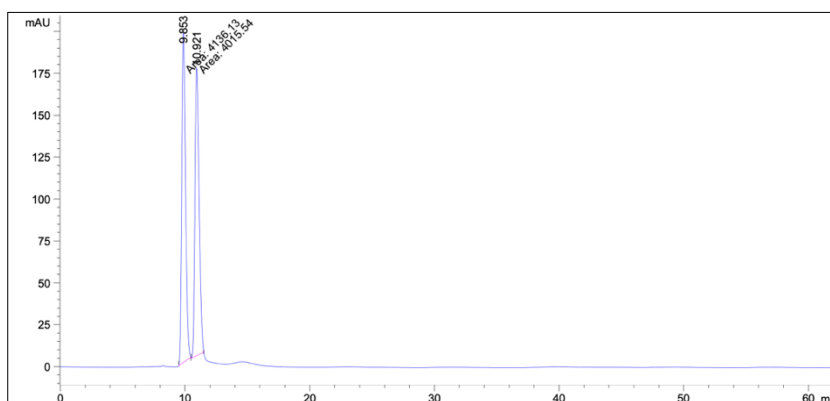


Figure 31. HPLC chromatogram of compound **21** (Chiralcel OD-H, eluent 90:10 n-hexane:isopropanol, flow rate 1.0 mL/min, t_R :9.8, 10.9)

With the analysis of the enantiomers using a chiral column, we decided to analyze the spiropyrans by using a reversed phase achiral column in the first place. The reason was that the spiropyrans synthesized in this study were obtained to be a diastereomeric mixture. The diastereomers would have a different affinity to the nonpolar stationary phase since their physical properties are different. Accordingly, **SPA-II** was loaded to achiral C18 column. However, the separation of the diastereomers could not be observed (Figure 32), which is ascribed to the fact that the polarity difference between the diastereomers is too small to be monitored.

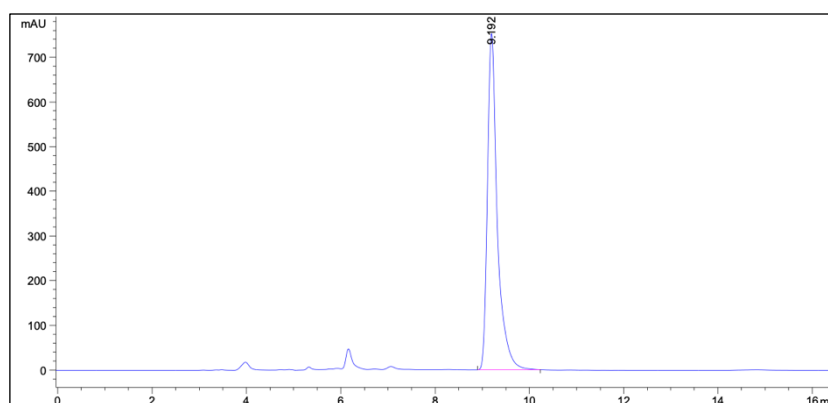


Figure 32. HPLC chromatogram of **SPA-II** (Phenomenex ODS C18, eluent 90:10 methanol:water, flow rate 1.0 mL/min, t_R : 9.2)

With these in mind, chiral OD-H column was attempted to separate the diastereomers (Figure 33). It was concluded that there is no significant difference between the ratio of the diastereomers after photoisomerization.

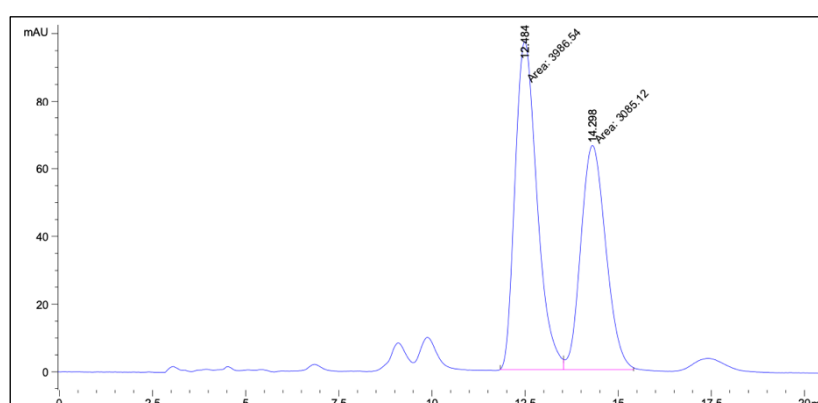


Figure 33. HPLC Chromatogram of **SPA-II** (Chiralpak OD-H, eluent 75:25 hexane:isopropanol, flow rate 1.0 mL/min, t_R : 12.4, 14.9)

CHAPTER 4

CONCLUSION

In this thesis, chiral units attached spiropyrans were studied. In this context, four new compounds were synthesized. The synthesized spiropyrans contained both enantiomers of amino protected alanine and phenylalanine. ¹H NMR spectra of **SPA-I**, **SPA-II**, **SPA-III**, and **SPA-IV** were consistent with the structures. This multistep synthesis were proved to be efficient for the synthesis of these compounds. The compounds were characterized and studied with optical spectroscopic methods; UV-Vis, Circular Dichroism and Fluorescence Spectroscopies. With UV-Vis spectroscopy, the photoisomerization of the spiropyrans to the corresponding merocyanines was monitored. It was seen that there is different kinetics of the photoisomerization in different solvents. The conversion of the merocyanine forms into the spiropyrans was also investigated. It was observed this conversion is faster in the spiropyran containing phenylalanine unit compared to that of bearing alanine derivative. This was attributed to the hydrophobic nature of benzyl group.

In the CD measurements, we expected that the effect of the chiral unit on the merocyanine form is observed to be a stereospecific ring closure when the merocyanine transforms into the spiropyran. In this study, contrary to expectations, we did not observe such a phenomenon. This may primarily arise from the distance between the chiral center and chromophore. To obtain chiral spiropyrans and to prevent racemization, chiral centers might be introduced closer to spiropyrans.

HPLC studies were conducted to monitor the ratio between the diastereomers after photoisomerization. Nevertheless, any significant difference was not observed as a result of the analyses.

CHAPTER 5

EXPERIMENTAL

5.1 Methods and Materials

All starting materials and solvents except ethyl acetate and hexane were purchased from Sigma Aldrich and were used without further purifications. Solvents used for Flash Chromatography were distilled prior to use (EtOAc and Hexane over CaCl₂). The reactions were monitored by thin layer chromatography (TLC) (Merck Silica Gel 60 F254) and visualized by UV light at 254 nm.

Structural evaluation of the synthesized compounds was accomplished with the instruments stated below.

¹H and ¹³C nuclear magnetic resonance spectra of the compounds were recorded in deuterated solvents with Bruker Avance III Ultrashield 400 Hz NMR spectrometer. The chemical shifts were stated in parts per million (ppm) with tetramethylsilane (TMS) as internal reference. Spin multiplicities were indicated as s (singlet), d (doublet), dd (doublet of doublet), t (triplet), tt (triplet of triplet), m (multiplet) and coupling constants (J) were reported as in Hz (Hertz). ¹H NMR, ¹³C NMR, and other NMR techniques spectra of compounds were given in Appendix A. NMR spectra were processed with MestReNova program.

Infrared (IR) Spectra were recorded with Thermo Scientific Nicolet iS10 ATR-IR spectrometer. Signal locations were reported in reciprocal centimeter (cm⁻¹). The IR spectra of the compounds synthesized are given in Appendix B.

UV-Vis measurements were recorded with Shimadzu UV-2450 spectrophotometer. Spectroscopic measurements were carried out in methanol, isopropanol,

dichloromethane, and hexane. UV absorption spectra were processed with Microsoft Excel and OriginPro 2019.

High Resolution Mass Spectra (HRMS) were processed in positive mode on (ES+) using Time of Flight mass analyzer. The high-resolution mass spectra of compounds synthesized are given in Appendix C.

Fluorescence measurements were recorded with Perkin Elmer LS55 spectrofluorometer. Spectroscopic measurements were carried out in isopropanol of spectroscopic grade. The fluorescence spectra of the compounds synthesized are given in Appendix D. Fluorescence spectra were processed with OriginPro 2019 program.

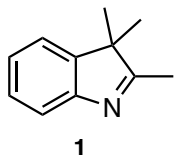
High Performance Liquid Chromatography (HPLC) was carried out with Agilent 1100 Series equipped a diode array detector for absorption measurements at room temperature. Chiralcel OD-H column and Phenomenex ODS (C18) column were used.

Irradiation experiments were performed with fluorescence light source emitting 365 nm. This light is usually used in TLC monitoring.

CD measurements were recorded with Jasco J-1500 CD Spectrometer. Spectroscopic measurements were carried out in isopropanol of spectroscopic grade. CD spectra were processed with Microsoft Excel.

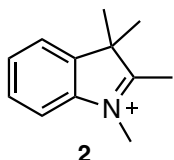
5.2 Synthesis of the Chiral Unit Attached Spiropyrans

5.2.1 Synthesis of 2,3,3-trimethyl-3*H*-indole⁶¹



Isopropyl methyl ketone (5.48 mL, 50.0 mmol, 1.0 eq.) and phenyl hydrazine (4.95 mL, 50.0 mmol, 1.0 eq.) were mixed in a 50 mL round-bottomed flask. The mixture was then refluxed for 4 hours with stirring. After cooled down to room temperature, it was extracted with water and diethyl ether. The organic layer was separated and dried over anhydrous MgSO₄. Red liquid was obtained after removing diethyl ether under vacuum. The resulting product was mixed with acetic acid (15 mL). Then, the reaction mixture was stirred at 90°C for 3 hours. After it was cooled to ambient temperature, ethyl acetate was added, and the mixture was neutralized with saturated Na₂CO₃ solution. The aqueous layer was washed with ethyl acetate several times and dried with anhydrous MgSO₄. After removal of the solvent under vacuum, the product was used in the next step without any further purification. (5.5 g, 68%) ¹H NMR (400 MHz, Chloroform-*d*) δ 7.6 (d, *J* = 7.5 Hz, 1H), 7.34 – 7.21 (m, 2H), 7.17 (m, 1H), 2.26 (s, 3H), 1.27 (s, 6H).

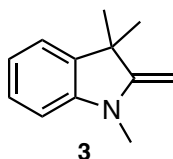
5.2.2 Synthesis of 1,2,3,3-tetrimethyl-3*H*-indolium iodide⁶¹



2,3,3-trimethyl-3*H*-indole (**1**) (7.39, 45.0 mmol, 1.0 eq.) was dissolved in 30 mL of acetonitrile. To the solution was then added iodomethane (5.7 mL, 90.0 mmol, 2.0 eq.). The reaction was carried out under reflux for 5 hours with stirring. The yellow

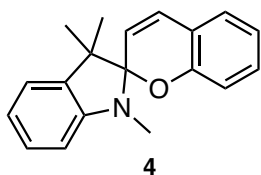
precipitate was obtained. After being collected by filtration, the product was recrystallized in ethanol. (9.1g, 67%) ^1H NMR (400 MHz, DMSO-d_6) δ 7.94 – 7.89 (m, 1H), 7.85 – 7.81 (m, 1H), 7.65 – 7.60 (m, 2H), 4.02 – 3.97 (s, 3H), 2.76 (s, 3H), 1.53 (s, 6H).

5.2.3 Synthesis of 1,3,3-trimethyl-2-methyleneindoline⁶²



10 mL Et_2O and 30 mL of 2M NaOH solution was mixed in a 100 mL round bottomed flask. Then, 1,2,3,3-tetrimethyl-3*H*-indolium iodide (0.72 g, 2.12 mmol, 1.0 eq.) was added and the mixture was allowed to stir at room temperature for 30 min. After the phases are separated, the organic layer was washed with water twice, and dried over MgSO_4 . The pink oil was obtained after evaporation of the solvent under vacuum. (0.35 g, 93 %) ^1H NMR (400 MHz, CDCl_3) δ 7.21 – 7.12 (m, 2H), 6.81 (t, $J = 7.4$, 1H), 6.59 (d, $J = 7.8$ Hz, 1H), 3.90 (s, 2H), 3.08 (s, 3H), 1.43 (s, 6H).

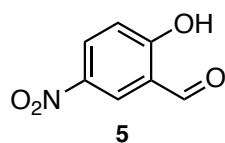
5.2.4 Synthesis of (*R/S*)- 1',3',3'-trimethylspiro[chromene-2,2'-indoline]⁵⁸



1,3,3-trimethyl-2-methyleneindoline (**3**) (1.8 g, 10 mmol, 1.0 eq.) and salicylaldehyde (1.1 mL, 10.0 mmol, 1.0eq.) were mixed in the presence of ethanol (50.0 mL). The mixture was then heated under reflux overnight before being concentrated under vacuum. The residue was dissolved in chloroform and washed with 3 M NaOH solution. The combined organic phases were dried over MgSO_4 and concentrated under vacuum. The crude product was purified by column

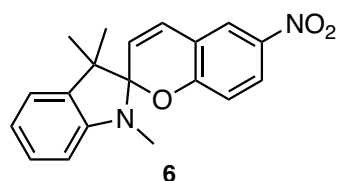
chromatography on silica gel (EtOAc/Hexane 1:5) to yield pink solid. (2.5g, 90%)¹H NMR (400 MHz, CDCl₃) δ 7.19 (t, *J* = 7.8 Hz, 1H), 7.13 – 7.02 (m, 3H), 6.89 – 6.79 (m, 3H), 6.72 (d, *J* = 8.1 Hz, 1H), 6.54 (d, *J* = 7.8 Hz, 1H), 5.68 (d, *J* = 10.2 Hz, 1H), 2.74 (s, 3H), 1.31 (s, 3H), 1.17 (s, 3H).

5.2.5 Synthesis of 2-hydroxy-5-nitrobenzaldehyde⁶³



Salicylaldehyde (2.55 mL, 24 mmol, 1.0 eq.) was dissolved in 13.5 mL of acetic acid. Then, nitric acid (9.0 mL, 120.0 mmol, 5.0 eq.) was added dropwise. The reaction mixture was allowed to stir at room temperature overnight. A pale-yellow precipitate was collected by filtration, which was then washed with distilled water. The crude product was purified by column chromatography on silica gel (EtOAc/Hexane) to afford as a white solid. (3.3 g, 83%) ¹H NMR (400 MHz, CDCl₃) δ 11.62 (s, 1H), 10.00 (s, 1H), 8.57 (d, *J* = 2.8 Hz, 1H), 8.42 (dd, *J* = 9.2, 2.8 Hz, 1H), 7.13 (d, *J* = 9.4 Hz, 1H).

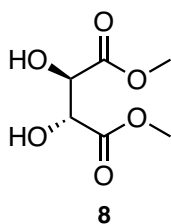
5.2.6 Synthesis of (*R/S*)-1',3',3'-trimethyl-6-nitrospiro[chromene-2,2'-indoline]⁶⁴



2-hydroxy-5-nitrobenzaldehyde (1.9 g, 11.7 mmol, 1.0 eq.) was mixed with 1,2,3,3-tetramethyl-3*H*-indolium iodide (**2**) (2.0 g, 11.7 mmol, 1.0 eq.) in 50.0 mL of ethanol. Piperidine (0.6 mL) was added to the reaction mixture. Subsequently, the solution was refluxed for 4 hours. After cooling, it was allowed to stand overnight, the yellow

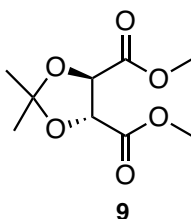
precipitate was collected by filtration and washed with methanol. (2.8 g, 74%) ^1H NMR (400 MHz, CDCl_3) δ 8.03 (d, $J = 2.8$ Hz, 1H), 8.00 (s, 1H), 7.23-7.18 (m, 1H), 7.10 (dd, $J = 7.3, 1.3$ Hz, 1H), 6.97 – 6.86 (m, 2H), 6.77 (d, $J = 8.3$ Hz, 1H), 6.57 (d, $J = 7.8$ Hz, 1H), 5.86 (d, $J = 10.3$ Hz, 1H), 2.74 (s, 3H), 1.30 (s, 3H), 1.19 (s, 3H).

5.2.7 Synthesis of (2*R*,3*R*) dimethyl 2,3-dihydroxysuccinate⁶⁵



Thionyl chloride (17.5 mL, 0.24 mol, 3.5 eq.) was added dropwise to a solution of *L*-tartaric acid (10.0 g, 66 mmol, 1.0 eq.) in methanol (150 mL) at 0°C. The reaction was maintained at this for an hour. Then, it was refluxed for 3 hours. After cooled down to ambient temperature, excess methanol, thionyl chloride, and gaseous hydrogen were removed under vacuum. The crude product was sufficiently pure to be used directly in the next step. (11.2 g, 100%) ^1H NMR (400 MHz, CDCl_3) δ 4.50 (s, 2H), 3.80 (s, 6H).

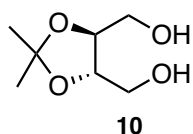
5.2.8 Synthesis of (4*R*,5*R*) dimethyl 2,2-dimethyl-1,3-dioxolane-4,5-dicarboxylate⁶⁵



p-toluenesulfonic acid monohydrate (3.0 g, 15.8 mmol, 0.25 eq.) was added to the mixture of compound **8** (11.2 g, 62.8 mmol, 1.0 eq.) and 2,2 dimethoxy propane (47.26 mL, 38.6 mmol, 6.14 eq.) in DMF (25 mL). The reaction mixture was heated

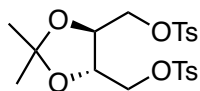
to reflux. It was stirred and maintained for 4 hours. After cooling, the solution was neutralized with NaHCO_3 , and then extracted with ethyl acetate. Organic phases were collected and washed with water several times in order to remove DMF. Then, it was dried over MgSO_4 . After removal of ethyl acetate, the product was obtained as a reddish oil and used in the next step without any further purification. (13.7, 83%) ^1H NMR (400 MHz, CDCl_3) δ 4.75 (s, 2H), 3.76 (s, 6H), 1.43 (s, 6H). ^{13}C NMR (101 MHz, CDCl_3) δ 170.0, 113.8, 76.9, 52.8, 26.2.

5.2.9 Synthesis of ((4*S*,5*S*)-2,2-dimethyl-1,3-dioxolane-4,5 diyl)dimethanol⁶⁵



(4*R*,5*R*) dimethyl 2,2-dimethyl-1,3-dioxolane-4,5-dicarboxylate (**9**) (1.0 g, 45.0 mmol, 1.0 eq.) was dissolved in methanol (20 mL). The solution was cooled down to 0°C. Then, NaBH_4 (0.846 g, 220 mmol, 4.97 eq.) was added in small portion at this temperature. The reaction mixture was allowed to stir at room temperature overnight. After methanol was evaporated, the mixture was dissolved in ethyl acetate and washed with water and saturated NH_4Cl solution respectively. The organic layers were combined and dried over anhydrous MgSO_4 . It was concentrated to be obtained as a pale-yellow oil, which was used in the next step without any further purification. (0.1 g, 15%) ^1H NMR (400 MHz, CDCl_3) δ 4.0-3.96 (m, 2H), 3.82-3.75 (m, 2H), 3.72-3.66 (m, 2H), 1.43 (s, 6H).

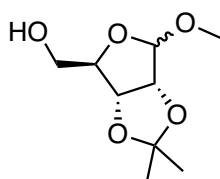
5.2.10 Synthesis of ((4*S*,5*S*)-2,2-dimethyl-1,3-dioxolane-4,5-diyl)bis(methylene)bis(4-methylbenzenesulfonate)⁶⁶



11

((4*S*,5*S*)-2,2-dimethyl-1,3-dioxolane-4,5-diyl)dimethanol (**10**) (0.69 g, 4.27 mmol, 1.0 eq.) was dissolved in DCM (25 mL) and solution was cooled down to 0°C. Then, Et₃N (1.25 mL, 8.9 mmol, 2.1 eq.) and TsCl (1.7 g, 8.9 mmol, 2.1 eq.) was added. The reaction mixture was allowed to stir at room temperature overnight. It was washed with water, 5% CuSO₄ solution, saturated NaHCO₃ and brine respectively. The organic phases were combined, dried over MgSO₄, and then filtered. After DCM was removed, the target compound was purified with column chromatography on silica gel (EtOAc: Hexane, 1:5) to obtain white solid. (0.04 g, 10%) ¹H NMR (400 MHz, CDCl₃) 7.77 (d, *J* = 8.4 Hz, 4H), 7.36 (d, *J* = 7.96 Hz, 4H), 4.09 (m, 4H), 4.01 (m, 2H), 2.45 (s, 6H), 1.29 (s, 6H). ¹³C NMR (101 MHz, CDCl₃) δ 145.2, 132.4, 130.0, 128.0, 110.8, 75.0, 68.4, 26.7, 21.6.

5.2.11 Synthesis of Methyl 2,3-O-isopropylidene-β-*D*-ribofuranoside⁶⁷

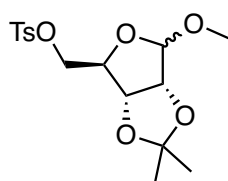


14

D-ribose (10.0 g, 67.0 mmol, 1.0 eq.), acetone (38.4 mL, 0.5 mol, 7.86 mmol), conc. HCl (6 mL) and methanol (75 mL) were mixed, and the reaction mixture was heated under reflux. After cooled to room temperature, the solution was neutralized with saturated aq. KHCO₃. It was concentrated under vacuum and then extracted with chloroform. The combined organic phases were washed with water several times and

dried over Na₂SO₄. The solvent was evaporated to get yellowish oily product. (9.8 g, 72%). ¹H NMR (400 MHz, CDCl₃) δ 4.87 (s, 1H), 4.72 (d, *J* = 6.0 Hz, 1H), 4.49 (d, *J* = 5.9 Hz, 1H), 4.33 – 4.28 (m, 1H), 3.59-3.48 (m, 2H), 3.32 (s, 3H), 1.41 (s, 3H), 1.22 (s, 3H).

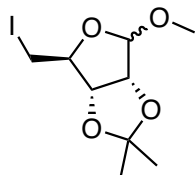
5.2.12 Synthesis of ((3*aR*,4*R*,6*aR*)-6-methoxy-2,2-dimethyltetrahydrofuro[3,4-*d*][1,3]dioxol-4-yl)methyl 4-methylbenzenesulfon⁶⁸



15

To a solution of methyl 2,3-*O*-isopropylidene- β -D-ribofuranoside (3.0 g, 14.6 mmol, 1.0 eq.) in pyridine (8 mL) *p*-toluenesulfonyl chloride (3.8 g, 22.0 mmol, 1.5 eq.) was added. The reaction was stirred at room temperature until the complete disappearance of the starting material. Then, the mixture was poured into slurry ice-water. After stirring vigorously, the product precipitated. It was washed with water and dried to be obtained as a white solid. (4.8 g, 96%) ¹H NMR (400 MHz, CDCl₃) δ 7.80 (d, *J* = 8.4 Hz, 2H), 7.36 (d, *J* = 7.9 Hz, 2H), 4.93 (s, 1H), 4.56 (dd, *J* = 20.36, 6.0, 2H), 4.53 (d, *J* = 5.9 Hz, 1H), 4.36 – 4.25 (m, 1H), 4.09 – 3.95 (m, 2H), 3.23 (s, 3H), 2.46 (s, 3H), 1.44 (s, 3H), 1.28 (s, 3H).

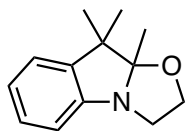
5.2.13 Synthesis of (3a*S*,4*S*,6*S*,6a*R*)-4-(iodomethyl)-6-methoxy-2,2-dimethyltetrahydrofuro[3,4-*d*][1,3]dioxole⁶⁹



17

NaI (0.88 g, 5.8 mmol, 2.0 eq.) was added to the solution compound **15** (1.0 g, 2.9 mmol, 1.0 eq.) in methyl ethyl ketone. The reaction mixture was allowed to reflux for 24 hours. After cooled down to ambient temperature, the solvent was removed under reduced pressure. The resulting mixture was extracted with ethyl acetate and washed with water and brine. After dried over MgSO₄ and concentrated under vacuum, reddish oily product was obtained. (0.54 g, 59%) ¹H NMR (400 MHz, CDCl₃) δ 5.08 – 5.01 (m, 1H), 4.76 (m, 1H), 4.62 (t, *J* = 5.3 Hz, 1H), 4.47-4.39 (m, 1H), 3.40 – 3.33 (m, 3H), 3.33 – 3.23 (m, 1H), 3.16 (m, 1H), 1.48 (s, 3H), 1.32 (s, 3H).

5.2.14 Synthesis of (*R/S*)-9,9,9a-Trimethyl-2,3,9,9a-tetrahydrooxazolo[3,2-*a*]indole⁷⁰

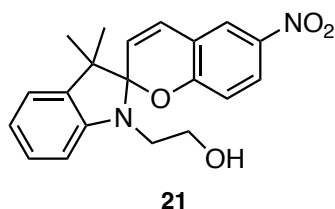


19

2-bromoethanol (9.17 mL, 73.0 mmol, 1.5 eq) was added to a solution of 2,3,3-trimethyl-3*H*-indole (**1**) (9.17 g, 49.0 mmol, 1.0 eq.) in 40 mL of acetonitrile. The reaction mixture was heated under reflux for 1 d. After cooled down to room temperature, acetonitrile was removed under reduced pressure. The viscous red residue was taken up in chloroform, and then washed with water. The aqueous layer was made basic upon addition of 1 M KOH solution. the color of the solution became

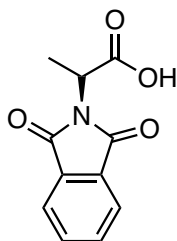
milky white, and the solution was extracted with diethyl ether. The organic phase was washed with water, brine and then dried over MgSO₄. (5.9 g, 56%) ¹H NMR (400 MHz, CDCl₃) δ 7.21 – 7.14 (m, 1H), 7.12 (d, *J* = 7.4, 1H), 6.96 (t, *J* = 7.4, Hz, 1H), 6.79 (d, *J* = 7.8 Hz, 1H), 3.89 – 3.81 (m, 1H), 3.76 – 3.67 (m, 1H), 3.62 – 3.49 (m, 2H), 1.49 (s, 3H), 1.43 (s, 3H), 1.23 (s, 3H).

5.2.15 Synthesis of (*R/S*)-2-(3',3'-dimethyl-6-nitrospiro[chromene-2,2'-indolin]-1'-yl)ethan-1-ol⁷⁰



A solution of (*R/S*)-9,9,9a-Trimethyl-2,3,9,9a-tetrahydrooxazolo[3,2-*a*]indole (**19**) (0.6 g, 2.6 mmol, 1.0 eq.) and 2-hydroxy-5-nitrobenzaldehyde (0.72g, 4.1 mmol, 1.5 eq.) was mixed in the presence of 15 mL of ethanol. The reaction mixture was heated under reflux for 3 hours. After cooled down to ambient temperature, it was filtered. The resultant purple solid was washed with ethanol. The crude product was purified by recrystallization from ethanol. (0.5g, 59 %) ¹H NMR (400 MHz, CDCl₃) δ 8.06 – 7.97 (m, 2H), 7.24 – 7.17 (m, 1H), 7.15 – 7.07 (m, 2H), 6.93-6.87 (m, 2H), 6.77 (d, *J* = 8.0 Hz, 1H), 6.68 (d, *J* = 7.1 Hz, 1H), 5.89 (d, *J* = 10.4 Hz, 1H), 3.85-3.77 (m, 1H), 3.77-3.69 (m, 1H), 3.37-3.29 (m, 1H), 3.52 – 3.42 (m, 1H), 1.29 (s, 3H), 1.20 (s, 3H).

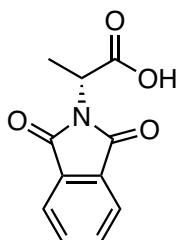
5.2.16 Synthesis of (*S*)-2-(1,3-dioxoisindolin-2-yl)propanoic acid⁷¹



22a-S

L-alanine (1.0 g, 11.22 mmol, 1.0 eq.) and phthalic anhydride (1.66 g, 11.22 mmol, 1.0 eq.) were mixed in the presence 15 mL of acetic acid. The reaction mixture was allowed to reflux overnight. After acetic acid was evaporated under reduced pressure. Distilled water was then added to the resulting white solid. The solution was heated to reflux for 1 h. After filtration, white solid was obtained. (1.46 g, 68%)
¹H NMR (400 MHz, CDCl₃) δ 7.93-7.82 (m, 2H), 7.79-7.69 (m, 2H), 5.04 (m, 1H), 1.72 (d, *J* = 7.4 Hz, 3H).

5.2.17 Synthesis of (*R*)-2-(1,3-dioxoisindolin-2-yl)propanoic acid⁷¹

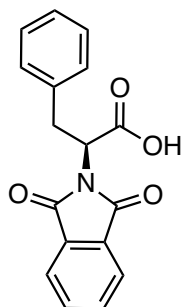


22a-R

D-alanine (1.0 g, 11.22 mmol, 1.0 eq.) and phthalic anhydride (1.66 g, 11.22 mmol, 1.0 eq.) were mixed in the presence 15 mL of acetic acid. The reaction mixture was allowed to reflux overnight. After acetic acid was evaporated under reduced pressure. Distilled water was then added to the resulting white solid. The solution was heated to reflux for 1 h. After filtration, white solid was obtained. (1.9 g, 85%)

^1H NMR (400 MHz, CDCl_3) δ 7.86 – 7.84 (m, 2H), 7.77-7.71 (m, 2H), 5.05 (p, J = 7.4, 5.8 Hz, 1H), 1.72 (d, J = 7.1 Hz, 3H).

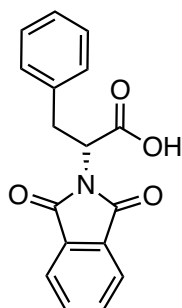
5.2.18 Synthesis of (*S*)-2-(1,3-dioxisoindolin-2-yl)propanoic acid⁷¹



22b-S

L-phenylalanine (1.0 g, 11.22 mmol, 1.0 eq.) and phthalic anhydride (1.66 g, 11.22 mmol, 1.0 eq.) were mixed in the presence 15 mL of acetic acid. The reaction mixture was allowed to reflux overnight. After acetic acid was evaporated under reduced pressure. Distilled water was then added to the resulting white solid. The solution was heated to reflux for 1 h. After filtration, white solid was obtained. (1.5 g, 81%) ^1H NMR (400 MHz, CDCl_3) δ 7.79-7.75 (m, 2H), 7.71-7.65 (m, 2H), 7.21 – 7.12 (m, 5H), 5.22 (dd, J = 9.1, 7.4 Hz, 1H), 3.59 (d, J = 8.8 Hz, 2H).

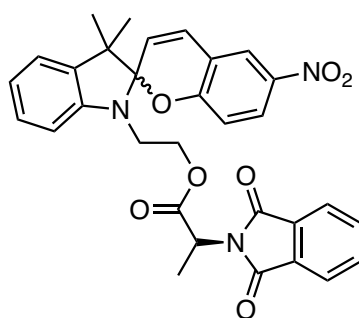
5.2.19 Synthesis of (*R*)-2-(1,3-dioxisoindolin-2-yl)-3-phenylpropanoic acid



22b-R

D-phenylalanine (1.0 g, 11.22 mmol, 1.0 eq.) and phthalic anhydride (1.66 g, 11.22 mmol, 1.0 eq.) were mixed in the presence 15 mL of acetic acid. The reaction mixture was allowed to reflux overnight. After acetic acid was evaporated under reduced pressure. Distilled water was then added to the resulting white solid. The solution was heated to reflux for 1 h. After filtration, white solid was obtained. (1.5 g, 86%) ¹H NMR (400 MHz, CDCl₃) δ 7.87 – 7.74 (m, 2H), 7.73-7.64 (m, 2H), 7.25 – 7.09 (m, 5H), 5.23 (m, 1H), 3.60 (d, *J* = 6.4 Hz, 2H).

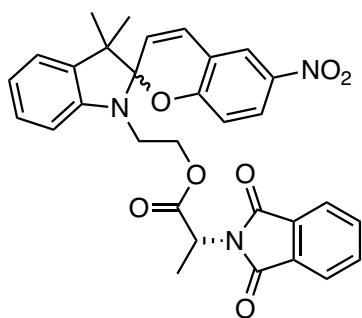
5.2.20 Synthesis of SPA-I



Spiropyran (0.1 g, 0.28 mmol, 1.0 eq.) and protected amino acid **22a-S** (0.08 g, 0.34 mmol, 1.2 eq.) were mixed in 50 mL of DCM. The mixture was cooled down to 0°C under argon. DCC (0.07 g, 1.02 mmol, 1.2 eq.) and DMAP (4 mg, 0.03 mmol, 0.1 eq.) were added respectively. The color of the solution was initially purple red. After addition of DMAP, it became dark blue, then yellow. The ice-bath was removed, and the reaction mixture was allowed to stir at room temperature. After completion of the reaction, the mixture was washed with water and dried over MgSO₄. The crude product was purified by column chromatography on silica gel (EtOAc: Hexane, 1:25) to yield pink solid. (80 mg, 52%) ¹H NMR (400 MHz, CDCl₃) δ 8.03 – 7.96 (m, 3H), 7.90 (d, *J* = 2.8 Hz, 1H), 7.88-7.83 (m, 2H), 7.78-7.70 (m, 6H), 7.15-7.10 (m, 1H), 7.08 – 6.95 (m, 3H), 6.89-6.82 (m, 2H), 6.77 – 6.68 (m, 4H), 6.57 (dd, *J* = 16.5, 7.8 Hz, 2H), 5.79 (dd, *J* = 20.2, 10.3 Hz, 2H), 4.93 (qd, *J* = 7.3, 2.4 Hz, 2H), 4.37 – 4.20 (m, 4H), 3.56 – 3.28 (m, 4H), 1.65 (dd, *J* = 8.6, 7.3 Hz, 6H), 1.23 (s, 6H), 1.13 (s, 3H), 1.05 (s, 3H). ¹³C NMR (101 MHz, CDCl₃) δ 169.7, 169.6, 167.2, 167.1, 159.3,

159.2, 146.61, 146.4, 141.1, 141.0, 141.0, 135.6, 135.4, 134.2, 134.1, 131.8, 131.8, 128.3, 128.1, 127.8, 127.7, 125.9, 123.5, 123.4, 122.8, 122.7, 121.7, 121.7, 121.7, 121.7, 121.5, 119.9, 118.4, 118.3, 115.5, 115.5, 106.6, 106.5, 106.4, 106.4, 77.3, 77.0, 76.7, 64.4, 63.7, 52.7, 52.6, 47.5, 47.3, 47.2, 42.2, 42.1, 25.81, 25.71, 22.6, 22.6, 22.3, 19.8, 15.3, 15.2. IR: 1779 cm^{-1} , 1743 cm^{-1} , 1710 cm^{-1} (C=O), 1517 cm^{-1} , 1338 cm^{-1} (NO_2), 951 cm^{-1} (C_{spiro}) HRMS: (ESI-MS) m/z : $[\text{M}+\text{H}]^+$ Calcd for $\text{C}_{31}\text{H}_{28}\text{N}_3\text{O}_7^+$ 554.1927, found 554.1927

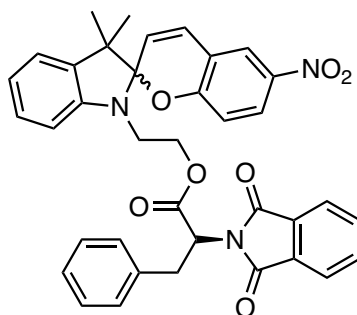
5.2.21 Synthesis of SPA-II



Spiropyran (0.1 g, 0.28 mmol, 1.0 eq.) and protected amino acid **22a-R** (0.08 g, 0.34 mmol, 1.2 eq.) were mixed in 50 mL of DCM. The mixture was cooled down to 0°C under argon. DCC (0.07 g, 1.02 mmol, 1.2 eq.) and DMAP (4 mg, 0.03 mmol, 0.1 eq.) were added respectively. The color of the solution was initially purple red. After addition of DMAP, it became dark blue, then yellow. The ice-bath was removed, and the reaction mixture was allowed to stir at room temperature. After completion of the reaction, the mixture was washed with water and dried over MgSO_4 . The crude product was purified by column chromatography on silica gel (EtOAc: Hexane, 1:25) to yield pink solid. (80 mg, 52%) ^1H NMR (400 MHz, CDCl_3) δ 8.03 – 7.97 (m, 3H), 7.90 (d, $J = 2.8$ Hz, 1H), 7.86 (dd, $J = 5.4, 3.1$ Hz, 2H), 7.80-7.70 (m, 6H), 7.15-7.08 (m, 1H), 7.08 – 6.94 (m, 4H), 6.89-6.81 (m, 2H), 6.78 – 6.67 (m, 4H), 6.57 (dd, $J = 16.4, 7.8$ Hz, 2H), 5.79 (dd, $J = 20.1, 10.4$ Hz, 2H), 4.93 (qd, $J = 7.4, 2.5$ Hz, 2H), 4.36-4.21 (m, 4H), 3.50 – 3.33 (m, 4H), 1.65 (t, $J = 7.9$ Hz, 6H), 1.23 (s, 6H), 1.13 (s, 3H), 1.05 (s, 3H). ^{13}C NMR (101 MHz, CDCl_3) δ 169.7, 169.6, 167.2, 167.1,

159.3, 159.3, 146., 146.49, 141.0, 135.6, 135.4, 134.2, 134.1, 131.8, 131.8, 128.3, 128.1, 127.8, 127.7, 125.9, 123.5, 123.4, 122.8, 122.7, 121.7, 121.7, 121.7, 121.5, 119.9, 118.4, 118.3, 115.5, 115.5, 106.6, 106.5, 106.4, 106.4, 77.3, 77.2, 77.0, 76.7, 64.4, 63.7, 52.7, 52.6, 47.3, 47.2, 42.2, 42.1, 25.8, 25.7, 22.6, 22.6, 22.3, 19.81, 15.3, 15.2. IR: 1779 cm^{-1} , 1743 cm^{-1} , 1710 cm^{-1} (C=O), 1517 cm^{-1} , 1338 cm^{-1} (NO_2), 951 cm^{-1} (C_{spiro}) HRMS: (ESI-MS) m/z : $[\text{M}+\text{H}]^+$ Calcd for $\text{C}_{31}\text{H}_{28}\text{N}_3\text{O}_7^+$ 554.1927, found 554.1926

5.2.22 Synthesis of SPA-III

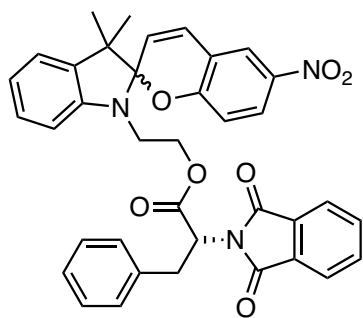


Spiropyran (0.1 g, 0.28 mmol, 1.0 eq.) and protected amino acid **22b-S** (0.1 g, 0.34 mmol, 1.2 eq.) were mixed in 50 mL of DCM. The mixture was cooled down to 0°C under argon. DCC (0.07 g, 1.02 mmol, 1.2 eq.) and DMAP (4 mg, 0.03 mmol, 0.1 eq.) were added respectively. The color of the solution was initially purple red. After addition of DMAP, it became dark blue, then yellow. The ice-bath was removed, and the reaction mixture was allowed to stir at room temperature. After completion of the reaction, the mixture was washed with water and dried over MgSO_4 . The crude product was purified by column chromatography on silica gel (EtOAc: Hexane, 1:25) to yield pink solid. (80 mg, 44%) ^1H NMR (400 MHz, CDCl_3) δ 8.02-7.96 (m, 3H), 7.90 (d, $J = 2.7$ Hz, 1H), 7.78-7.74 (m, 2H), 7.73 – 7.65 (m, 6H), 7.2-2.07 (m, 11H), 7.06 – 6.97 (m, 3H), 6.88 – 6.80 (m, 2H), 6.77 – 6.68 (m, 4H), 6.60 (d, $J = 7.8$ Hz, 1H), 6.55 (d, $J = 7.8$ Hz, 1H), 5.78 (dd, $J = 22.5, 10.4$ Hz, 2H), 5.09 (dt, $J = 11.3, 5.6$ Hz, 2H), 4.41-4.23 (m, 4H), 3.56 – 3.34 (m, 8H), 1.23 (s, 6H), 1.13 (s, 3H), 1.04 (s, 3H). ^{13}C NMR (101 MHz, CDCl_3) δ 168.9, 168.7, 167.2, 167.1, 159.3, 146.5,

146.4, 141.1, 136.5, 135.6, 135.5, 134.2, 134.1, 131.5, 131.4, 128.8, 128.8, 128.6, 128.5, 128.3, 128.1, 127.8, 127.7, 126.9, 125.9, 123.5, 123.4, 122.8, 122.7, 121.8, 121.7, 121.6, 121.6, 120.0, 118.3, 115.5, 115.5, 106.6, 106.5, 106.4, 106.3, 64.4, 63.9, 53.2, 53.1, 52.7, 52.7, 42.3, 42.2, 34.7, 34.6, 25.8, 25.7, 19.8, IR: 1773 cm^{-1} , 1732 cm^{-1} , 1711 cm^{-1} (C=O), 1514 cm^{-1} , 1335 cm^{-1} (NO_2), 955 cm^{-1} (C_{spiro}) HRMS: (ESI-MS) m/z : $[\text{M}+\text{H}]^+$ Calcd for $\text{C}_{37}\text{H}_{32}\text{N}_3\text{O}_7^+$ 630.2240, found 630.2240

Protected *L*-phenyl alanine **22b-S** (80 mg, 0.28 mmol, 1.0 eq.), EDC (0.06 mL, 0.34 mmol, 1.2 eq.) and DMAP (20 mg, 0.14 mmol, 0.5 eq.) were mixed in the presence of 5 mL of DCM at 0°C. After an hour, spiropyran (0.1 g, 0.28 mmol, 1.0 eq.) was added and then resulting mixture was allowed to stir at room temperature. The reaction was monitored by TLC. After 24 hours, it was quenched by the addition of water. The phases were separated, and organic phase was dried over MgSO_4 . The solvent was evaporated. The crude product was purified by column chromatography on silica gel (EtOAc:Hexane, 1:25). (50 mg, 28%)

5.2.23 Synthesis of SPA-IV



Spiropyran (0.1 g, 0.28 mmol, 1.0 eq.) and protected amino acid **22b-R** (0.1 g, 0.34 mmol, 1.2 eq.) were mixed in 50 mL of DCM. The mixture was cooled down to 0°C under argon. DCC (0.07 g, 1.02 mmol, 1.2 eq.) and DMAP (4 mg, 0.03 mmol, 0.1 eq.) were added respectively. The color of the solution was initially purple red. After addition of DMAP, it became dark blue, then yellow. The ice-bath was removed, and the reaction mixture was allowed to stir at room temperature. After completion of

the reaction, the mixture was washed with water and dried over MgSO₄. The crude product was purified by column chromatography on silica gel (EtOAc: Hexane, 1:25) to yield pink solid. (90 mg, 58%) ¹H NMR (400 MHz, CDCl₃) δ 8.03-7.96 (m, 3H), 7.90 (d, *J* = 2.7 Hz, 1H), 7.78-7.75 (m, 2H), 7.72-7.65 (m, 6H), 7.19 – 7.10 (m, 11H), 7.03-6.97 (m, 3H), 6.89 – 6.80 (m, 2H), 6.78 – 6.68 (m, 5H), 6.60 (d, *J* = 7.8 Hz, 1H), 6.55 (d, *J* = 7.7 Hz, 1H), 5.78 (dd, *J* = 22.9, 10.4 Hz, 2H), 5.10 (dt, *J* = 11.3, 5.6 Hz, 2H), 4.39 – 4.27 (m, 4H), 3.54 – 3.38 (m, 8H), 1.23 (s, 6H), 1.13 (s, 3H), 1.04 (s, 3H). ¹³C NMR (101 MHz, CDCl₃) δ 193.8, 167.2, 167.1, 165.6, 165.54, 157.6, 157.6, 144.9, 144.8, 139.4, 139.4, 134.8, 134.8, 134.0, 133.8, 132.55, 132.4, 132.3, 129.8, 129.7, 127., 127.15, 126.9, 126.9, 126.8, 126.6, 126.5, 126.1, 126.01, 125.3, 124., 121.86, 121.8, 121.1, 121.0, 120.2, 120.1, 120.0, 119.9, 118.37, 116.7, 116.7, 113.9, 113.8, 104.9, 104.9, 104.8, 104.7, 75.6, 75.3, 75.0, 62.8, 62.2, 61.3, 51.5, 51.4, 51.0, 51.0, 42.3, 40.6, 40.5, 33.0, 32.9, 28.0, 24.1, 24.0, 18.1. IR: 1774 cm⁻¹, 1743 cm⁻¹, 1712 cm⁻¹ (C=O), 1516 cm⁻¹, 1336 cm⁻¹ (NO₂), 953 cm⁻¹ (C_{spiro}) HRMS: (ESI-MS) *m/z*: [M+H]⁺ Calcd for C₃₇H₃₂N₃O₇⁺ 630.2240, found 630.2239

REFERENCES

- (1) Dürr, H.; Bouas-Laurent, H. Photochromism. In *Photochromism: Molecules and Systems*; Elsevier, **2003**. <https://doi.org/10.1016/B978-0-444-51322-9.X5000-3>.
- (2) Bouas-Laurent, H.; Dürr, H. Organic Photochromism (IUPAC Technical Report). *Pure Appl. Chem.* **2007**. <https://doi.org/10.1351/pac200173040639>.
- (3) Davies, M. J.; Truscott, R. J. W. Photo-Oxidation of Proteins and Its Role in Cataractogenesis. *J. Photochem. Photobiol. B Biol.* **2001**, *63*, 114–125. [https://doi.org/10.1016/S1011-1344\(01\)00208-1](https://doi.org/10.1016/S1011-1344(01)00208-1).
- (4) Kathan, M.; Hecht, S. Photoswitchable Molecules as Key Ingredients to Drive Systems Away from the Global Thermodynamic Minimum. *Chem. Soc. Rev.* **2017**, *46*, 5536–5550. <https://doi.org/10.1039/c7cs00112f>.
- (5) Fleming, C. L.; Li, S.; Grøtli, M.; Andréasson, J. Shining New Light on the Spiropyran Photoswitch: A Photocage Decides between Cis – Trans or Spiro-Merocyanine Isomerization. *J. Am. Chem. Soc.* **2018**, *140*, 14069–14072. <https://doi.org/10.1021/jacs.8b09523>.
- (6) Jia, S.; Fong, W. K.; Graham, B.; Boyd, B. J. Photoswitchable Molecules in Long-Wavelength Light-Responsive Drug Delivery: From Molecular Design to Applications. *Chem. Mater.* **2018**, *30*, 2873–2887. <https://doi.org/10.1021/acs.chemmater.8b00357>.
- (7) Bléger, D.; Schwarz, J.; Brouwer, A. M.; Hecht, S. O -Fluoroazobenzenes as Readily Synthesized Photoswitches Offering Nearly Quantitative Two-Way Isomerization with Visible Light. *J. Am. Chem. Soc.* **2012**, *134*, 20597–20600. <https://doi.org/10.1021/ja310323y>.
- (8) Beharry, A. A.; Sadvoski, O.; Woolley, G. A. Azobenzene Photoswitching without Ultraviolet Light. *J. Am. Chem. Soc.* **2011**, *133*, 19684–19687. <https://doi.org/10.1021/ja209239m>.

- (9) Samanta, S.; Beharry, A. A.; Sadovski, O.; McCormick, T. M.; Babalhavaeji, A.; Tropepe, V.; Woolley, G. A. Photoswitching Azo Compounds in Vivo with Red Light. *J. Am. Chem. Soc.* **2013**, *135*, 9777–9784. <https://doi.org/10.1021/ja402220t>.
- (10) Irie, M. Diarylethenes for Memories and Switches. *Chem. Rev.* **2000**, *100*, 1685–1716. <https://doi.org/10.1021/cr980069d>.
- (11) Irie, M.; Fukaminato, T.; Matsuda, K.; Kobatake, S. Photochromism of Diarylethene Molecules and Crystals: Memories, Switches, and Actuators. *Chem. Rev.* **2014**, *114*, 12174–12277. <https://doi.org/10.1021/cr500249p>.
- (12) Baeyer, A. Systematik Und Nomenclatur Bicyclischer Kohlenwasserstoffe. *Berichte der Dtsch. Chem. Gesellschaft* **1900**, *33*, 3771–3775. <https://doi.org/10.1002/cber.190003303187>.
- (13) Beesley, R. M.; Ingold, C. K.; Thorpe, J. F. CXIX.—The Formation and Stability of Spiro-Compounds. Part I. Spiro-Compounds from Cyclohexane. *J. Chem. Soc., Trans.* **1915**, *107*, 1080–1106. <https://doi.org/10.1039/CT9150701080>.
- (14) Seiler, V.; Tumanov, N.; Robeyns, K.; Wouters, J.; Champagne, B.; Leyssens, T. A Structural Analysis of Spiropyran and Spirooxazine Compounds and Their Polymorphs. *Crystals* **2017**, *7*, 84. <https://doi.org/10.3390/cryst7030084>.
- (15) Xia, H.; Xie, K.; Zou, G. Advances in Spiropyran/Spirooxazines and Applications Based on Fluorescence Resonance Energy Transfer (FRET) with Fluorescent Materials. *Molecules* **2017**, *22*. <https://doi.org/10.3390/molecules22122236>.
- (16) Kortekaas, L.; Browne, W. R. The Evolution of Spiropyran: Fundamentals and Progress of an Extraordinarily Versatile Photochrome. *Chem. Soc. Rev.* **2019**, *48*, 3406–3424. <https://doi.org/10.1039/c9cs00203k>.
- (17) Bertelson, R. C. Spiropyran. In *Organic Photochromic and Thermochromic*

- Compounds*; Kluwer Academic Publishers: Boston, **2006**; pp 11–83.
https://doi.org/10.1007/0-306-46911-1_2.
- (18) Minkin, V. I. Photo-, Thermo-, Solvato-, and Electrochromic Spiroheterocyclic Compounds. *Chem. Rev.* **2004**, *104*, 2751–2776.
<https://doi.org/10.1021/cr020088u>.
- (19) Hirshberg, Y.; Fischer, E. 128. Low-Temperature Photochromism and Its Relation to Thermochromism. *J. Chem. Soc.* **1953**, 629–636.
<https://doi.org/10.1039/jr9530000629>.
- (20) Bittmann, S. F.; Dsouza, R.; Siddiqui, K. M.; Hayes, S. A.; Rossos, A.; Corthey, G.; Kochman, M.; Prokhorenko, V. I.; Murphy, R. S.; Schwoerer, H.; Miller, R. J. D. Ultrafast Ring-Opening and Solvent-Dependent Product Relaxation of Photochromic Spiroanthopyran. *Phys. Chem. Chem. Phys.* **2019**, *21*, 18119–18127. <https://doi.org/10.1039/C9CP02950H>.
- (21) Swansburg, S.; Buncel, E.; Lemieux, R. P. Thermal Racemization of Substituted Indolinobenzospiropyran: Evidence of Competing Polar and Nonpolar Mechanisms. *J. Am. Chem. Soc.* **2000**, *122*, 6594–6600.
<https://doi.org/10.1021/ja0001613>.
- (22) Keum, S. R.; Lee, M. J. Nonactivated Arylazaindolinobenzospiropyran Derivatives. Part 21 : Preparation and Kinetic Measurements of the Spiro-Ring Formation from the Merocyanine Form. *Bull. Korean Chem. Soc.* **1999**, *20*, 1464–1468.
- (23) Ivashenko, O.; Van Herpt, J. T.; Feringa, B. L.; Rudolf, P.; Browne, W. R. UV/Vis and NIR Light-Responsive Spiropyran Self-Assembled Monolayers. *Langmuir* **2013**, *29*, 4290–4297. <https://doi.org/10.1021/la400192c>.
- (24) Liu, F.; Morokuma, K. Multiple Pathways for the Primary Step of the Spiropyran Photochromic Reaction: A CASPT2//CASSCF Study. *J. Am. Chem. Soc.* **2013**, *135*, 10693–10702. <https://doi.org/10.1021/ja402868b>.
- (25) Harada, J.; Kawazoe, Y.; Ogawa, K. Photochromism of Spiropyran and

- Spirooxazines in the Solid State: Low Temperature Enhances Photocoloration. *Chem. Commun.* **2010**, *46*, 2593. <https://doi.org/10.1039/b925514a>.
- (26) Barachevsky, V. A.; Valova, T. M.; Atabekyan, L. S.; Lyubimov, A. V. Negative Photochromism of Water-Soluble Pyridine-Containing Nitro-Substituted Spiropyrans. *High Energy Chem.* **2017**, *51*, 415–419. <https://doi.org/10.1134/S0018143917060029>.
- (27) Buback, J.; Nuernberger, P.; Kullmann, M.; Langhojer, F.; Schmidt, R.; Würthner, F.; Brixner, T. Ring-Closure and Isomerization Capabilities of Spiropyran-Derived Merocyanine Isomers. *J. Phys. Chem. A* **2011**, *115*, 3924–3935. <https://doi.org/10.1021/jp108322u>.
- (28) Matczyszyn, K.; Olesiak-Banska, J.; Nakatani, K.; Yu, P.; Murugan, N. A.; Zalesny, R.; Roztoczyńska, A.; Bednarska, J.; Bartkowiak, W.; Kongsted, J.; Ågren, H.; Samoć, M. One- and Two-Photon Absorption of a Spiropyran–Merocyanine System: Experimental and Theoretical Studies. *J. Phys. Chem. B* **2015**, *119*, 1515–1522. <https://doi.org/10.1021/jp5071715>.
- (29) Tian, W.; Tian, J. An Insight into the Solvent Effect on Photo-, Solvato-Chromism of Spiropyran through the Perspective of Intermolecular Interactions. *Dye. Pigment.* **2014**, *105*, 66–74. <https://doi.org/10.1016/j.dyepig.2014.01.020>.
- (30) Lukyanov, B. S.; Lukyanova, M. B. Spiropyran: Synthesis, Properties, and Application. (Review). *Chem. Heterocycl. Compd.* **2005**, *41*, 281–311. <https://doi.org/10.1007/s10593-005-0148-x>.
- (31) Barachevsky, V. A. Negative Photochromism in Organic Systems. *Rev. J. Chem.* **2017**, *7*, 334–371. <https://doi.org/10.1134/s2079978017030013>.
- (32) Crano, C. J.; Guglielmetti, R. J. *Organic Photochromic and Thermochromic Compounds*; Crano, J. C., Guglielmetti, R. J., Eds.; Topics in Applied Chemistry; Kluwer Academic Publishers: Boston, **2002**. <https://doi.org/10.1007/b115590>.

- (33) Hatano, S.; Horino, T.; Tokita, A.; Oshima, T.; Abe, J. Unusual Negative Photochromism via a Short-Lived Imidazolyl Radical of 1,1'-Binaphthyl-Bridged Imidazole Dimer. *J. Am. Chem. Soc.* **2013**, *135*, 3164–3172. <https://doi.org/10.1021/ja311344u>.
- (34) Kim, N.; Lam, H.; Kyu, T. Photochromism and Photopolymerization Induced Mesophase Transitions in Mixtures of Spiropyran and Mesogenic Diacrylate. *J. Phys. Chem. B* **2010**, *114*, 16381–16387. <https://doi.org/10.1021/jp108113b>.
- (35) Qin, T.; Han, J.; Geng, Y.; Ju, L.; Sheng, L.; Zhang, S. X. A. A Multiaddressable Dyad with Switchable Cyan/Magenta/Yellow Colors for Full-Color Rewritable Paper. *Chem. - A Eur. J.* **2018**, *24*, 12539–12545. <https://doi.org/10.1002/chem.201801692>.
- (36) Reichardt, C.; Welton, T. *Solvents and Solvent Effects in Organic Chemistry*; Wiley-VCH Verlag GmbH & Co. KGaA: Weinheim, Germany, **2010**. <https://doi.org/10.1002/9783527632220>.
- (37) Nigam, S.; Rutan, S. Principles and Applications of Solvatochromism. *Appl. Spectrosc.* **2001**, *55*, 362A–370A. <https://doi.org/10.1366/0003702011953702>.
- (38) Murugan, N. A.; Chakrabarti, S.; Ågren, H. Solvent Dependence of Structure, Charge Distribution, and Absorption Spectrum in the Photochromic Merocyanine–Spiropyran Pair. *J. Phys. Chem. B* **2011**, *115*, 4025–4032. <https://doi.org/10.1021/jp2004612>.
- (39) Ernsting, N. P.; Dick, B.; Arthen-Engeland, T. The Primary Photochemical Reaction Step of Unsubstituted Indolino-Spiroyrans. *Pure Appl. Chem.* **1990**, *62*, 1483–1488. <https://doi.org/10.1351/pac199062081483>.
- (40) Wu, Y.; Sasaki, T.; Kazushi, K.; Seo, T.; Sakurai, K. Interactions between Spiroyrans and Room-Temperature Ionic Liquids: Photochromism and Solvatochromism. *J. Phys. Chem. B* **2008**, *112*, 7530–7536. <https://doi.org/10.1021/jp800957c>.

- (41) Schenderlein, H.; Voss, A.; Stark, R. W.; Biesalski, M. Preparation and Characterization of Light-Switchable Polymer Networks Attached to Solid Substrates. *Langmuir* **2013**, *29*, 4525–4534. <https://doi.org/10.1021/la305073p>.
- (42) Rosario, R.; Gust, D.; Hayes, M.; Springer, J.; Garcia, A. A. Solvatochromic Study of the Microenvironment of Surface-Bound Spiropyrans. *Langmuir* **2003**, *19*, 8801–8806. <https://doi.org/10.1021/la0344332>.
- (43) Irving, F. CXLV.—Styrylpyrylium Salts. Part XII. Spiropyrans Derived from 9-Methyl- and 9-Ethyl-Xanthylium Salts. *J. Chem. Soc.* **1929**, 1093–1095. <https://doi.org/10.1039/JR9290001093>.
- (44) Roxburgh, C. On the Acid Catalysed Isomerisation of Some Substituted Spirobenzopyrans. *Dye. Pigment.* **1995**, *27*, 63–69. [https://doi.org/10.1016/0143-7208\(94\)00059-B](https://doi.org/10.1016/0143-7208(94)00059-B).
- (45) Zhou, J.; Li, Y.; Tang, Y.; Zhao, F.; Song, X.; Li, E. Detailed Investigation on a Negative Photochromic Spiropyran. *J. Photochem. Photobiol. A Chem.* **1995**, *90*, 117–123. [https://doi.org/10.1016/1010-6030\(95\)04082-Q](https://doi.org/10.1016/1010-6030(95)04082-Q).
- (46) Shiozaki, H. Molecular Orbital Calculations for Acid Induced Ring Opening Reaction of Spiropyran. *Dye. Pigment.* **1997**, *33*, 229–237. [https://doi.org/10.1016/S0143-7208\(96\)00051-4](https://doi.org/10.1016/S0143-7208(96)00051-4).
- (47) Cui, L.; Zhang, H.; Zhang, G.; Zhou, Y.; Fan, L.; Shi, L.; Zhang, C.; Shuang, S.; Dong, C. Substituent Effect on the Acid-Induced Isomerization of Spiropyran Compounds. *Spectrochim. Acta Part A Mol. Biomol. Spectrosc.* **2018**, *202*, 13–17. <https://doi.org/10.1016/j.saa.2018.04.076>.
- (48) Kortekaas, L.; Chen, J.; Jacquemin, D.; Browne, W. R. Proton-Stabilized Photochemically Reversible E/ Z Isomerization of Spiropyrans. *J. Phys. Chem. B* **2018**, *122*, 6423–6430. <https://doi.org/10.1021/acs.jpcc.8b03528>.
- (49) Day, J. H. Thermochromism. *Chem. Rev.* **1963**, *63*, 65–80. <https://doi.org/10.1021/cr60221a005>.

- (50) Mustafa, A. The Chemistry of Spiropyran. *Chem. Rev.* **1948**, *43*, 509–523. <https://doi.org/10.1021/cr60136a004>.
- (51) Heller, C. A.; Fine, D. A.; Henry, R. A. PHOTOCROMISM. *J. Phys. Chem.* **1961**, *65*, 1908–1909. <https://doi.org/10.1021/j100827a511>.
- (52) Koelsch, C. F. Steric Factors in Thermochromism of Spiropyran and in Reactivities of Certain Methylene Groups. *J. Org. Chem.* **1951**, *16*, 1362–1370. <https://doi.org/10.1021/jo50003a005>.
- (53) Hirshberg, Y.; Fischer, E. Multiple Reversible Color Changes Initiated by Irradiation at Low Temperature. *J. Chem. Phys.* **1953**, *21*, 1619–1620. <https://doi.org/10.1063/1.1699322>.
- (54) Razavi, B.; Abdollahi, A.; Roghani-Mamaqani, H.; Salami-Kalajahi, M. Light- and Temperature-Responsive Micellar Carriers Prepared by Spiropyran-Initiated Atom Transfer Polymerization: Investigation of Photochromism Kinetics, Responsivities, and Controlled Release of Doxorubicin. *Polymer (Guildf)*. **2020**, *187*, 122046. <https://doi.org/10.1016/j.polymer.2019.122046>.
- (55) Chen, S.; Jiang, F.; Cao, Z.; Wang, G.; Dang, Z.-M. Photo, PH, and Thermo Triple-Responsive Spiropyran-Based Copolymer Nanoparticles for Controlled Release. *Chem. Commun.* **2015**, *51*, 12633–12636. <https://doi.org/10.1039/C5CC04087F>.
- (56) Ali, A. A.; Kharbash, R.; Kim, Y. Chemo- and Biosensing Applications of Spiropyran and Its Derivatives - A Review. *Anal. Chim. Acta* **2020**, *1110*, 199–223. <https://doi.org/10.1016/j.aca.2020.01.057>.
- (57) Keum, S.-R.; Lee, K.-B.; Kazmaier, P. M.; Manderville, R. A.; Buncel, E. Thermo- and Photochromic Dyes: Spiro(Indolinebenzopyrans). 2—Detailed Assignment of The¹H NMR Spectra and Structural Aspects of the Closed Form of 1,3,3-Trimethylspiro(Indoline-2,2'-Benzopyrans). *Magn. Reson. Chem.* **1992**, *30*, 1128–1131. <https://doi.org/10.1002/mrc.1260301119>.

- (58) Balmond, E. I.; Tautges, B. K.; Faulkner, A. L.; Or, V. W.; Hodur, B. M.; Shaw, J. T.; Louie, A. Y. Comparative Evaluation of Substituent Effect on the Photochromic Properties of Spiropyrans and Spirooxazines. *J. Org. Chem.* **2016**, *81*, 8744–8758. <https://doi.org/10.1021/acs.joc.6b01193>.
- (59) Kim, D. W.; Kang, H.; Lee, Y.-S.; Kim, E.; Kang, Y.; Lee, C. Preparation of Merocyanine Salts by Treatment of Acids on Spiropyran and Investigation on Their Photochromic Behaviors. *J. Nonlinear Opt. Phys. Mater.* **2004**, *13*, 575–579. <https://doi.org/10.1142/S0218863504002286>.
- (60) Carroll, F. A. *Perspectives on Structure and Mechanism in Organic Chemistry*, 2nd ed.; Wiley, **2010**.
- (61) Li, T.; Yu, L.; Jin, D.; Chen, B.; Li, L.; Chen, L.; Li, Y. A Colorimetric and Fluorescent Probe for Fluoride Anions Based on a Phenanthroimidazole-Cyanine Platform. *Anal. Methods* **2013**, *5*, 1612–1616. <https://doi.org/10.1039/c3ay26461k>.
- (62) Natali, M.; Giordani, S. Interaction Studies between Photochromic Spiropyrans and Transition Metal Cations: The Curious Case of Copper. *Org. Biomol. Chem.* **2012**, *10*, 1162–1171. <https://doi.org/10.1039/C1OB06375H>.
- (63) Renuka, J.; Reddy, K. I.; Srihari, K.; Jeankumar, V. U.; Shravan, M.; Sridevi, J. P.; Yogeewari, P.; Babu, K. S.; Sriram, D. Design, Synthesis, Biological Evaluation of Substituted Benzofurans as DNA GyraseB Inhibitors of Mycobacterium Tuberculosis. *Bioorganic Med. Chem.* **2014**, *22*, 4924–4934. <https://doi.org/10.1016/j.bmc.2014.06.041>.
- (64) Zhang, Y.; Wang, S. Preparation of Smart Poly(SPAA-Co-MMA) Film Materials for Regulating Wettability and Humidity by Electrospinning. *Polym. Eng. Sci.* **2019**, *59*, E279–E286. <https://doi.org/10.1002/pen.24932>.
- (65) Kim, B. M.; Bae, S. J.; So, S. M.; Yoo, H. T.; Chang, S. K.; Lee, J. H.; Kang, J. Synthesis of a Chiral Aziridine Derivative as a Versatile Intermediate for HIV Protease Inhibitors. *Org. Lett.* **2001**, *3*, 2349–2351. <https://doi.org/10.1021/ol016147s>.

- (66) Bailey, S. J.; Wales, S. M.; Willis, A. C.; Keller, P. A. Ring-Opening and -Expansion of 2,2'-Biaziridine: Access to Diverse Enantiopure Linear and Bicyclic Vicinal Diamines. *Org. Lett.* **2014**, *16*, 4344–4347. <https://doi.org/10.1021/ol502164b>.
- (67) Gyepes, A.; Schäffer, R.; Bajor, G.; Woller, Á.; Fodor, P. Synthesis and Chromatographic Study of Methyl-2,3-O-Isopropylidene-5-Dimethyl-Arsinoyl- β -d-Ribofuranoside and Methyl-2,3-O-Isopropylidene-5-Deoxy-5-Dimethyl-Thioarsinoyl- β -d-Ribofuranoside. *Polyhedron* **2008**, *27*, 2655–2661. <https://doi.org/10.1016/j.poly.2008.04.049>.
- (68) Downey, A. M.; Pohl, R.; Roithová, J.; Hocek, M. Synthesis of Nucleosides through Direct Glycosylation of Nucleobases with 5- O -Monoprotected or 5-Modified Ribose: Improved Protocol, Scope, and Mechanism. *Chem. - A Eur. J.* **2017**, *23*, 3910–3917. <https://doi.org/10.1002/chem.201604955>.
- (69) Baird, L. J.; Timmer, M. S. M.; Teesdale-Spittle, P. H.; Harvey, J. E. Total Synthesis of Aigialomycin D Using a Ramberg–Bäcklund/RCM Strategy. *J. Org. Chem.* **2009**, *74*, 2271–2277. <https://doi.org/10.1021/jo802561s>.
- (70) Raymo, F. M.; Giordani, S.; White, A. J. P.; Williams, D. J. Digital Processing with a Three-State Molecular Switch. *J. Org. Chem.* **2003**, *68*, 4158–4169. <https://doi.org/10.1021/jo0340455>.
- (71) Baloch, S. K.; Ma, L.; Wang, X.-L.; Shi, J.; Zhu, Y.; Wu, F.-Y.; Pang, Y.-J.; Lu, G.-H.; Qi, J.-L.; Wang, X.-M.; Gu, H.-W.; Yang, Y.-H. Design, Synthesis and Mechanism of Novel Shikonin Derivatives as Potent Anticancer Agents. *RSC Adv.* **2015**, *5*, 31759–31767. <https://doi.org/10.1039/C5RA01872B>.

APPENDICES

A. NMR Spectra

NMR spectra were recorded at Bruker Avance III Ultrashield 400 Hz. CDCl_3 and DMSO were used as solvent in all records.

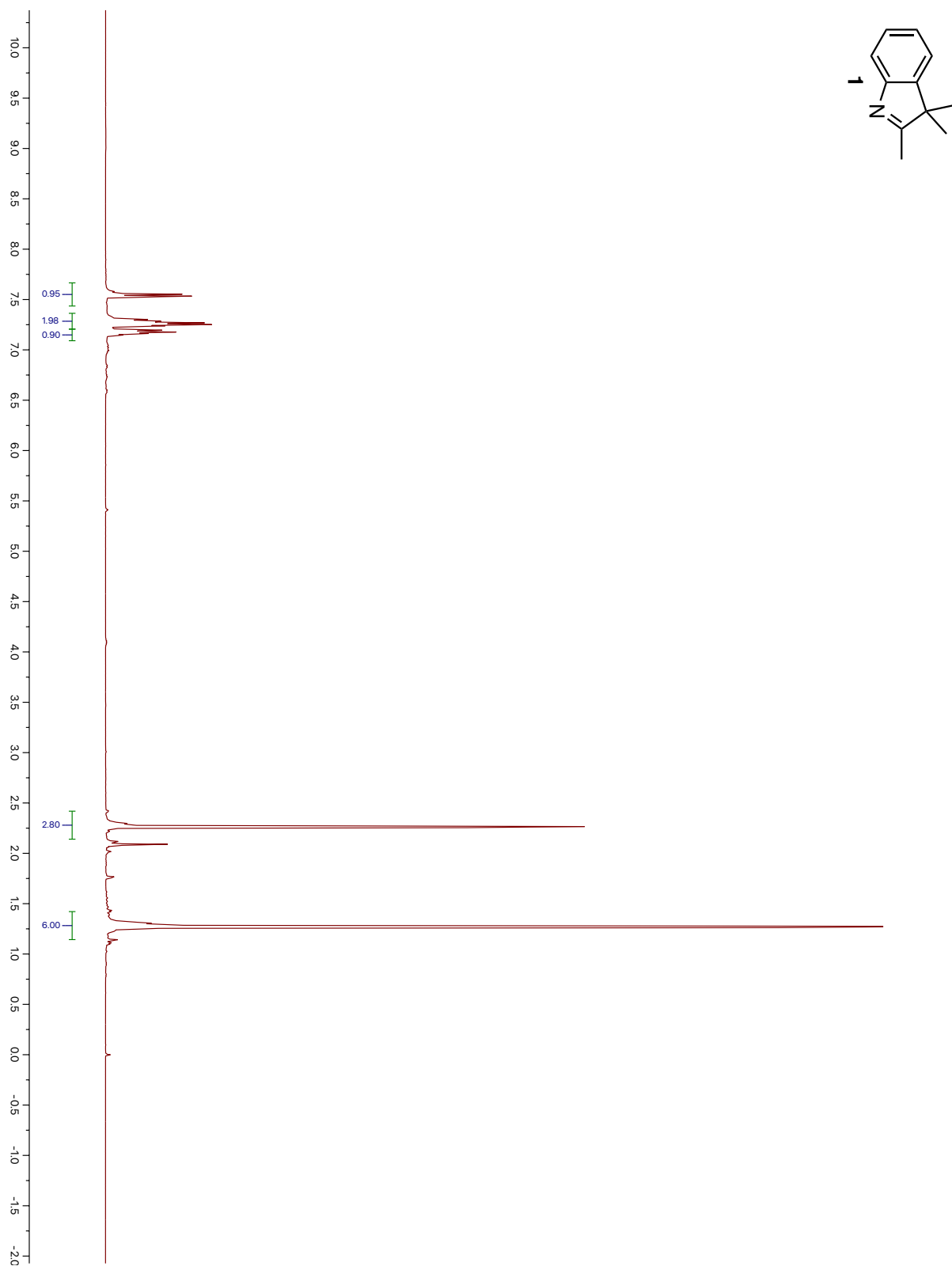


Figure 34. ¹H NMR spectrum of Compound 1

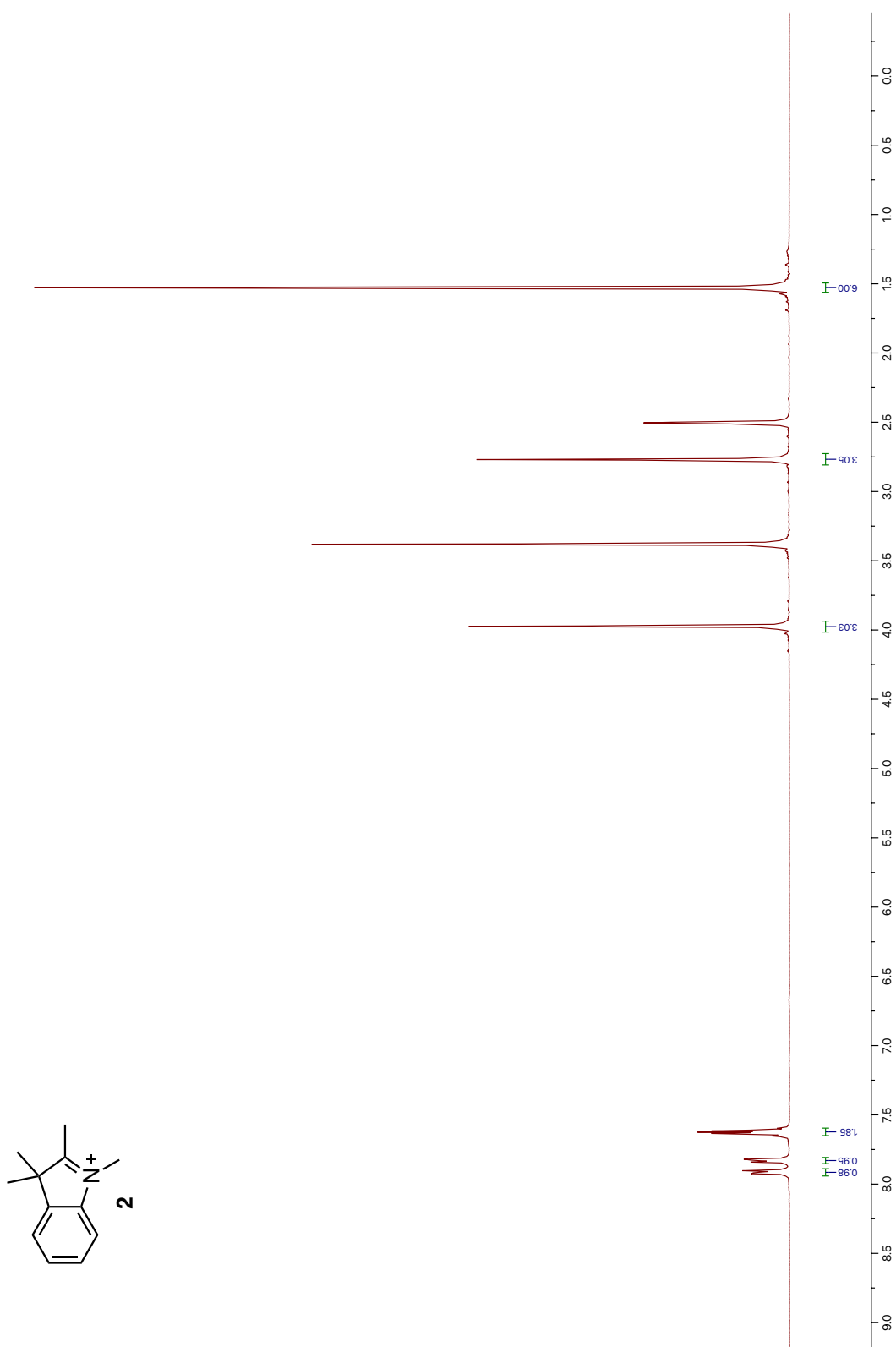


Figure 35. ¹H NMR spectrum of Compound 2

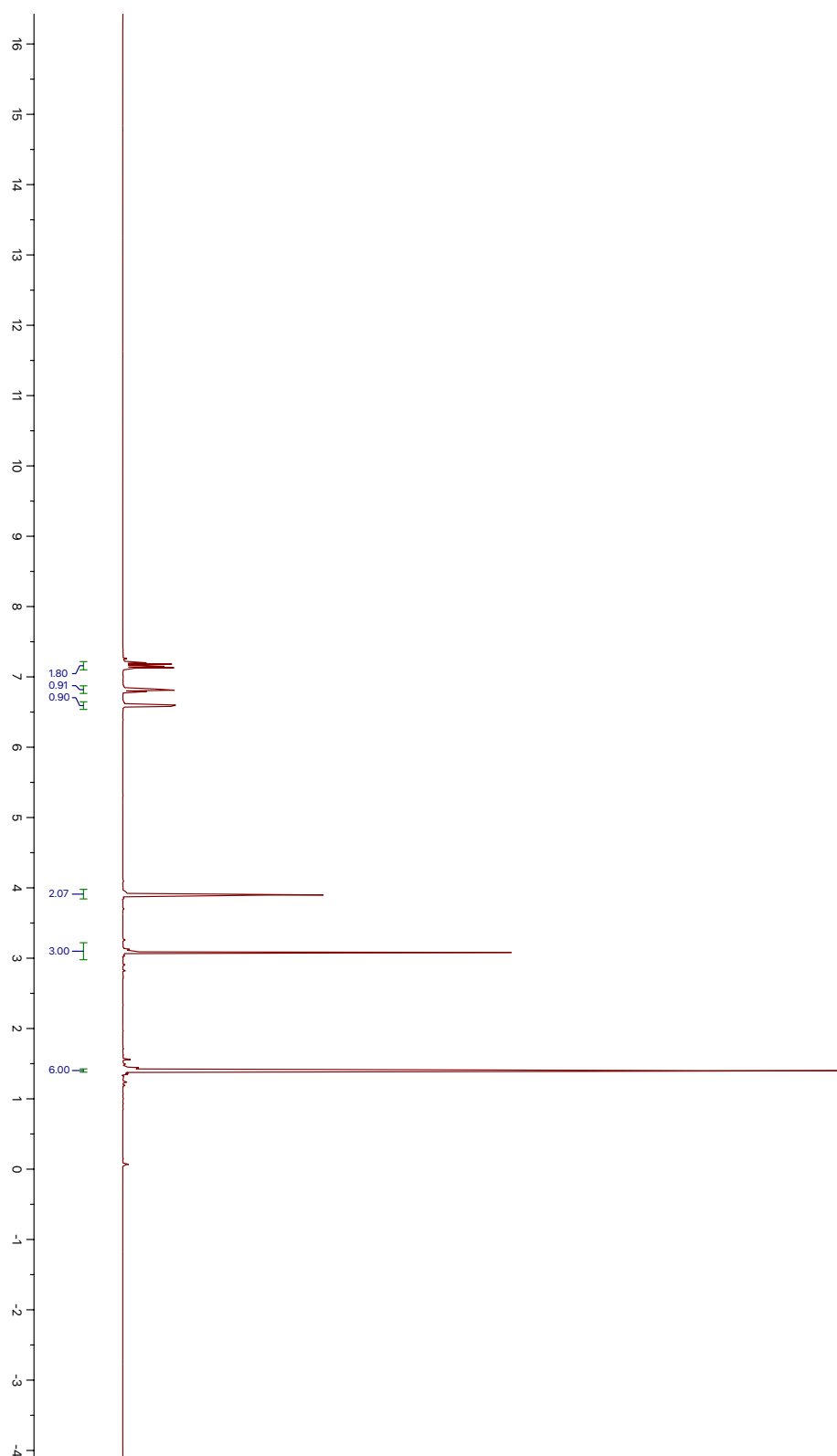
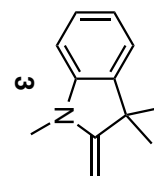


Figure 36. ^1H NMR spectrum of Compound 3

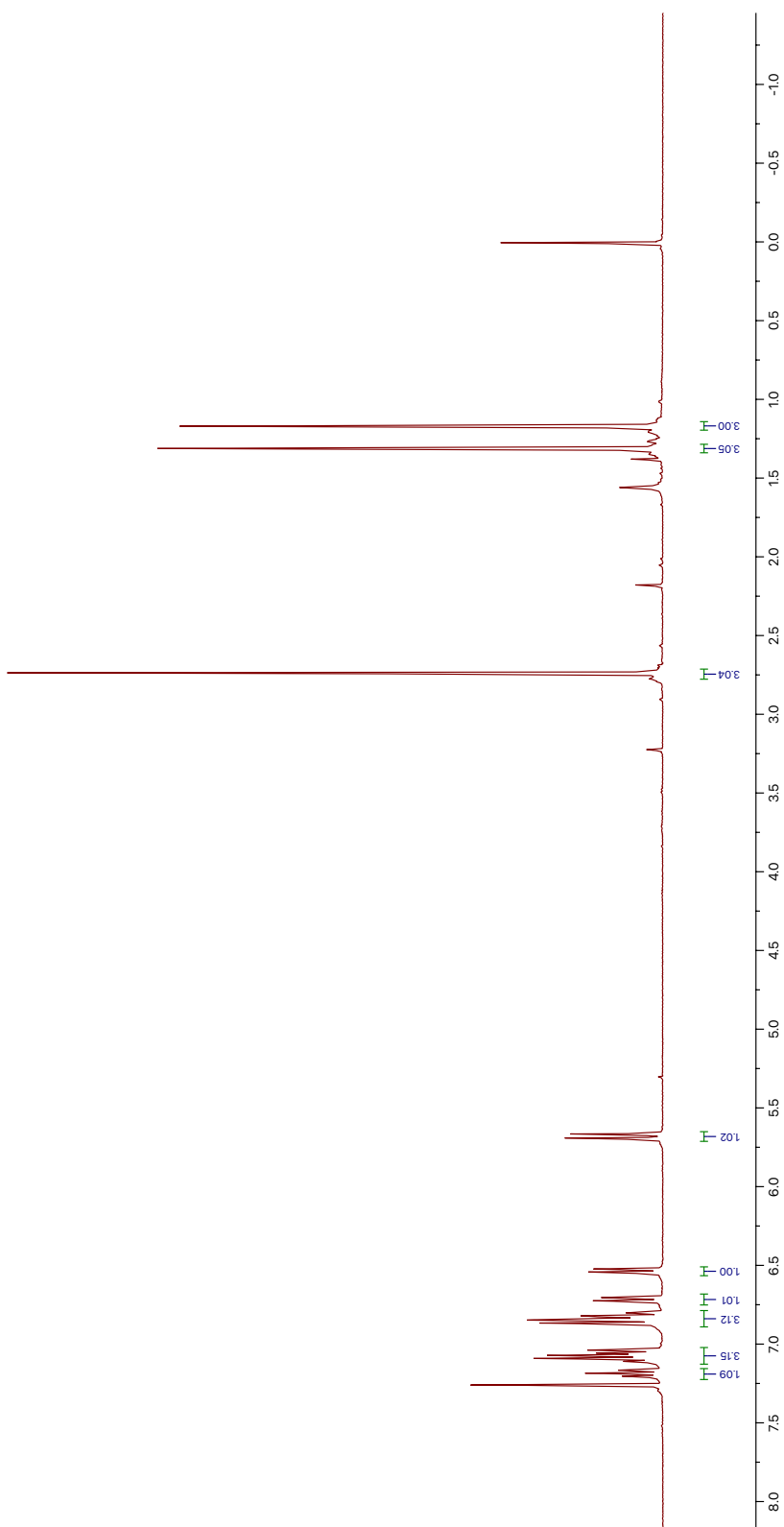
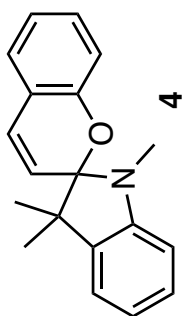


Figure 37. ¹H NMR spectrum of Compound 4

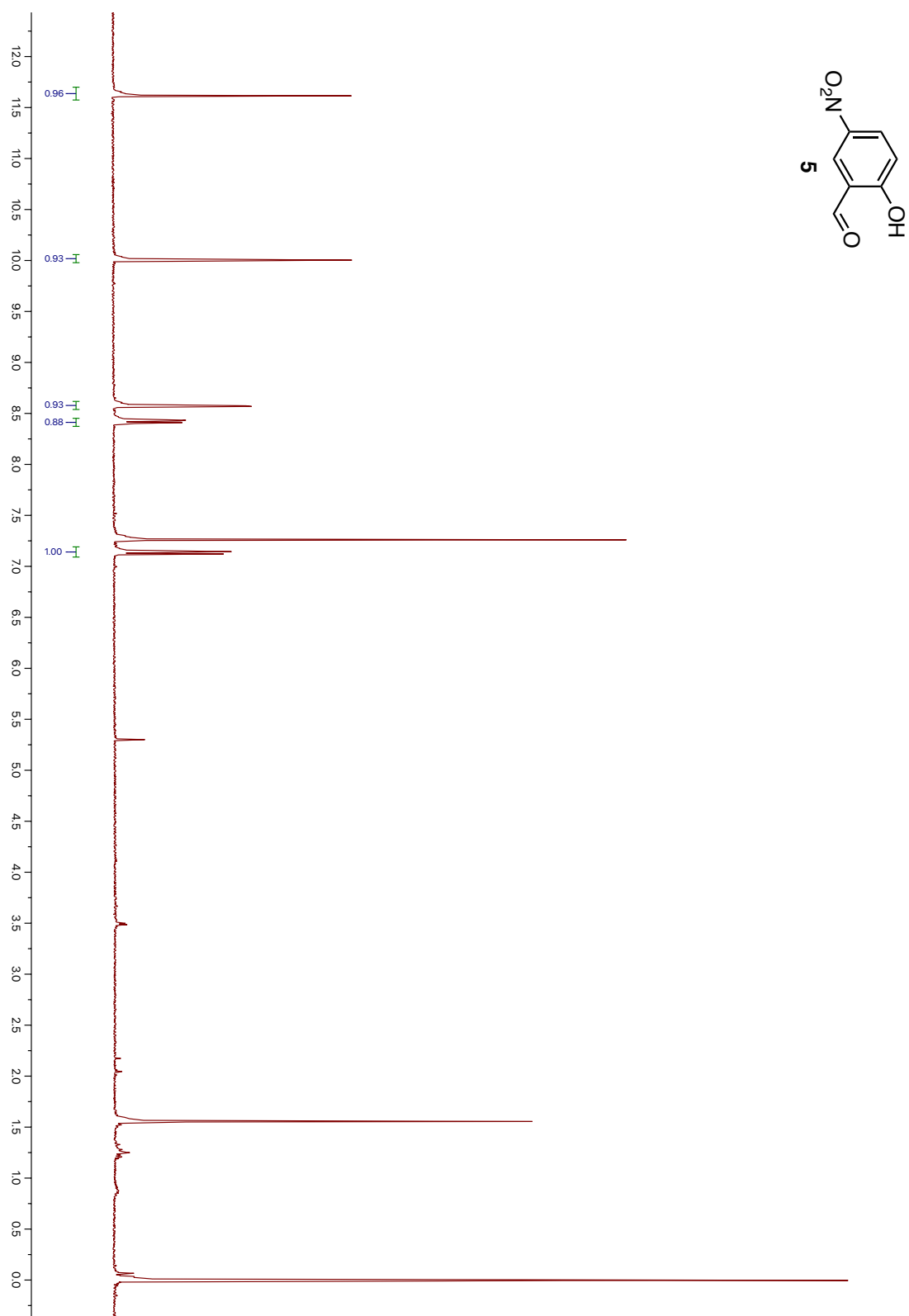


Figure 38. ¹H NMR spectrum of 2-hydroxy-5-nitrobenzaldehyde (**5**)

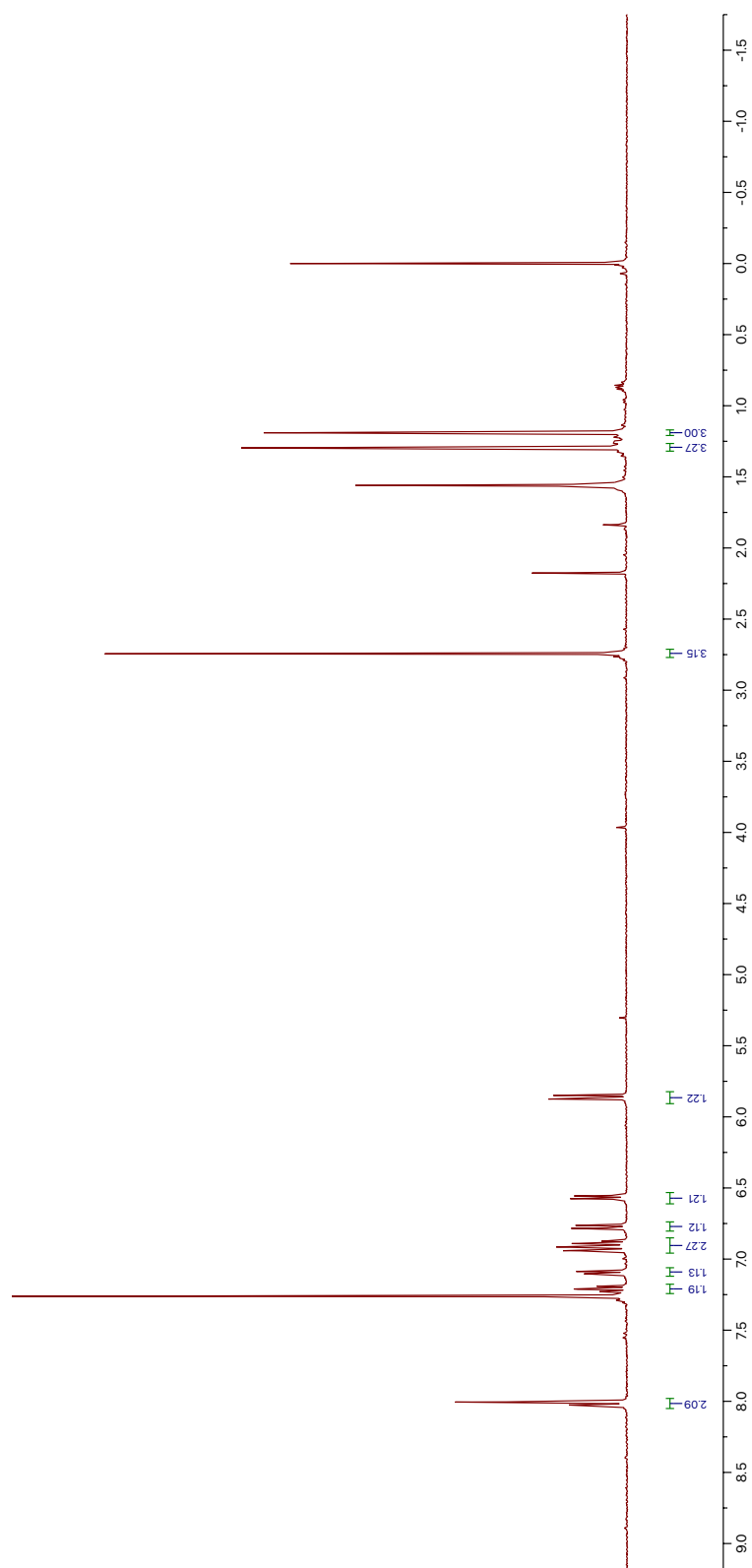
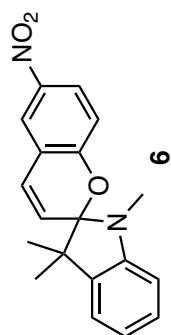


Figure 39. ¹H NMR spectrum of Compound 6

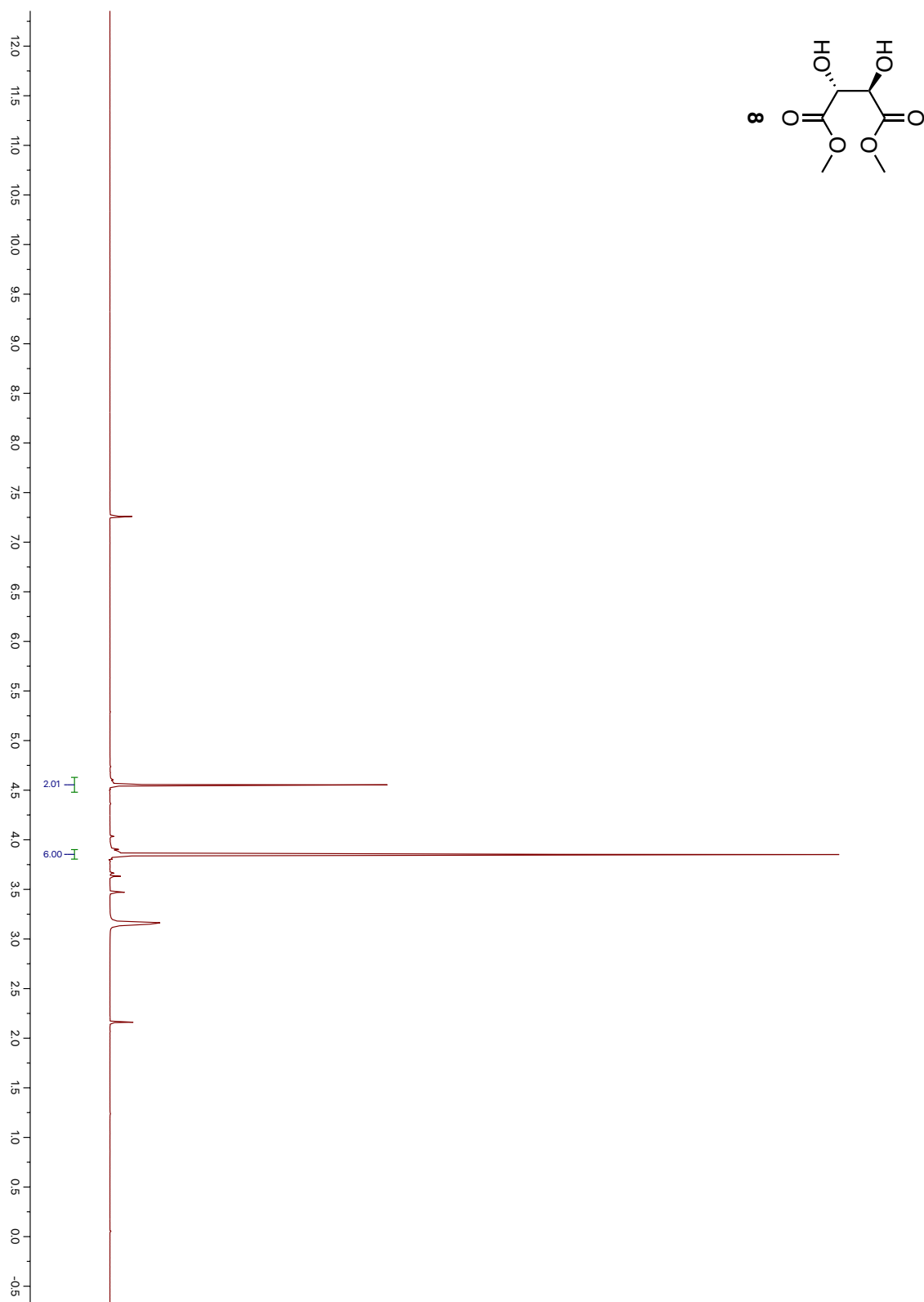


Figure 40. ¹H NMR spectrum of Compound 8

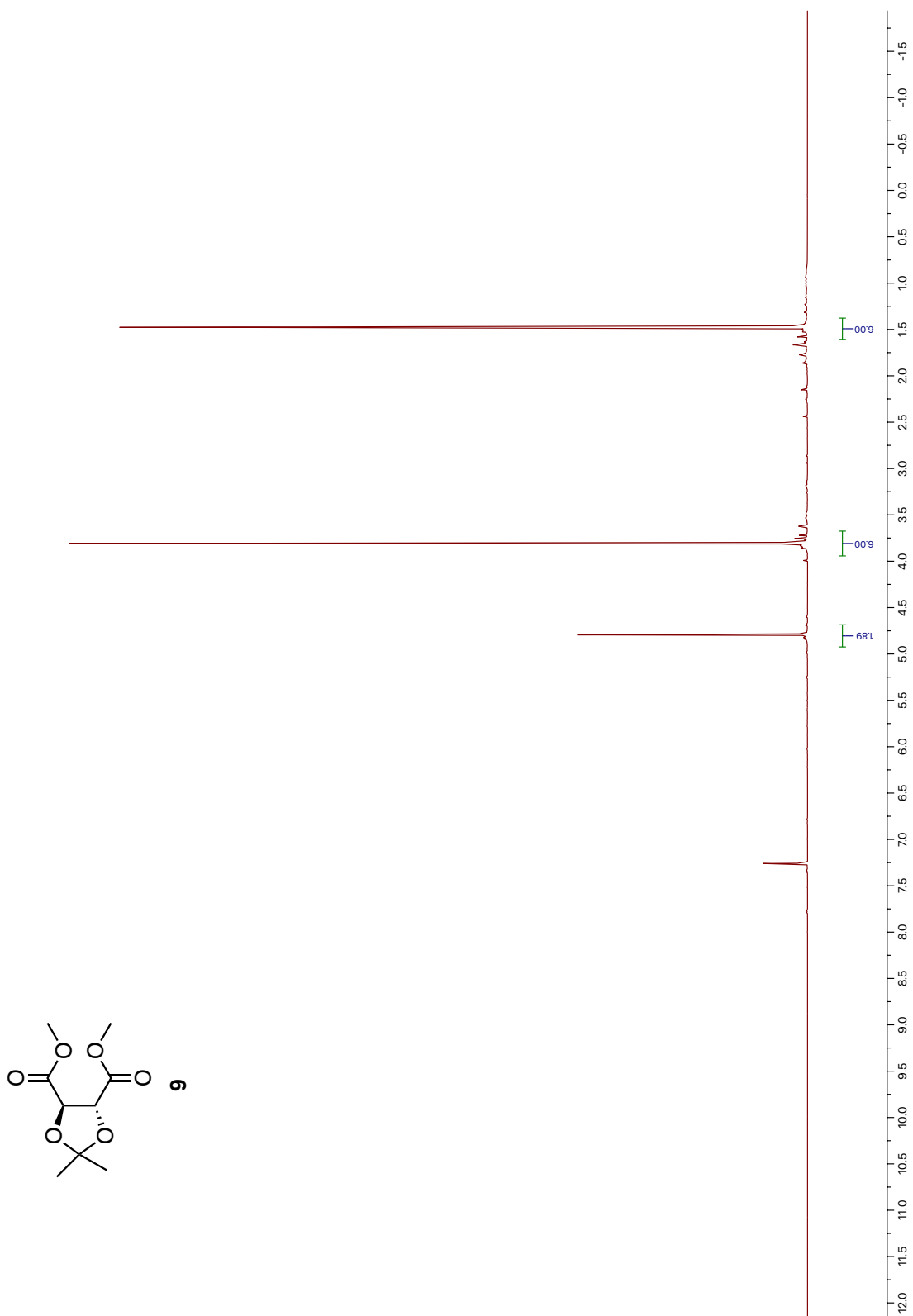


Figure 41. ¹H NMR spectrum of Compound 9

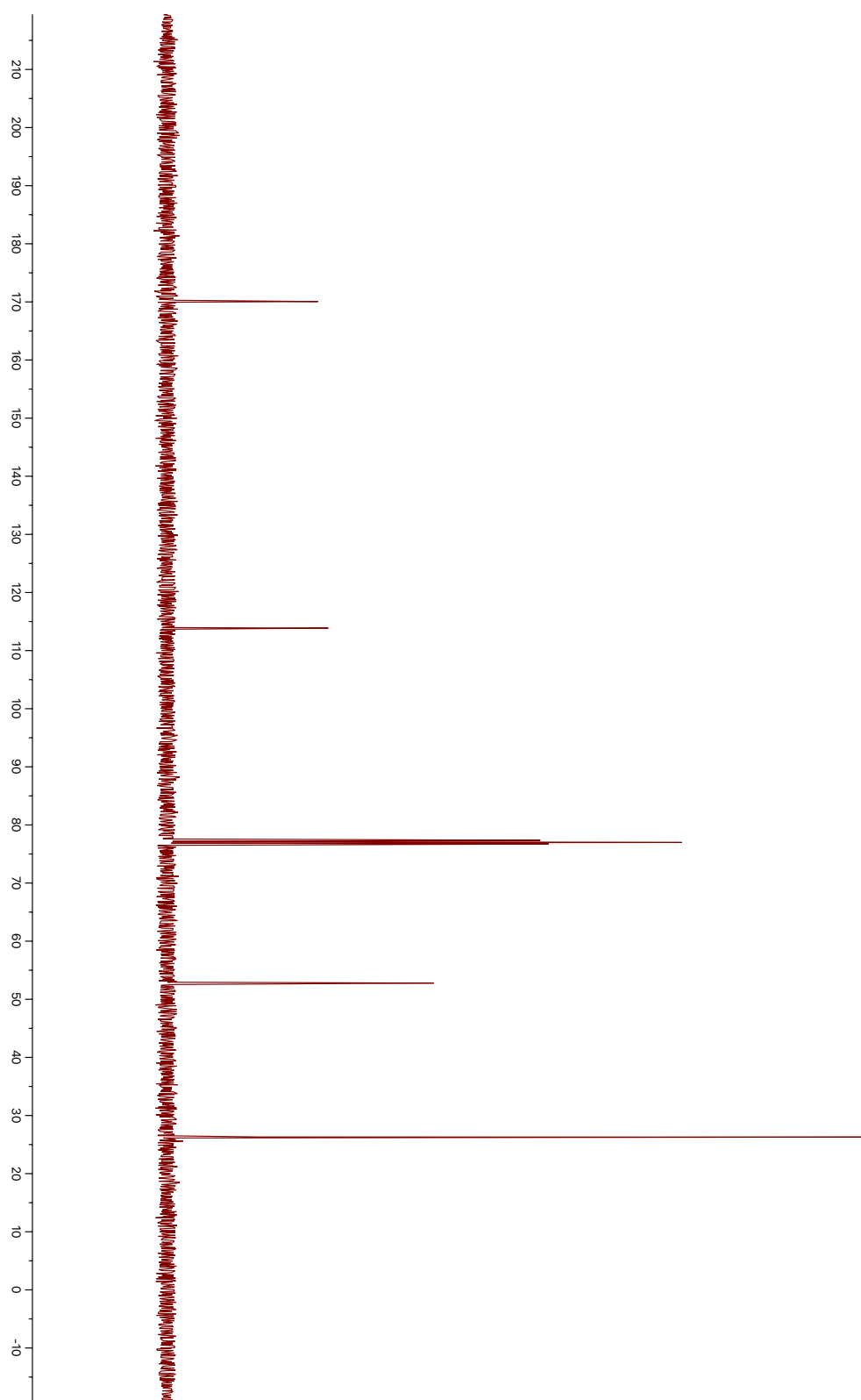


Figure 42. ^{13}C NMR spectrum of compound 9

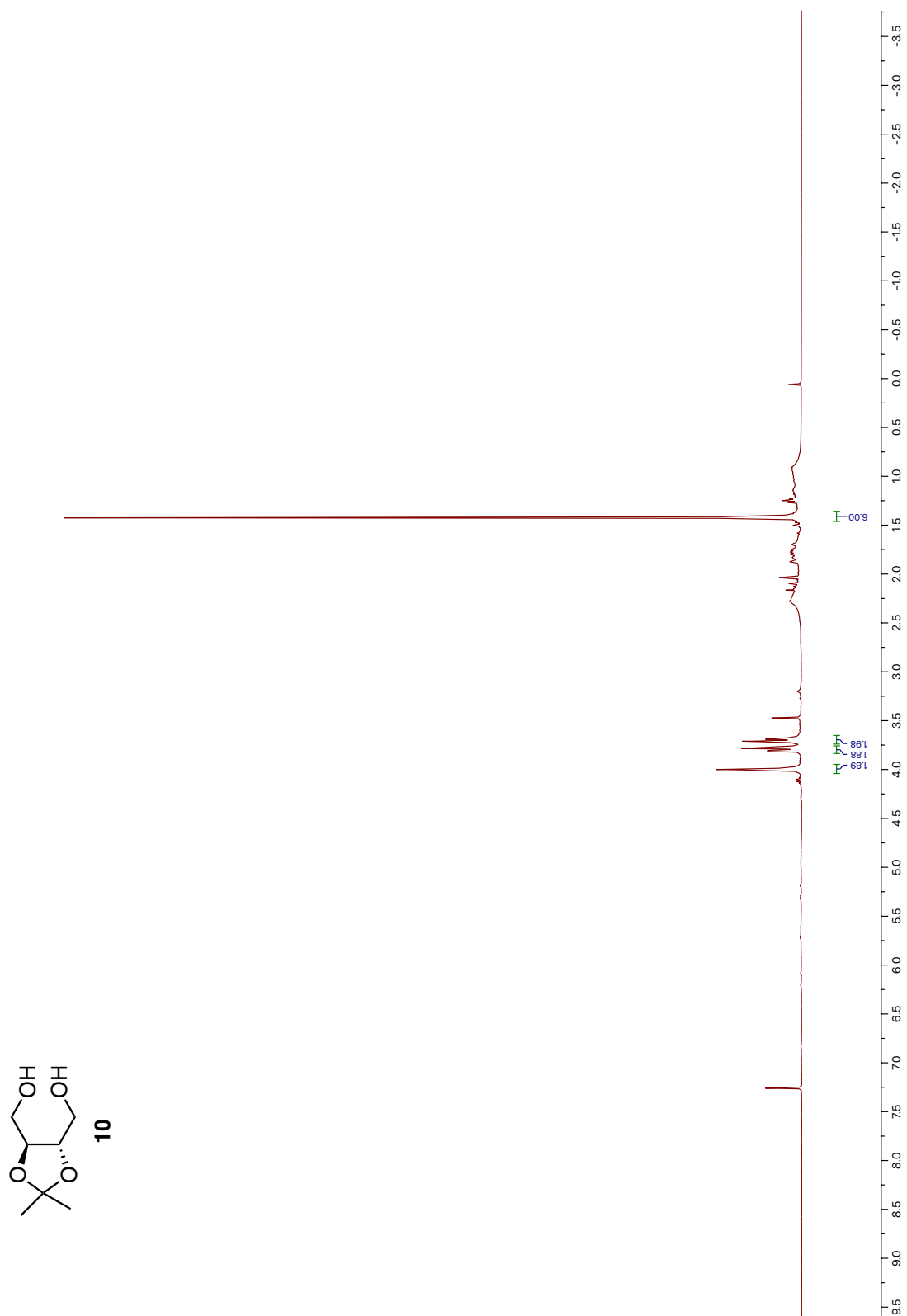


Figure 43. ¹H NMR spectrum of Compound 10

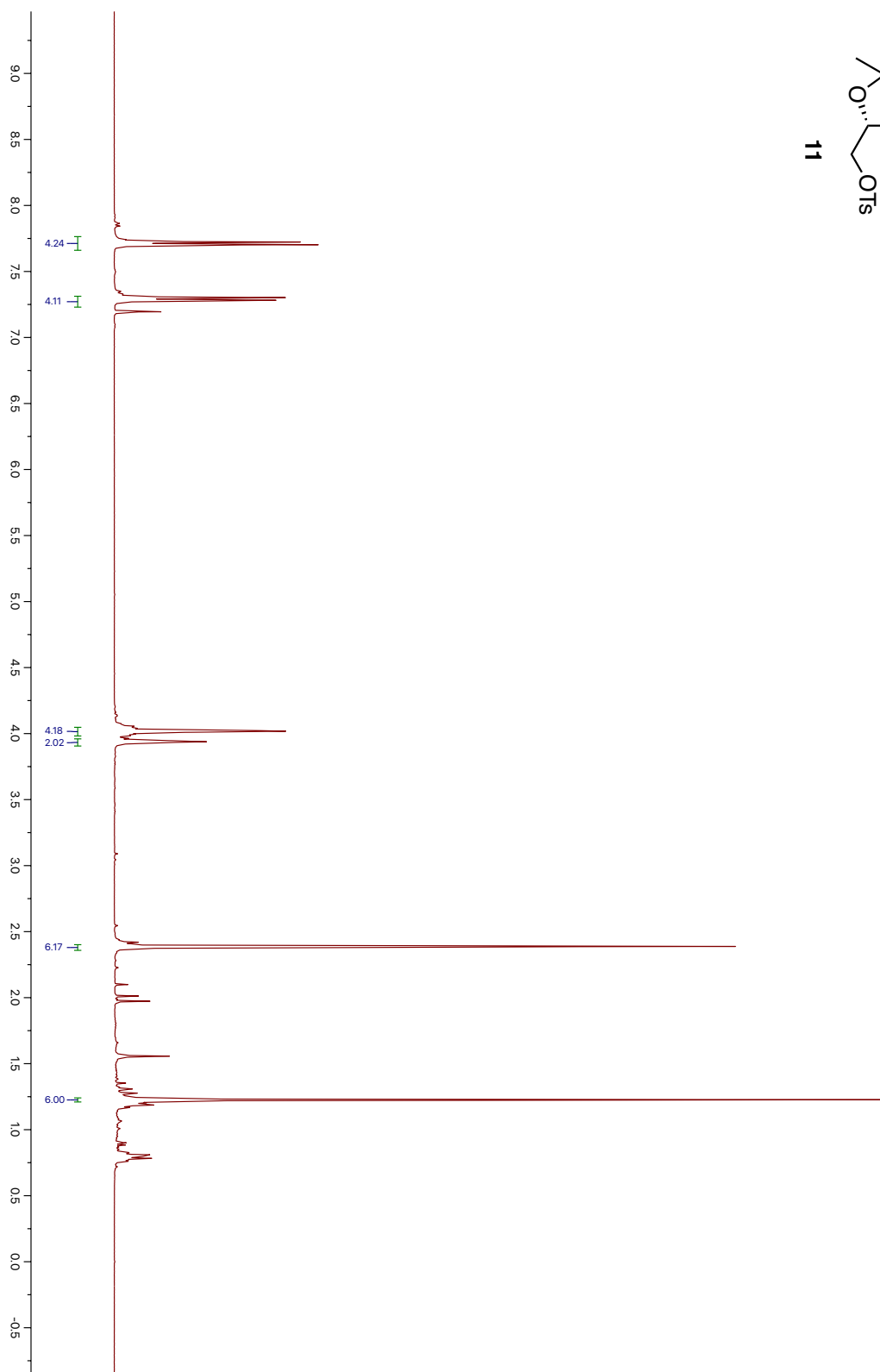
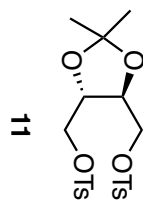


Figure 44. ¹H NMR spectrum of Compound 11

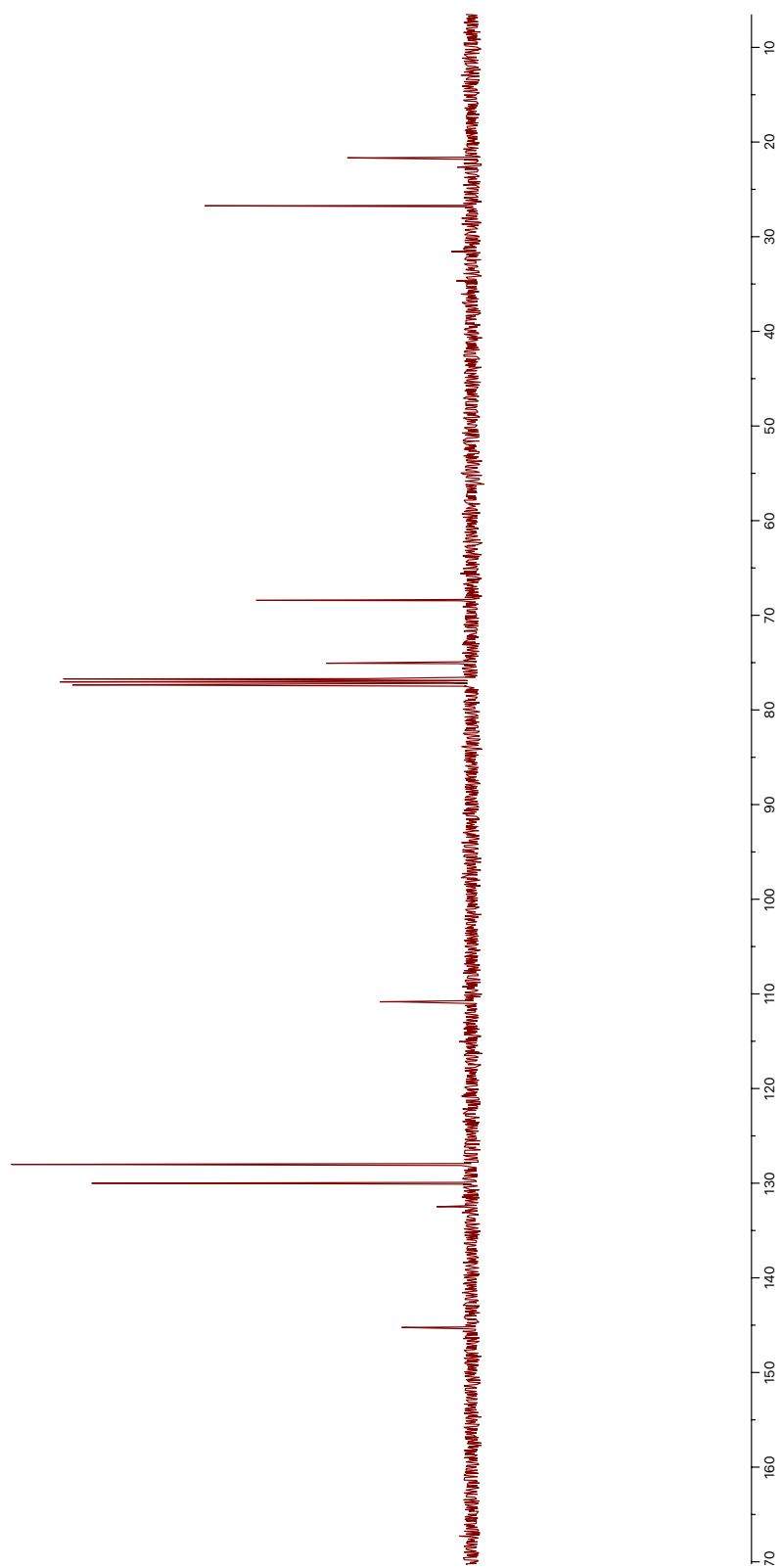


Figure 45. ^{13}C NMR spectrum of Compound 11

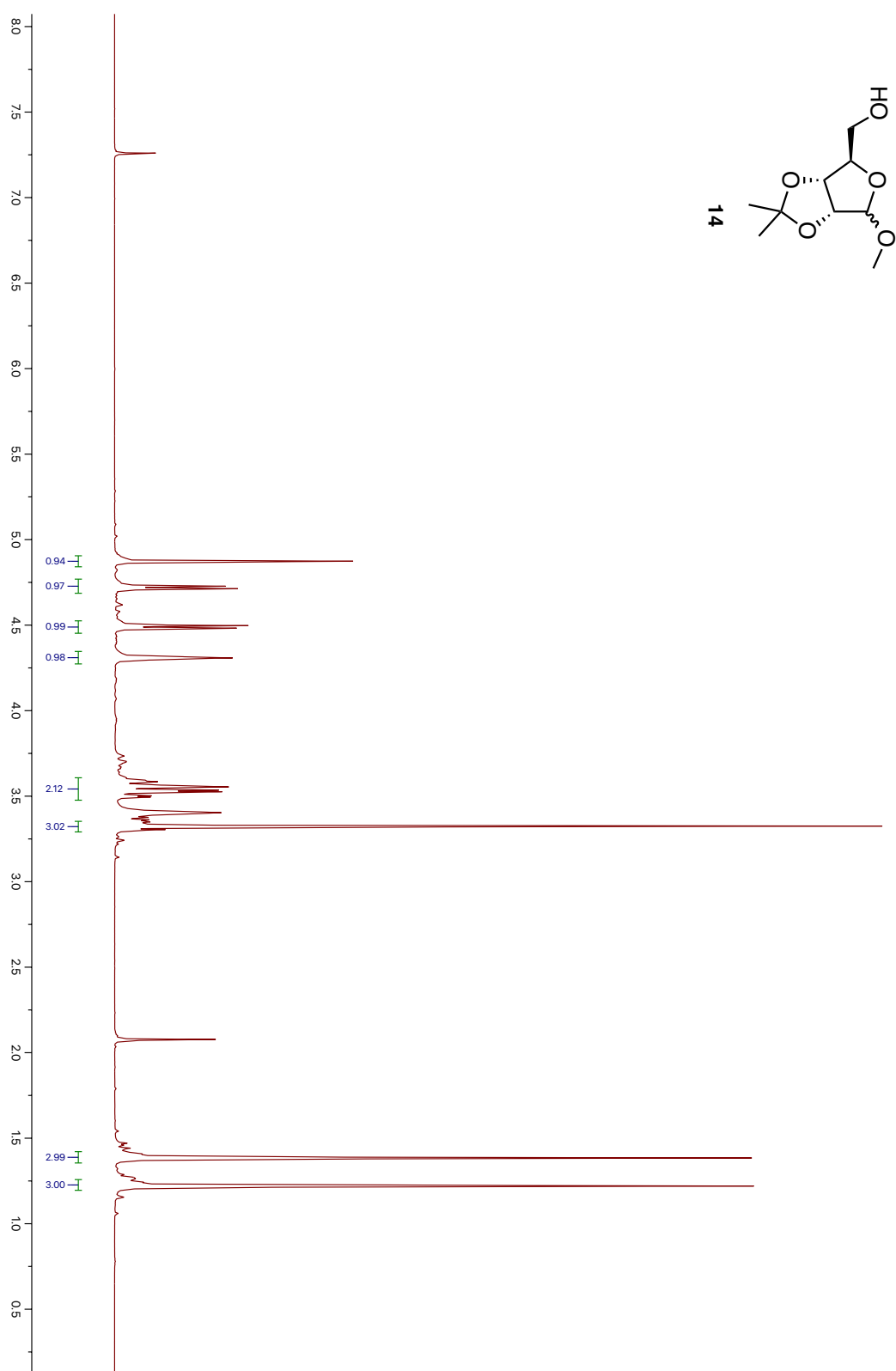


Figure 46. ¹H NMR spectrum of Compound 14

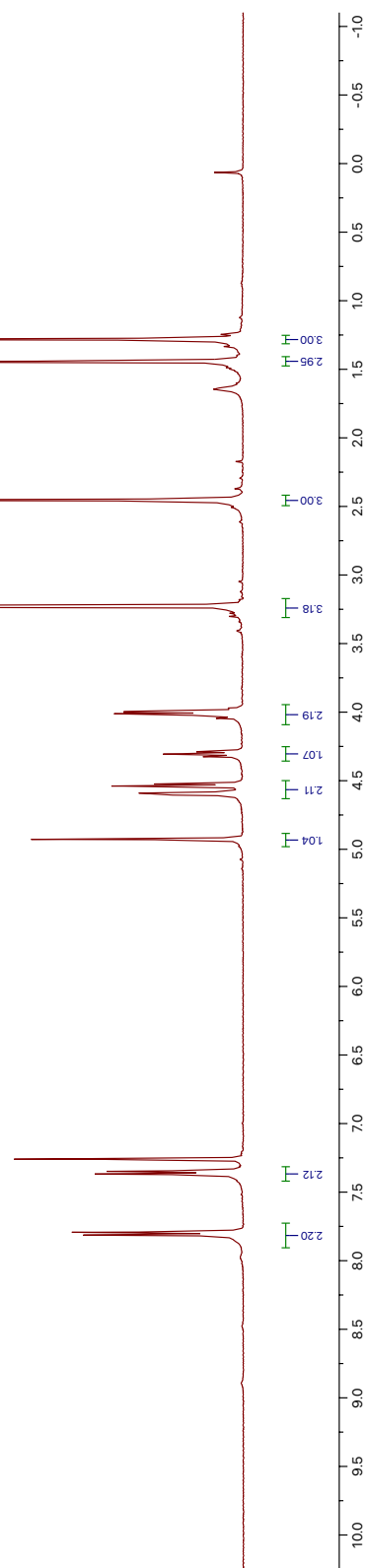
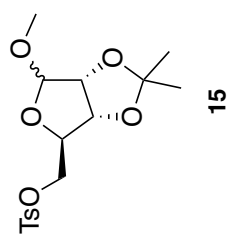


Figure 47. ¹H NMR spectrum of Compound 15

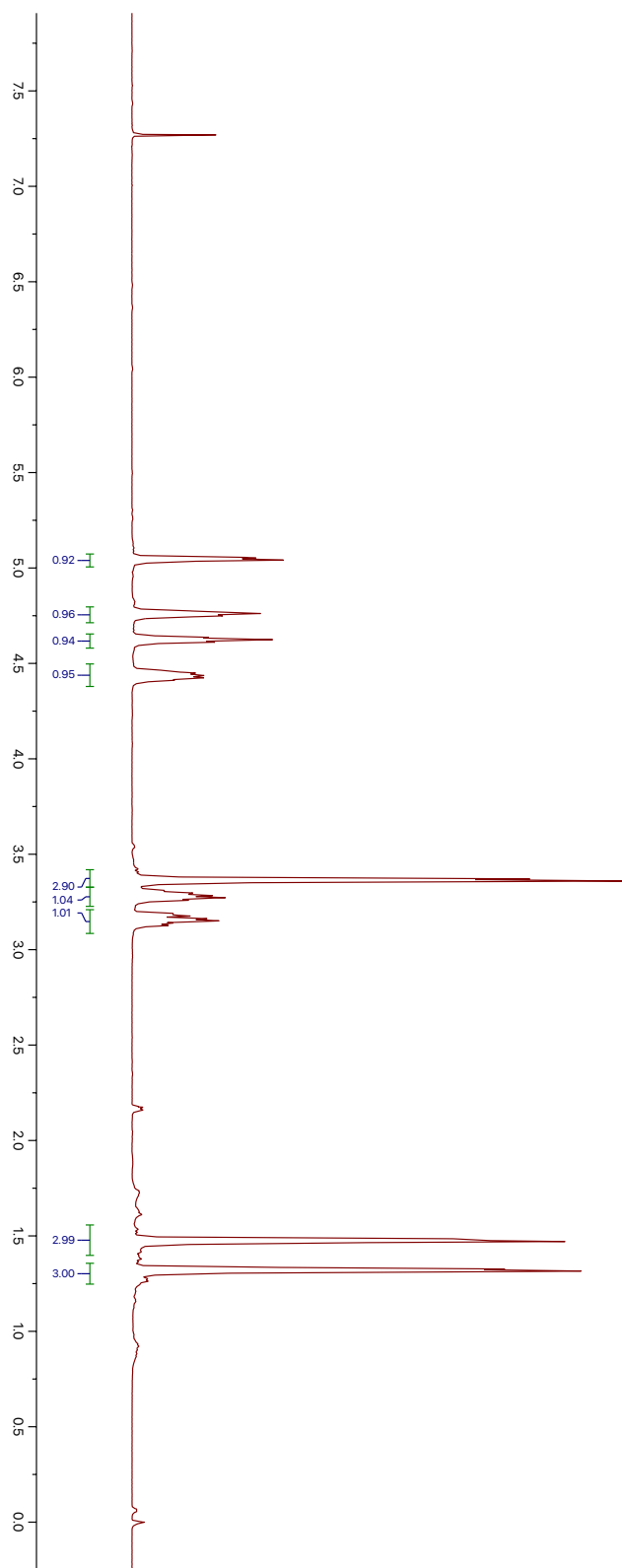
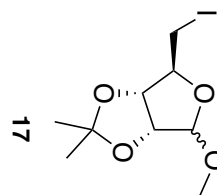


Figure 48. ¹H NMR spectrum of Compound 17

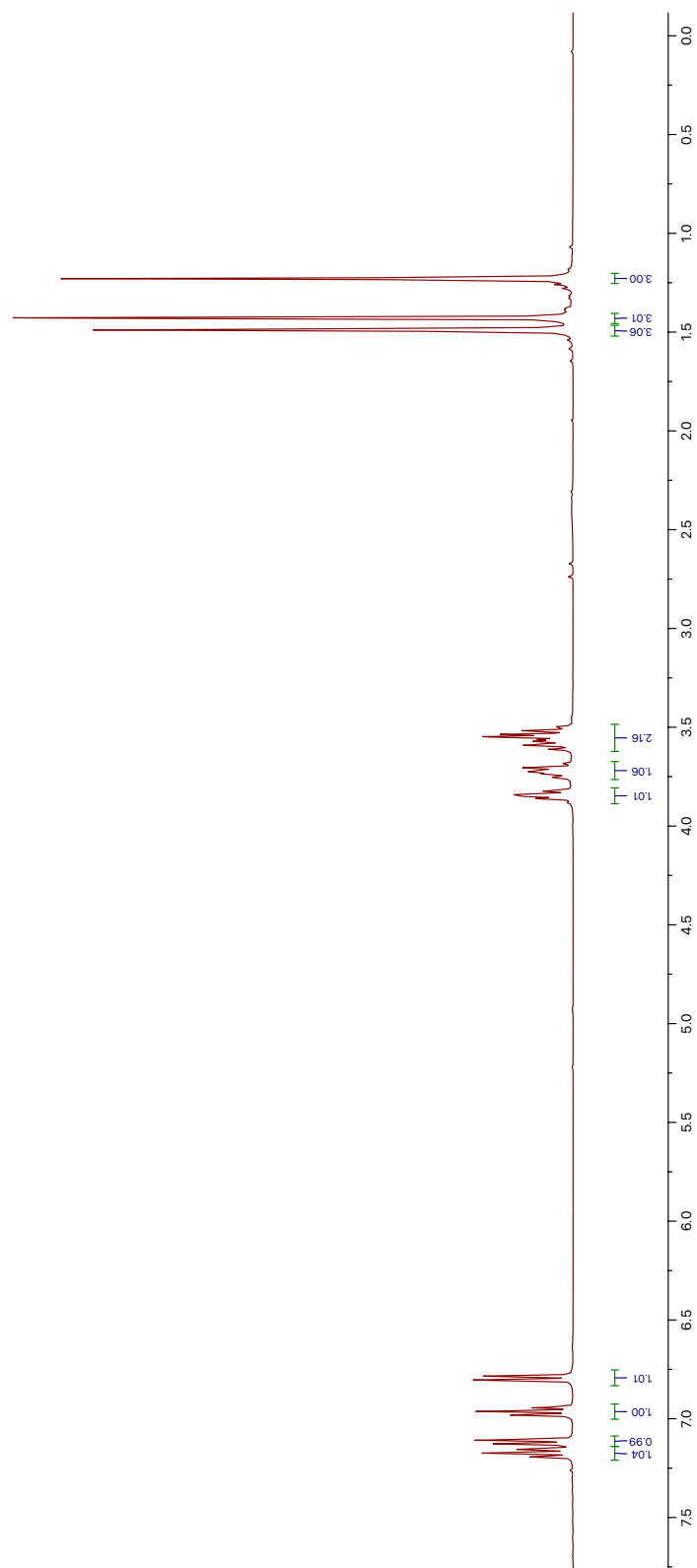
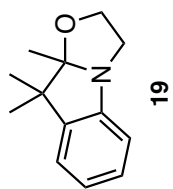


Figure 49. ¹H NMR spectrum of Compound 19

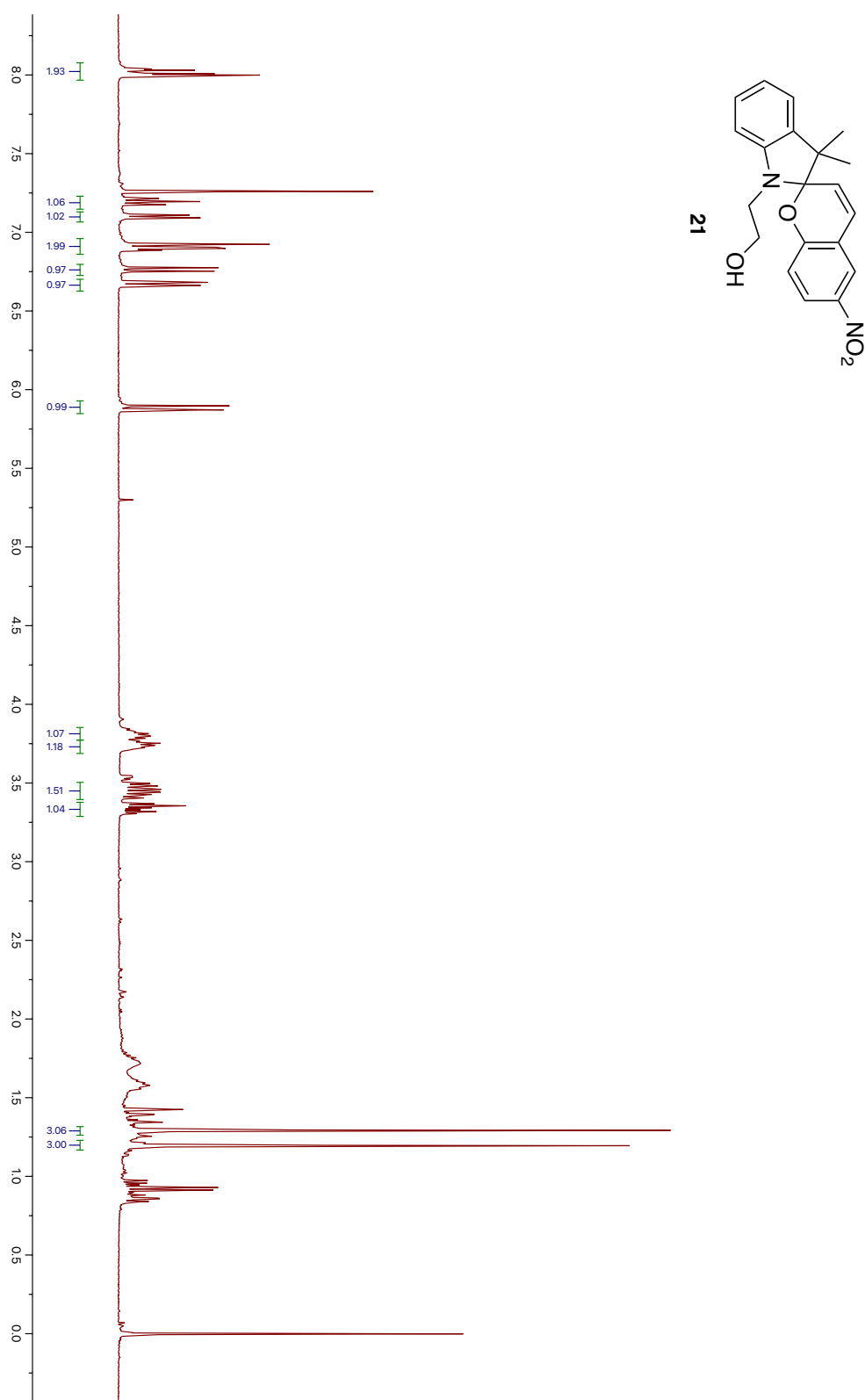


Figure 50. ¹H NMR spectrum of Compound 21

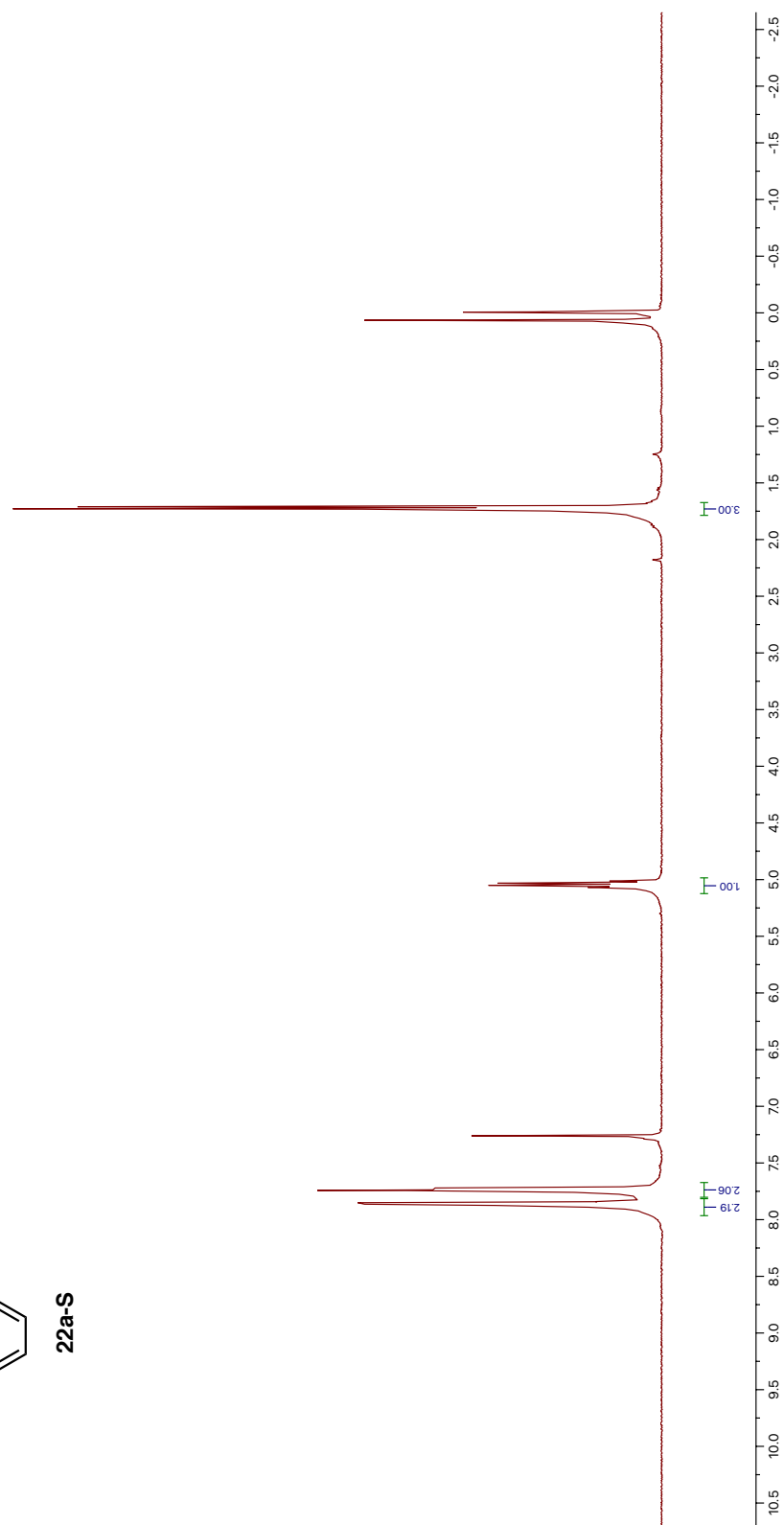
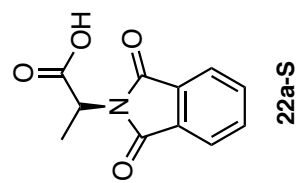


Figure 51. ¹H NMR spectrum of Compound 22a-S

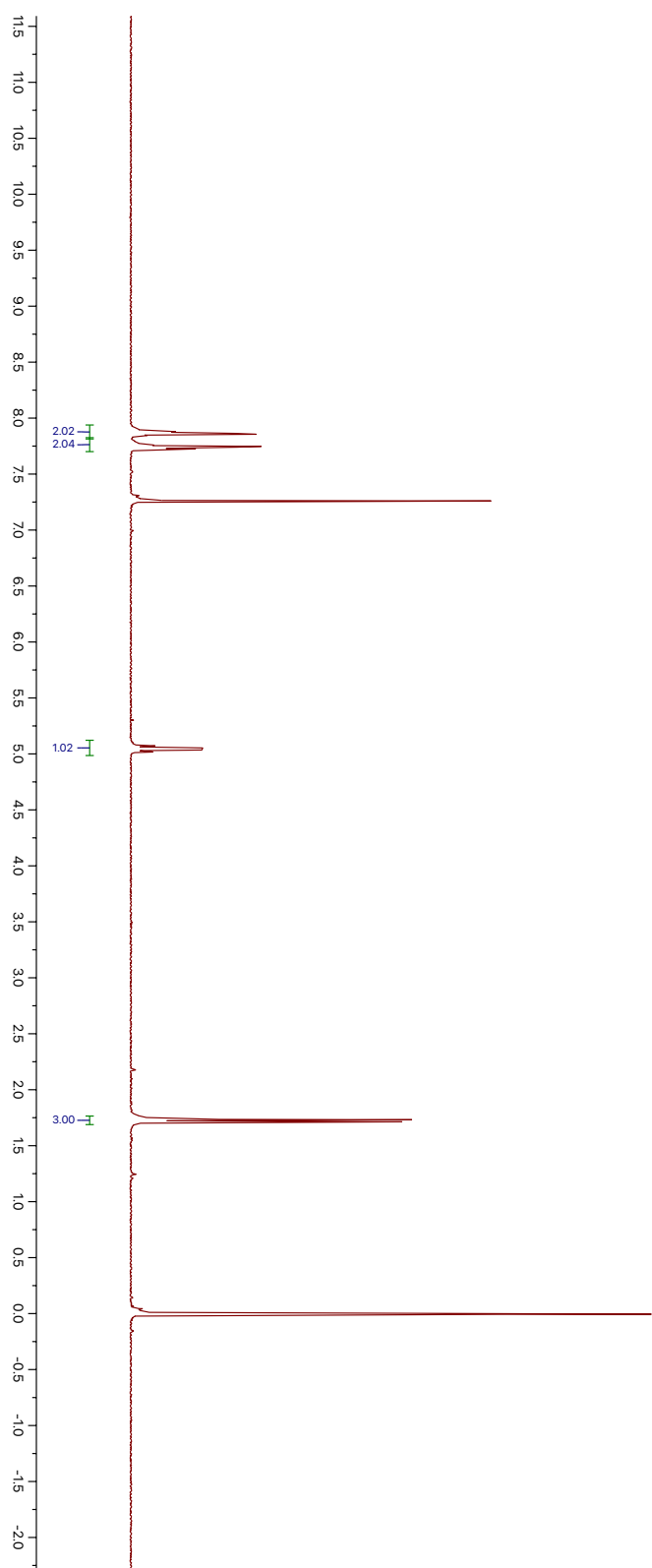
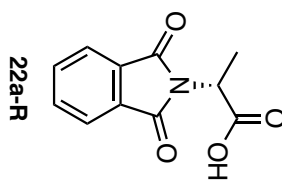


Figure 52. ¹H NMR spectrum of Compound 22a-R

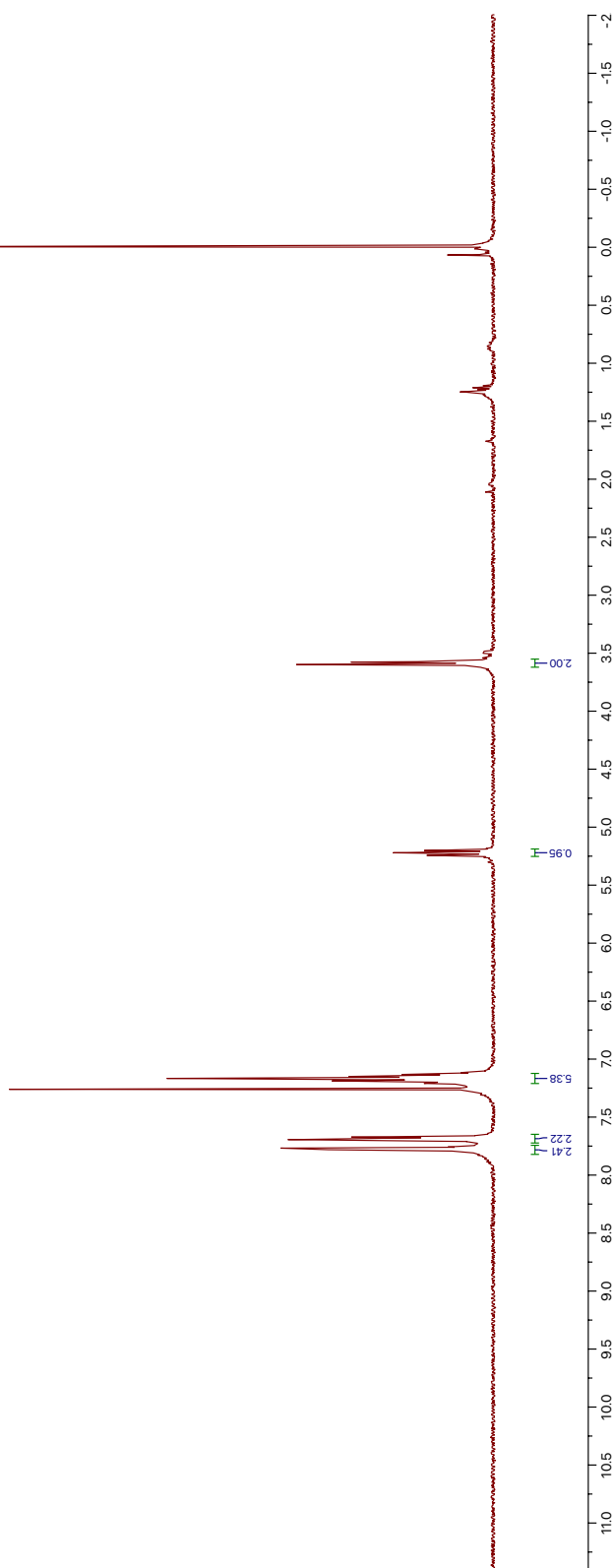
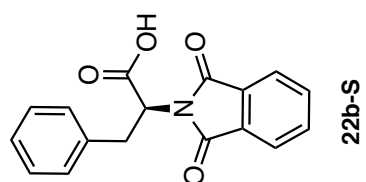


Figure 53. ¹H NMR spectrum of Compound **22b-S**

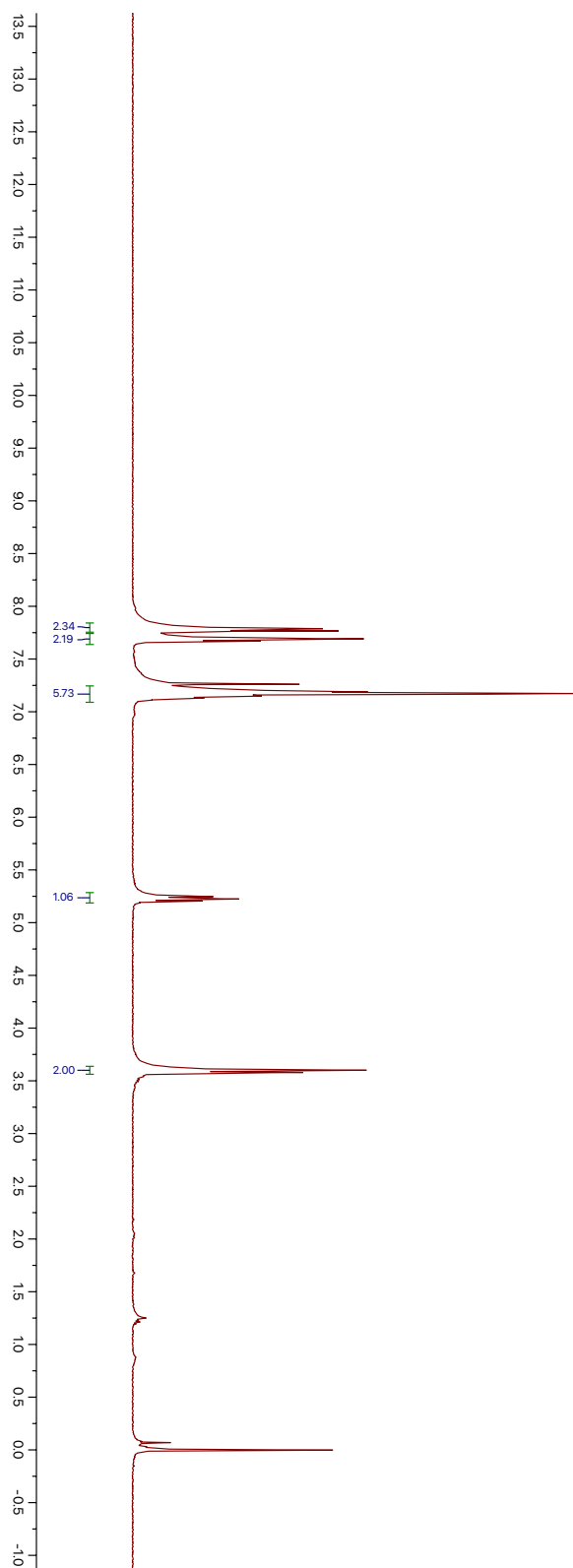
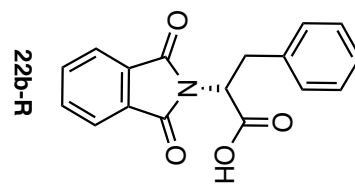


Figure 54. ^1H NMR spectrum of Compound **22b-R**

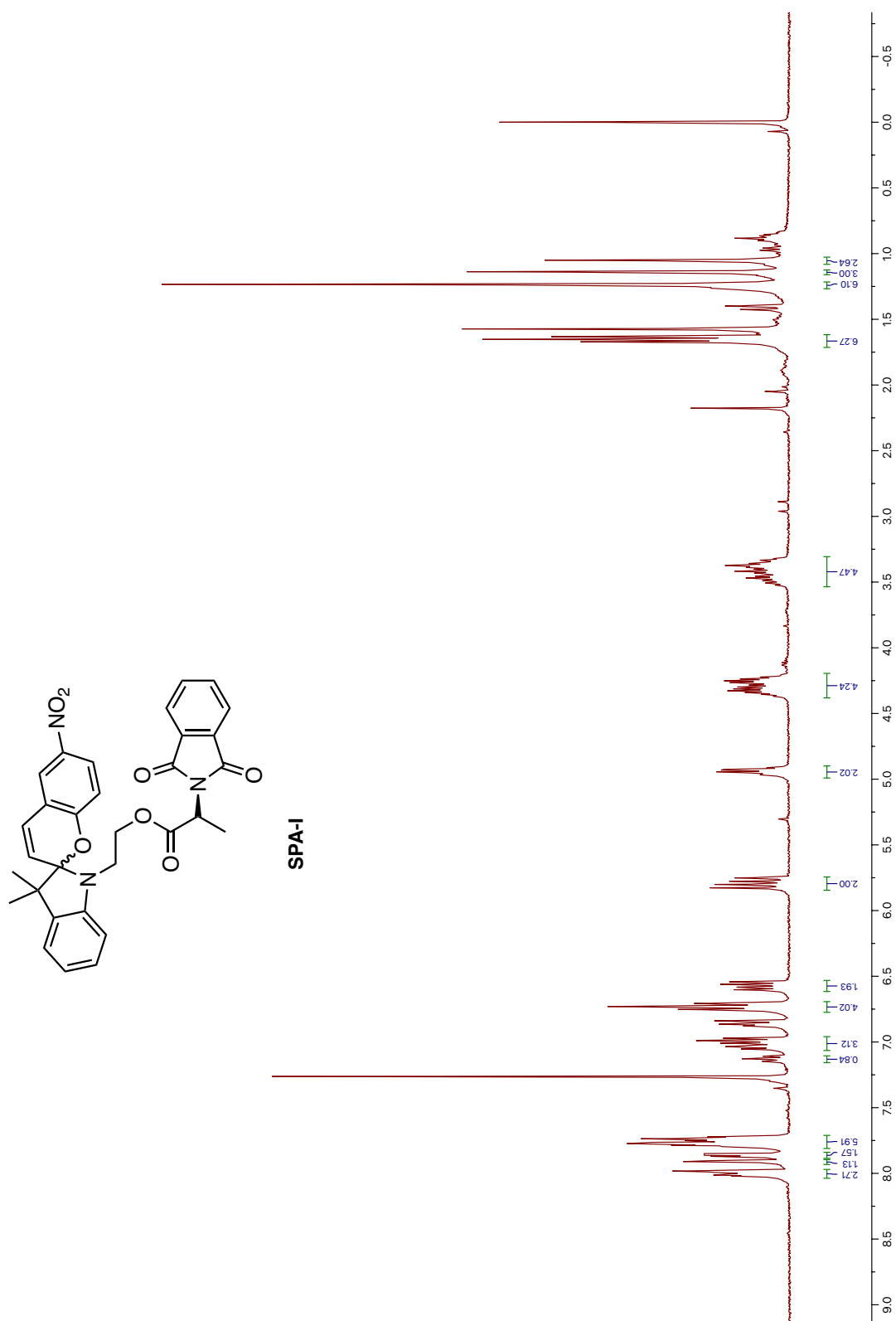


Figure 55. ¹H NMR spectrum of SPA-I

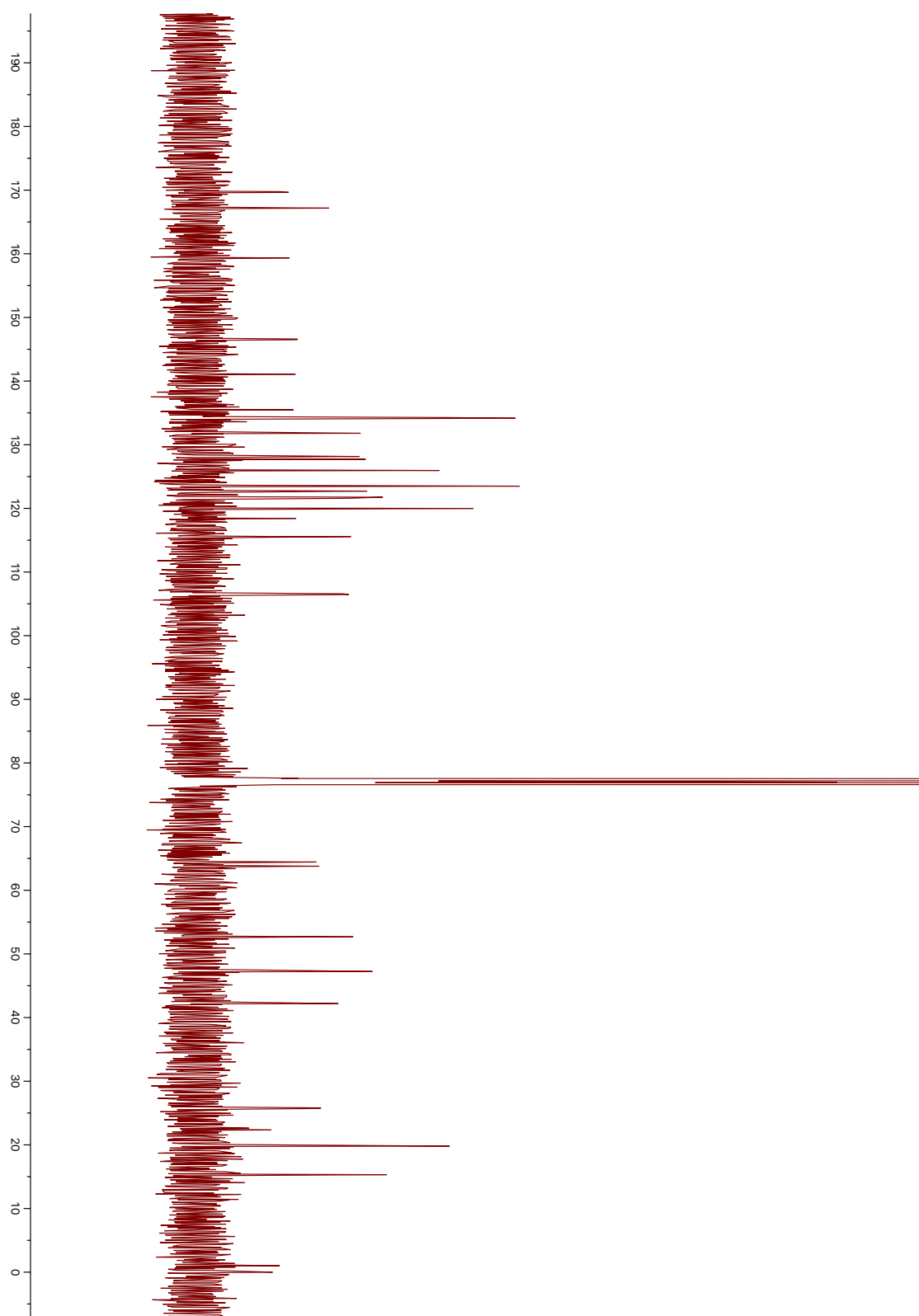


Figure 56. ^{13}C NMR spectrum of SPA-I

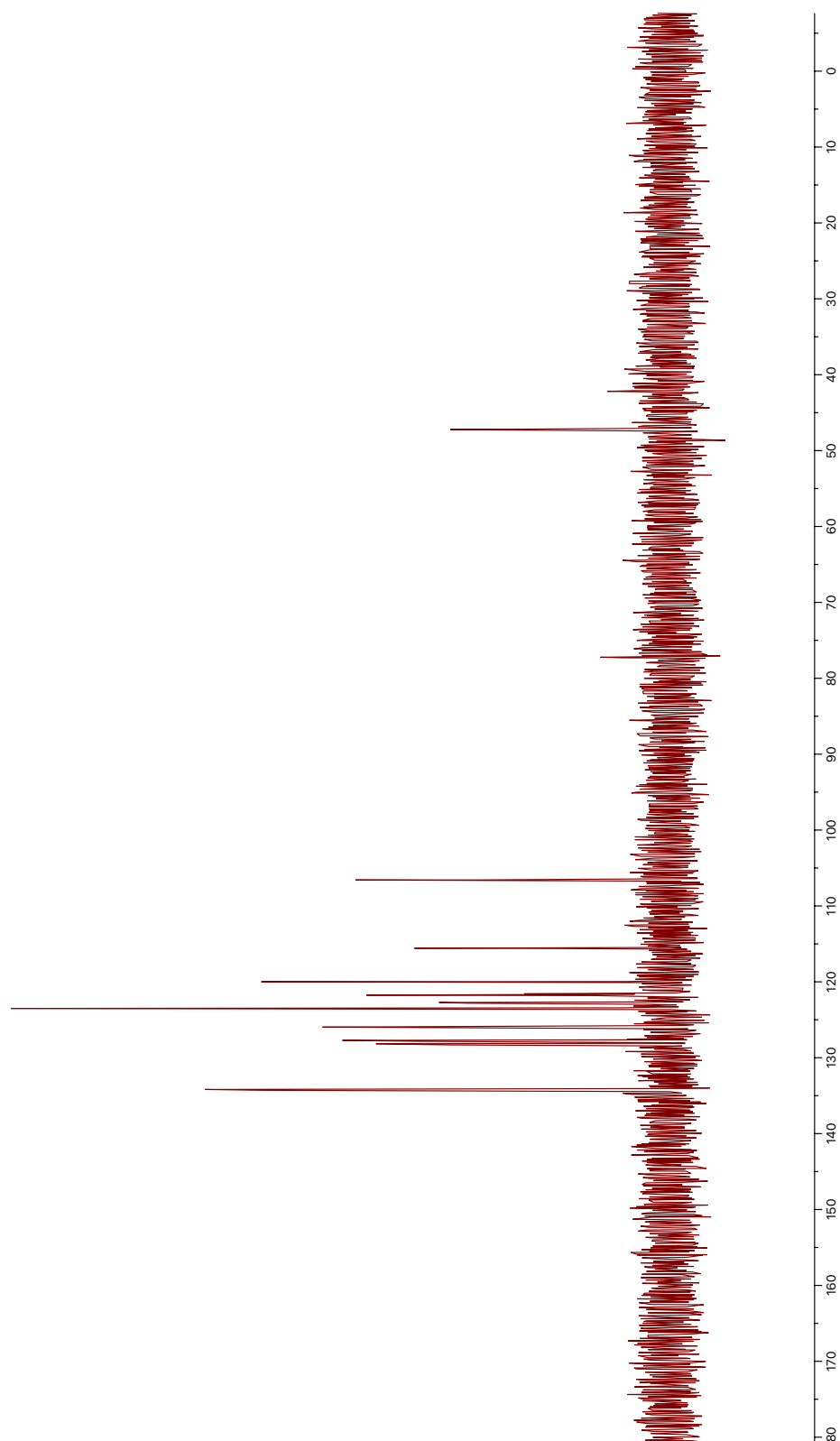


Figure 57. DEPT90 NMR spectrum of SPA-I

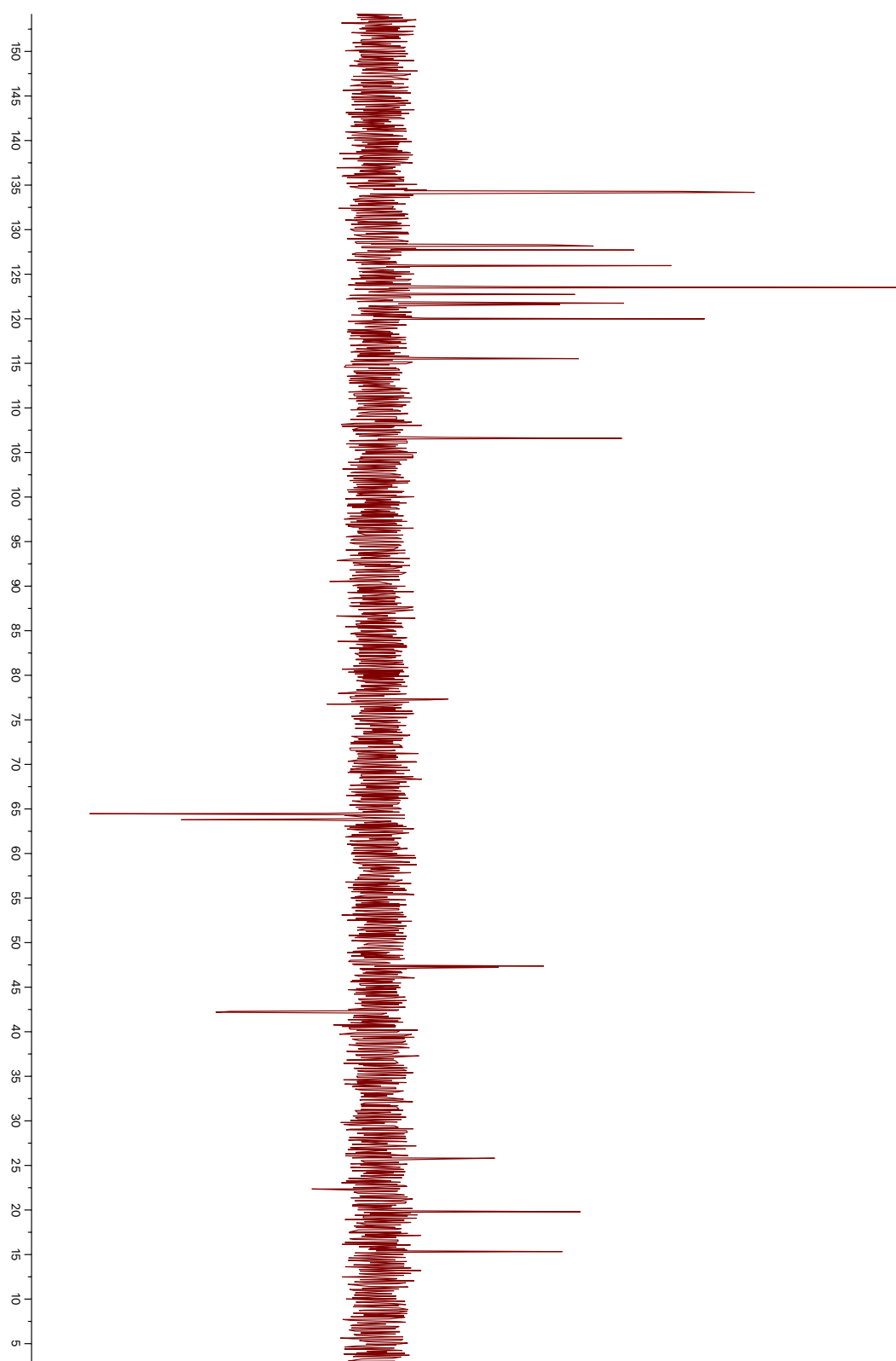


Figure 58. DEPT135 NMR spectrum of SPA-I

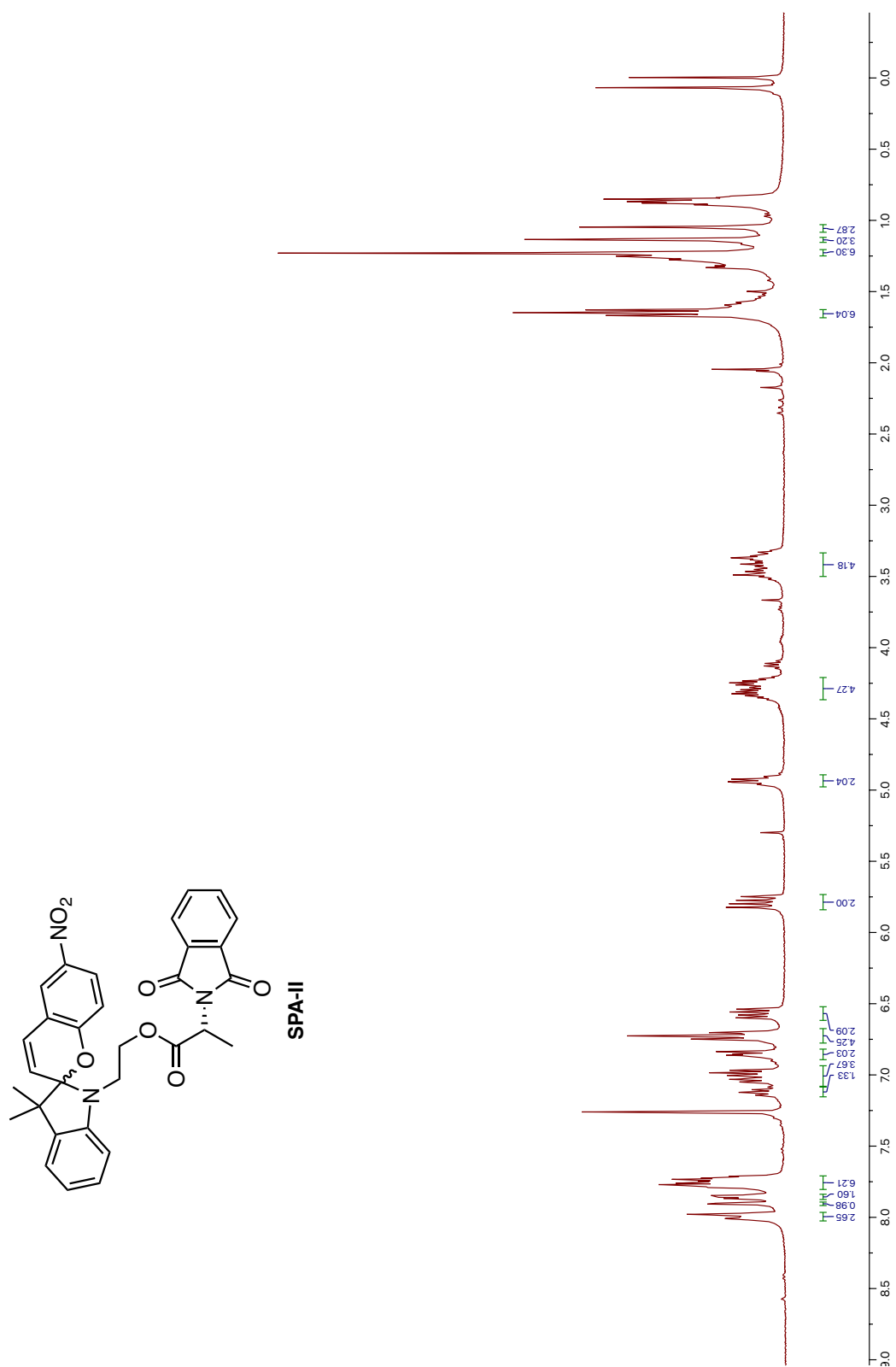


Figure 59. ¹H NMR spectrum of SPA-II

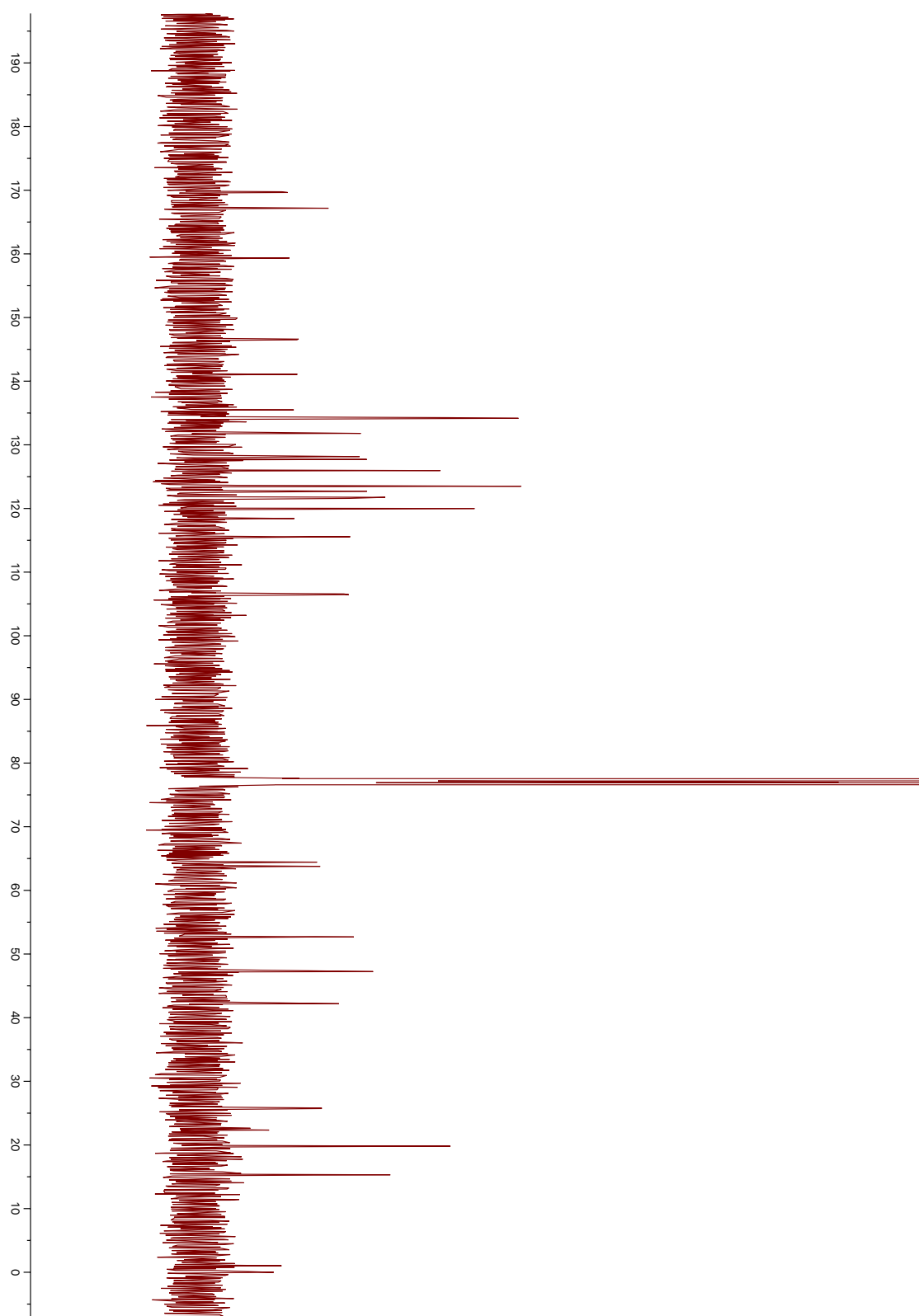


Figure 60. ^{13}C NMR spectrum of SPA-II

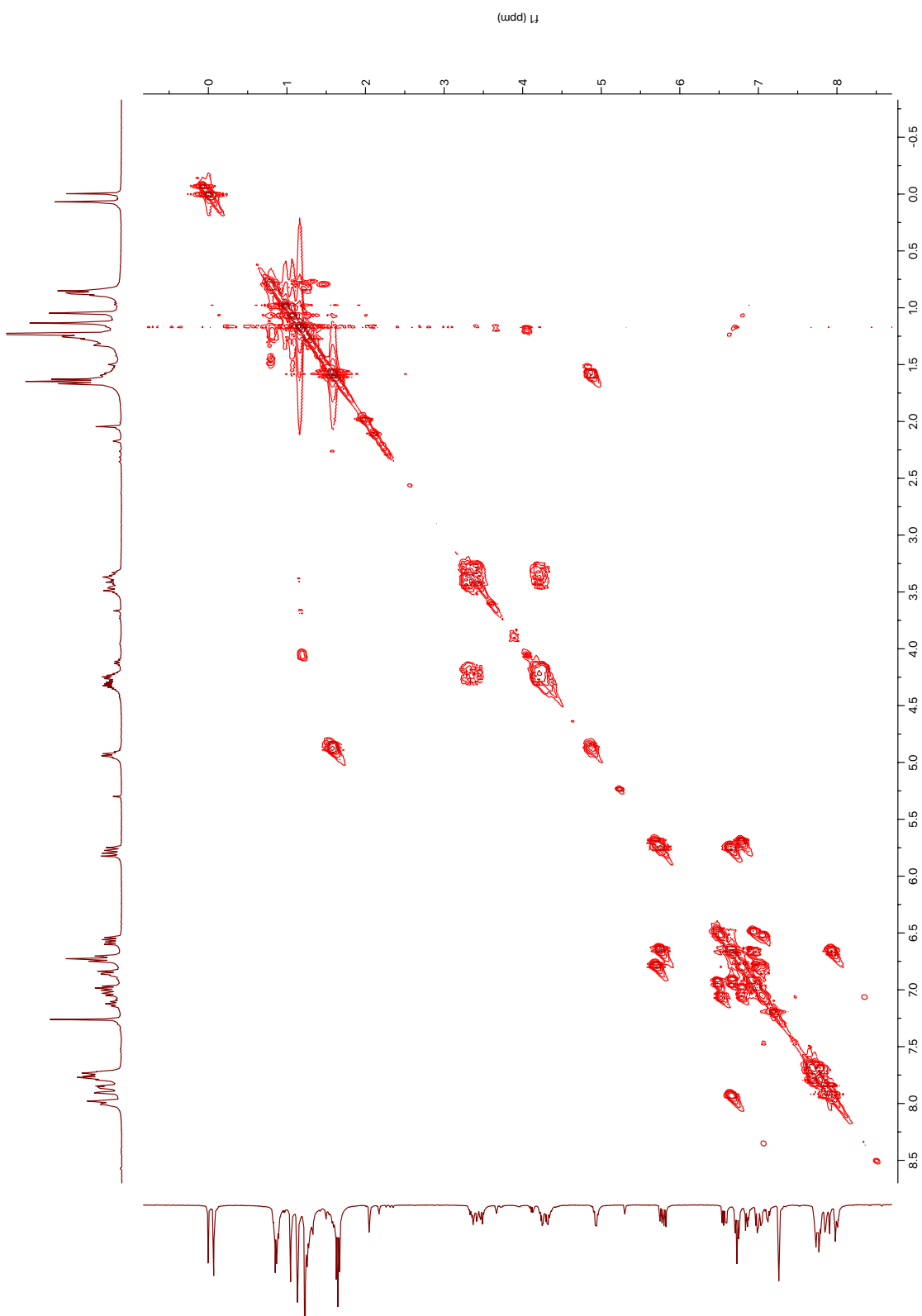


Figure 61. COSY NMR spectrum of SPA-II

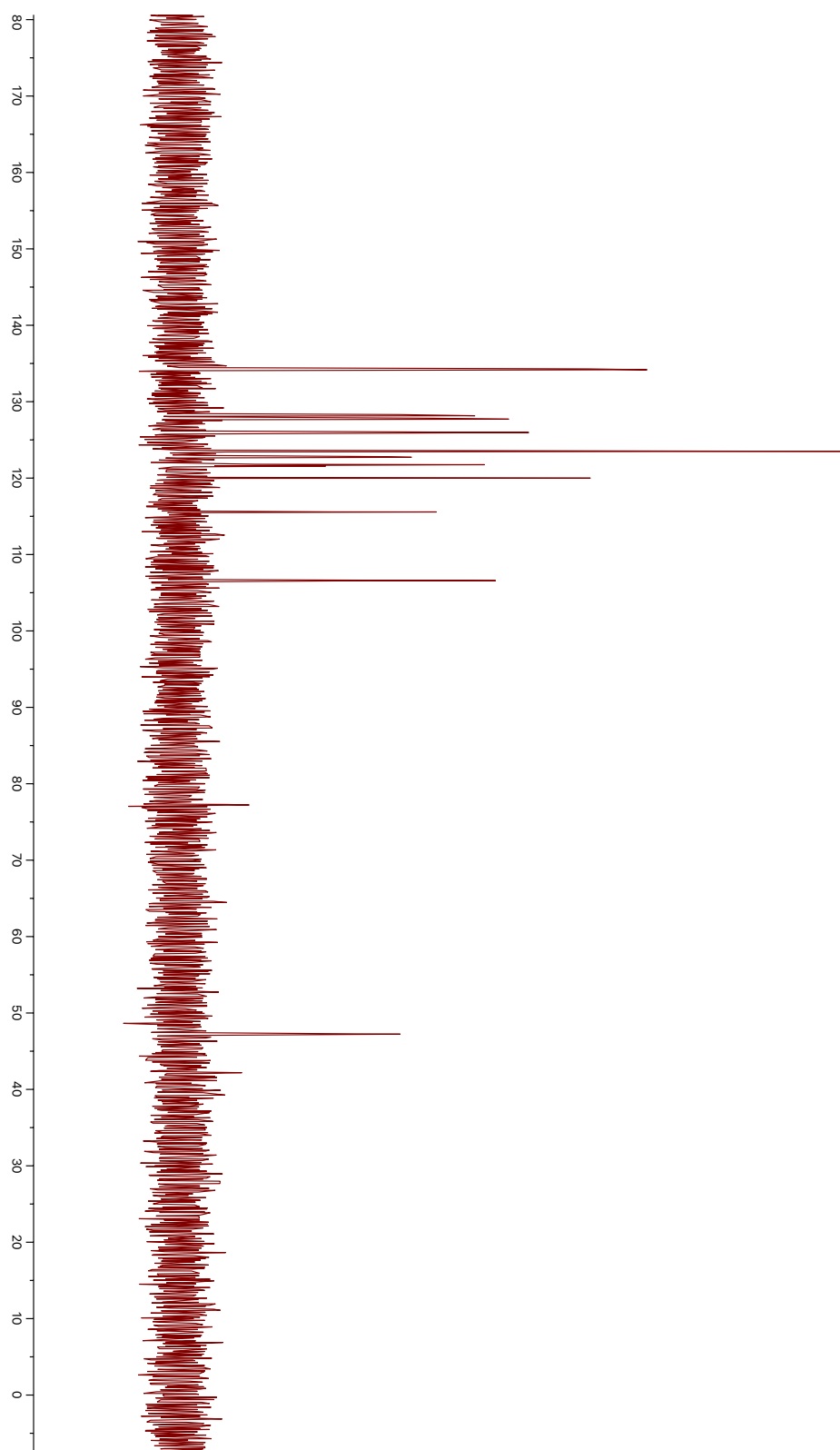


Figure 62. DEPT90 NMR spectrum of SPA-II

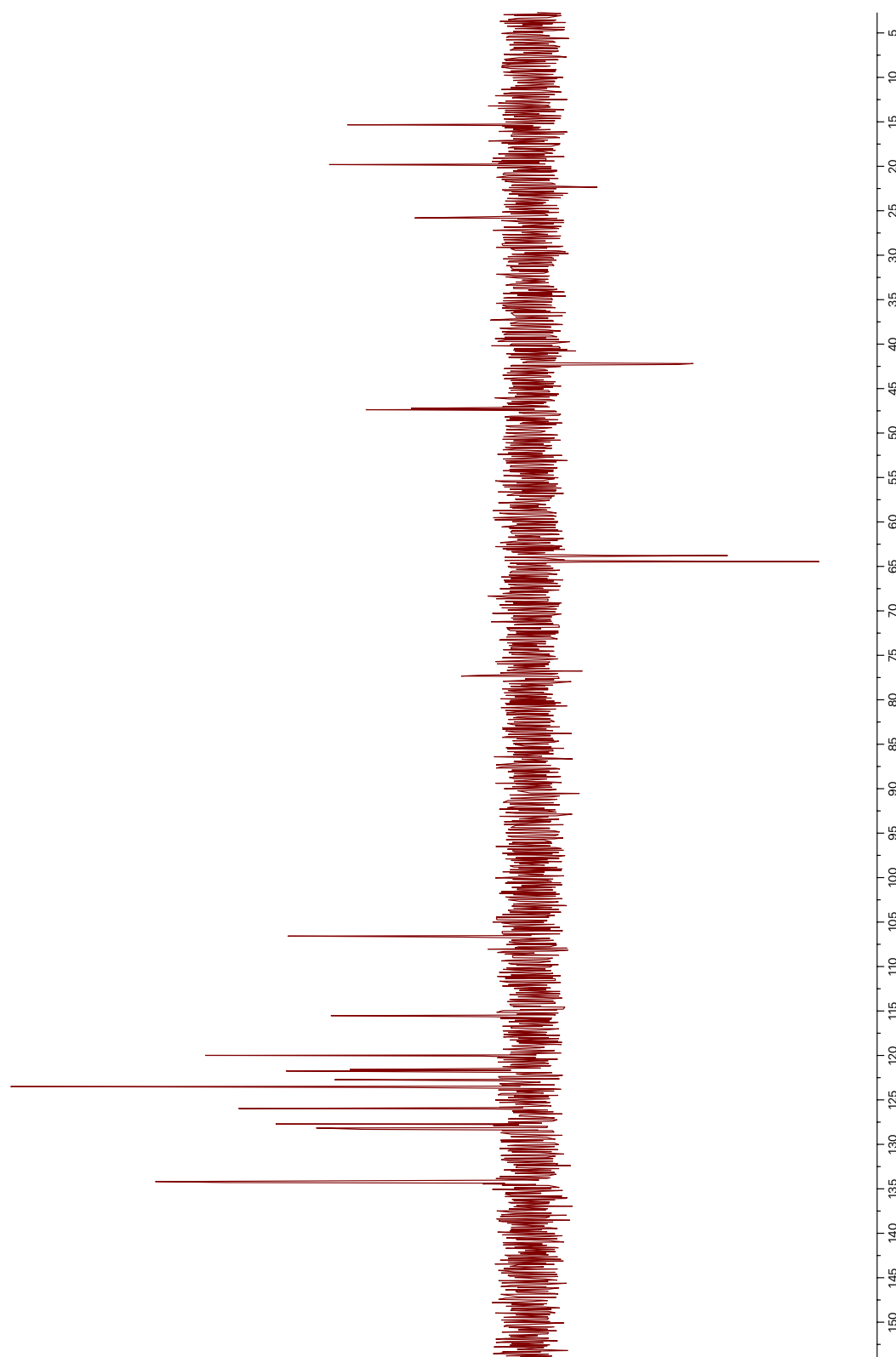


Figure 63. DEPT135 NMR spectrum of SPA-II

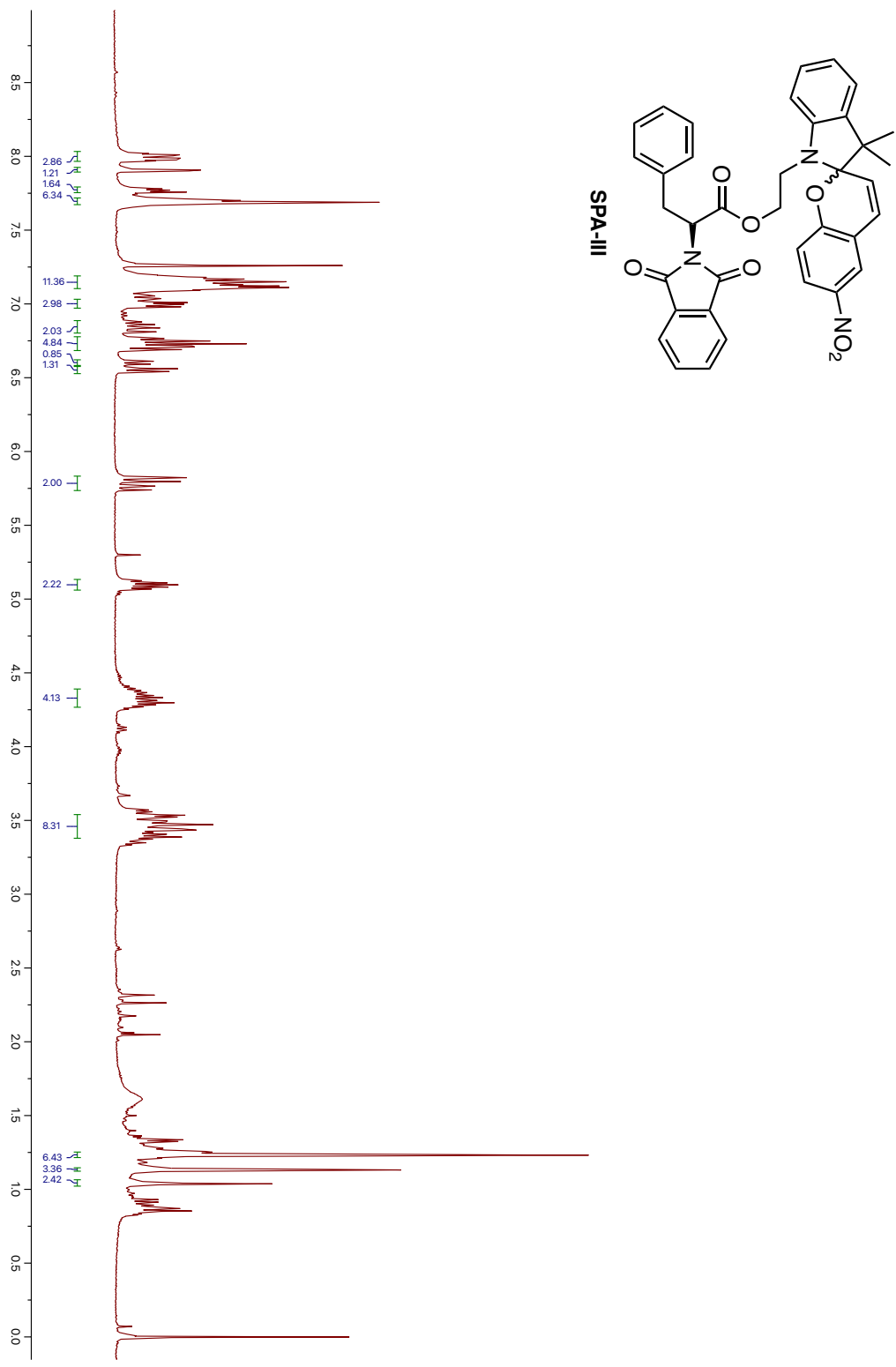


Figure 64. ¹H NMR spectrum of SPA-III

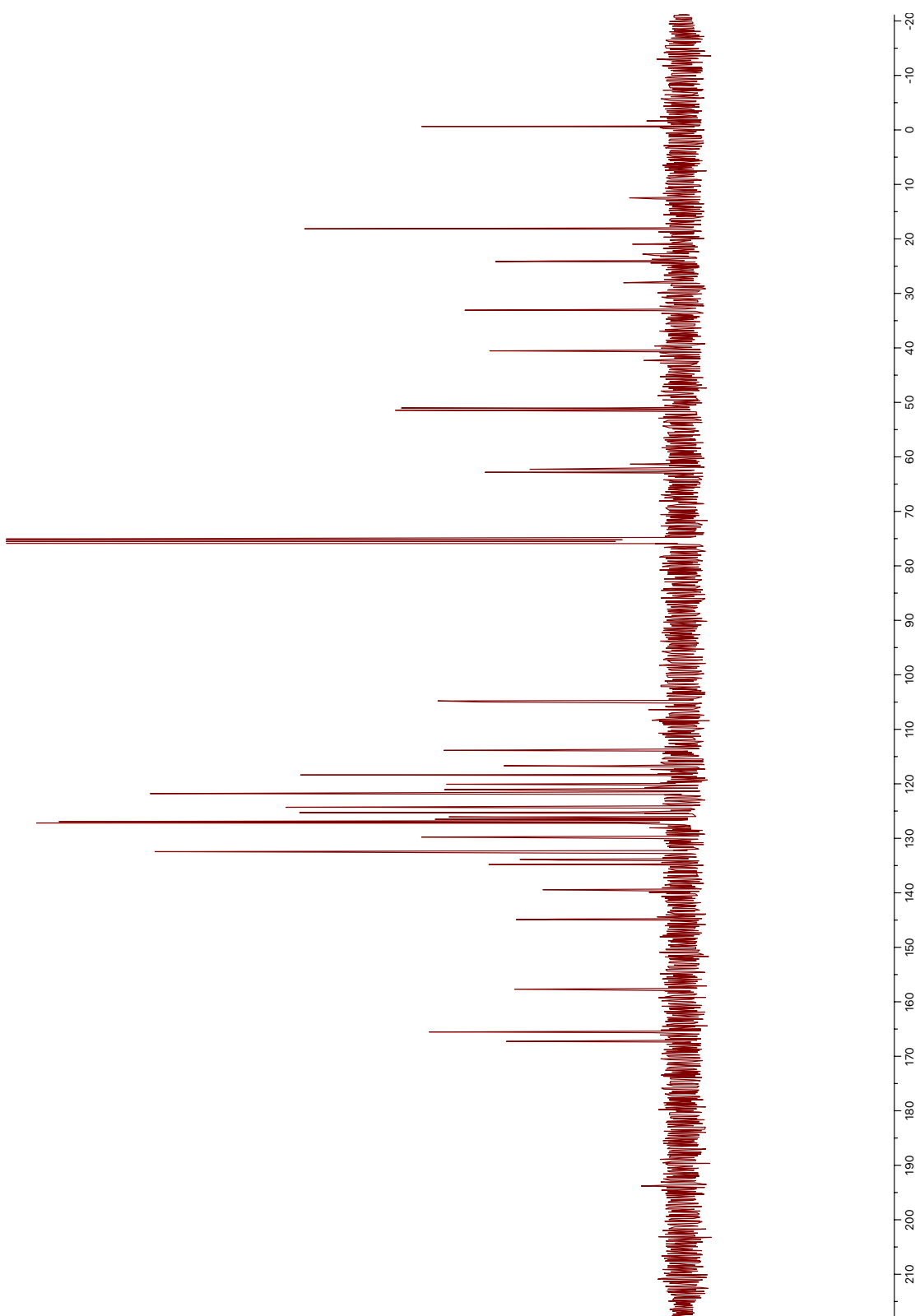


Figure 65. ^{13}C NMR spectrum of SPA-III

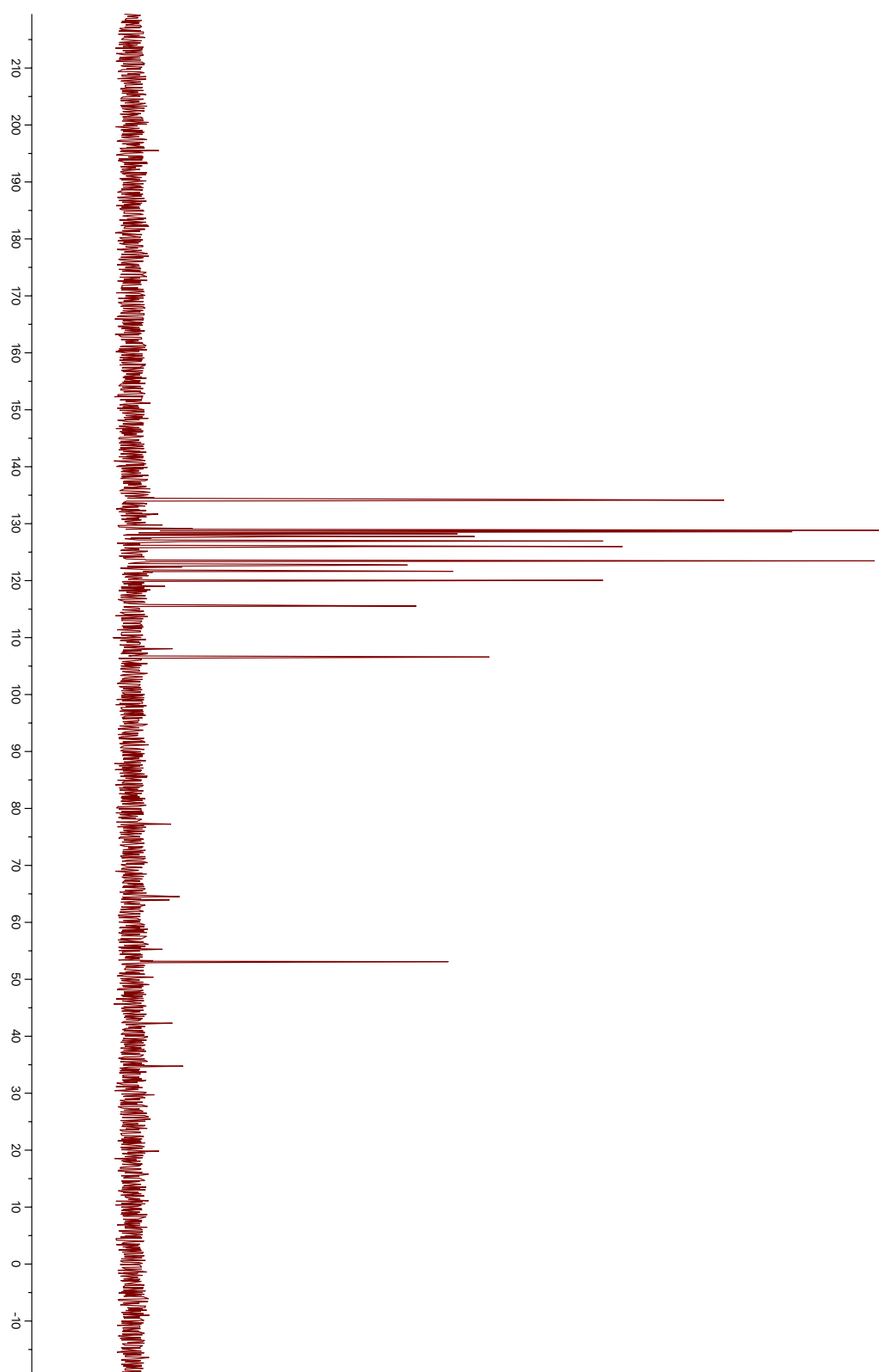


Figure 66. DEPT90 NMR spectrum of SPA-III

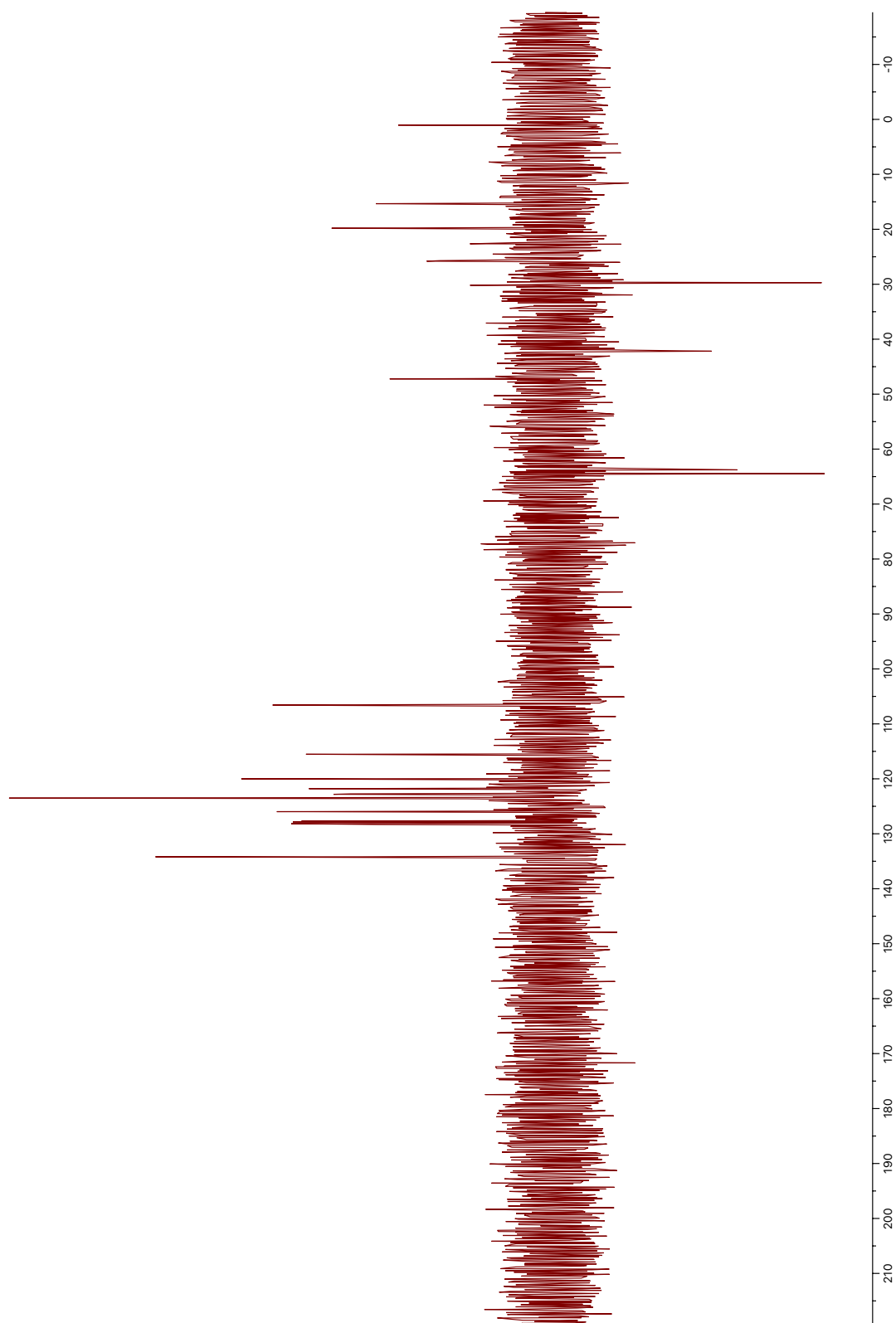


Figure 67. DEPT135 NMR spectrum of SPA-III

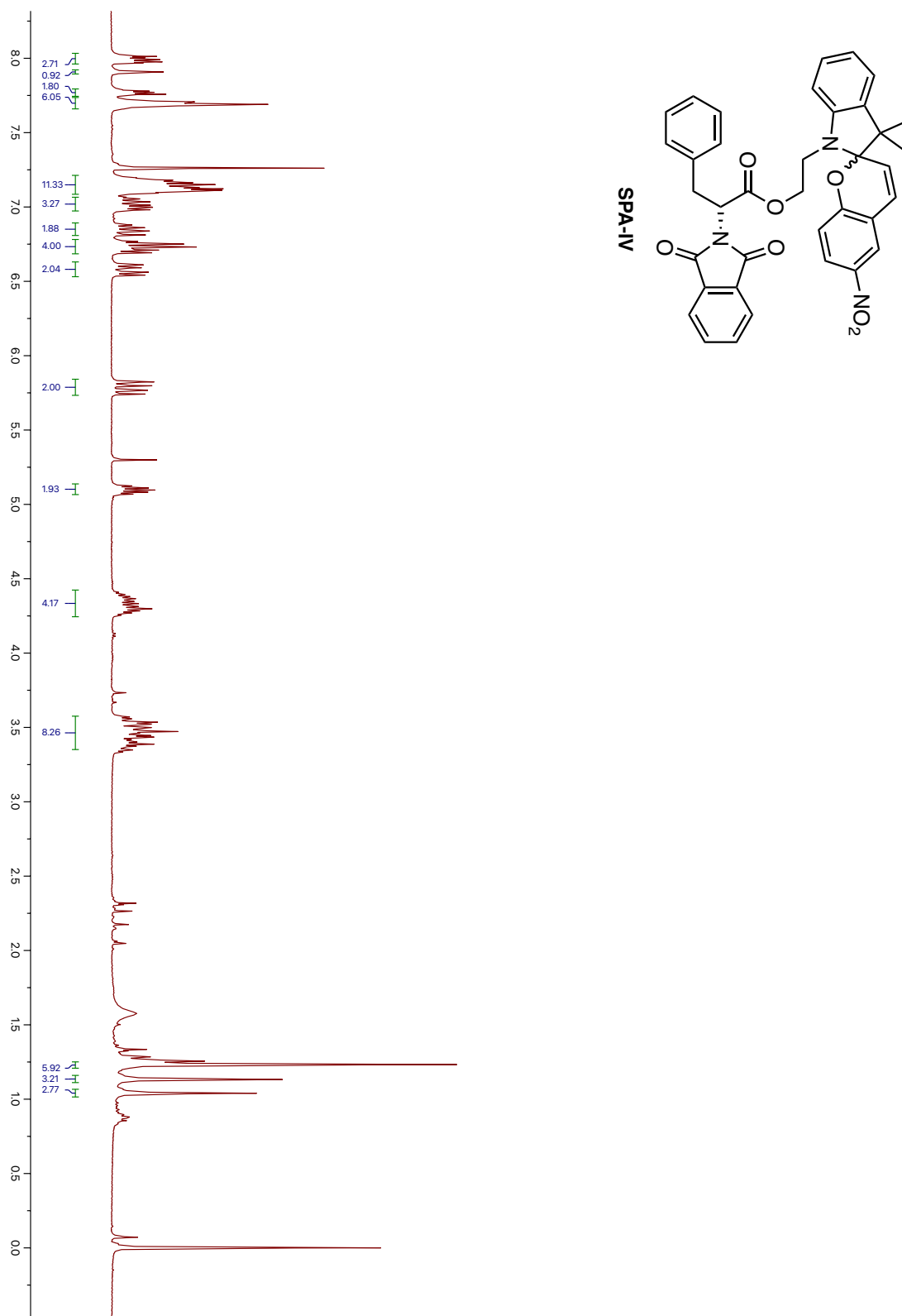


Figure 68. ¹H NMR spectrum of SPA-IV

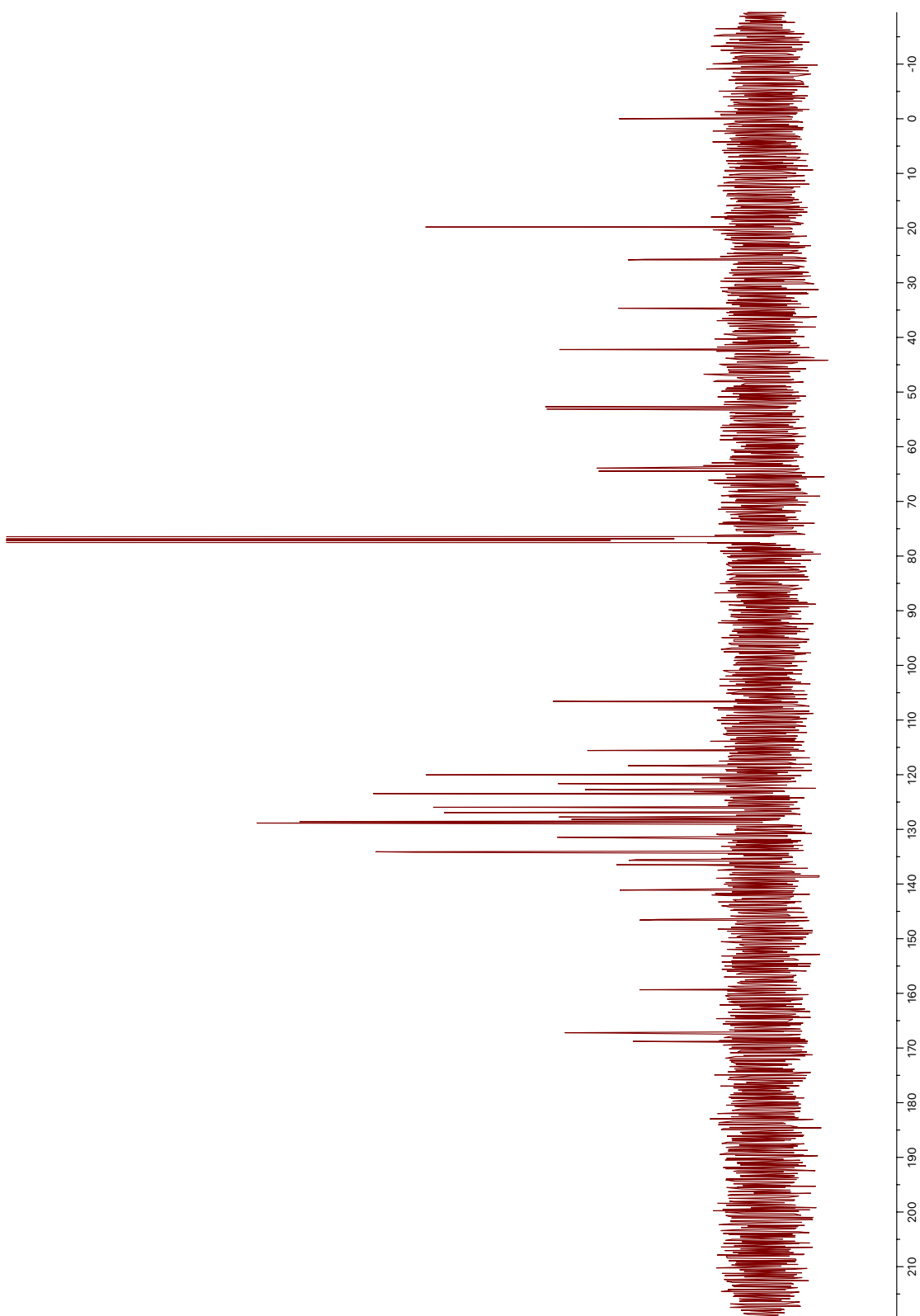


Figure 69. ^{13}C NMR spectrum of SPA-IV

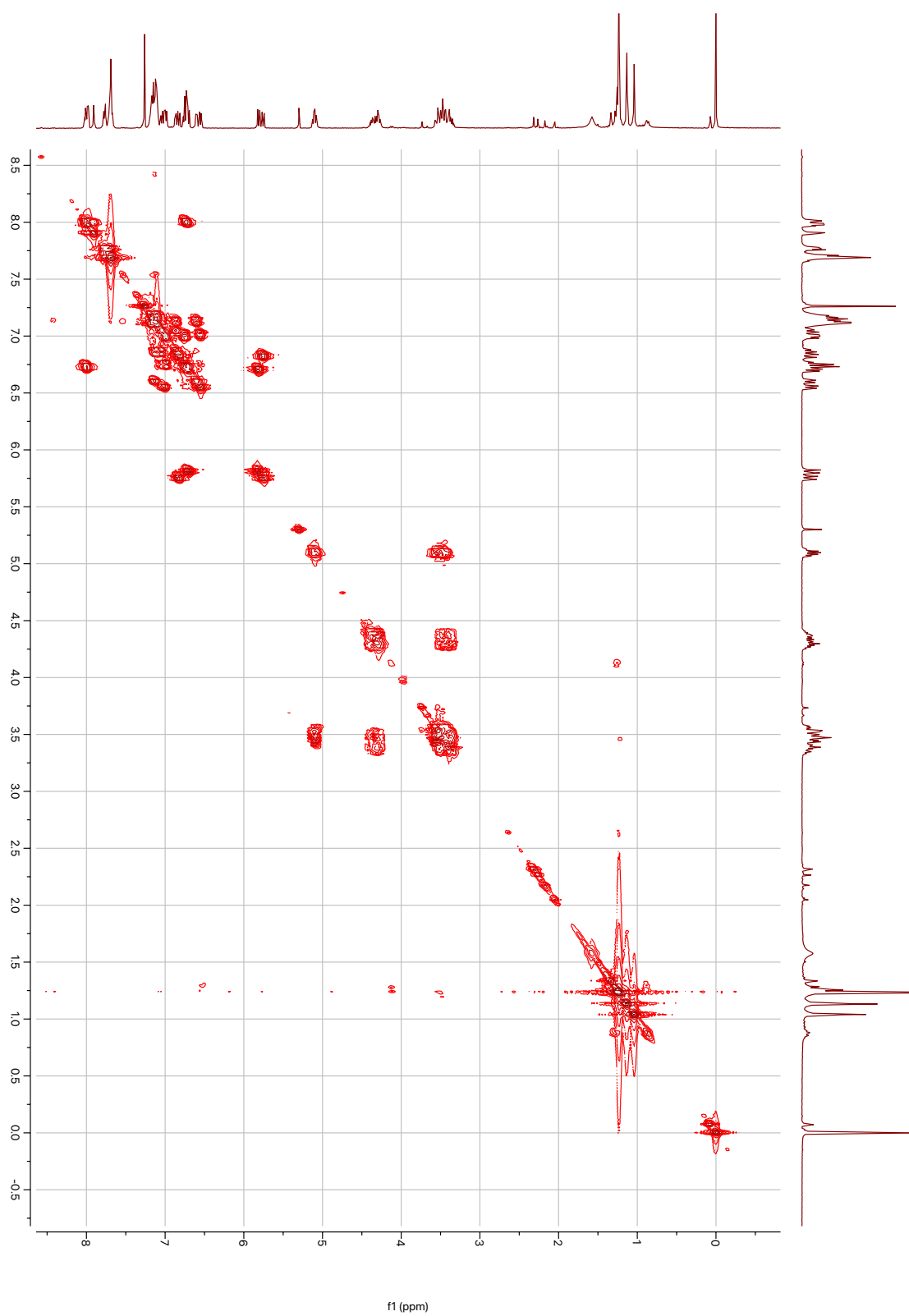


Figure 70. COSY NMR spectrum of SPA-IV

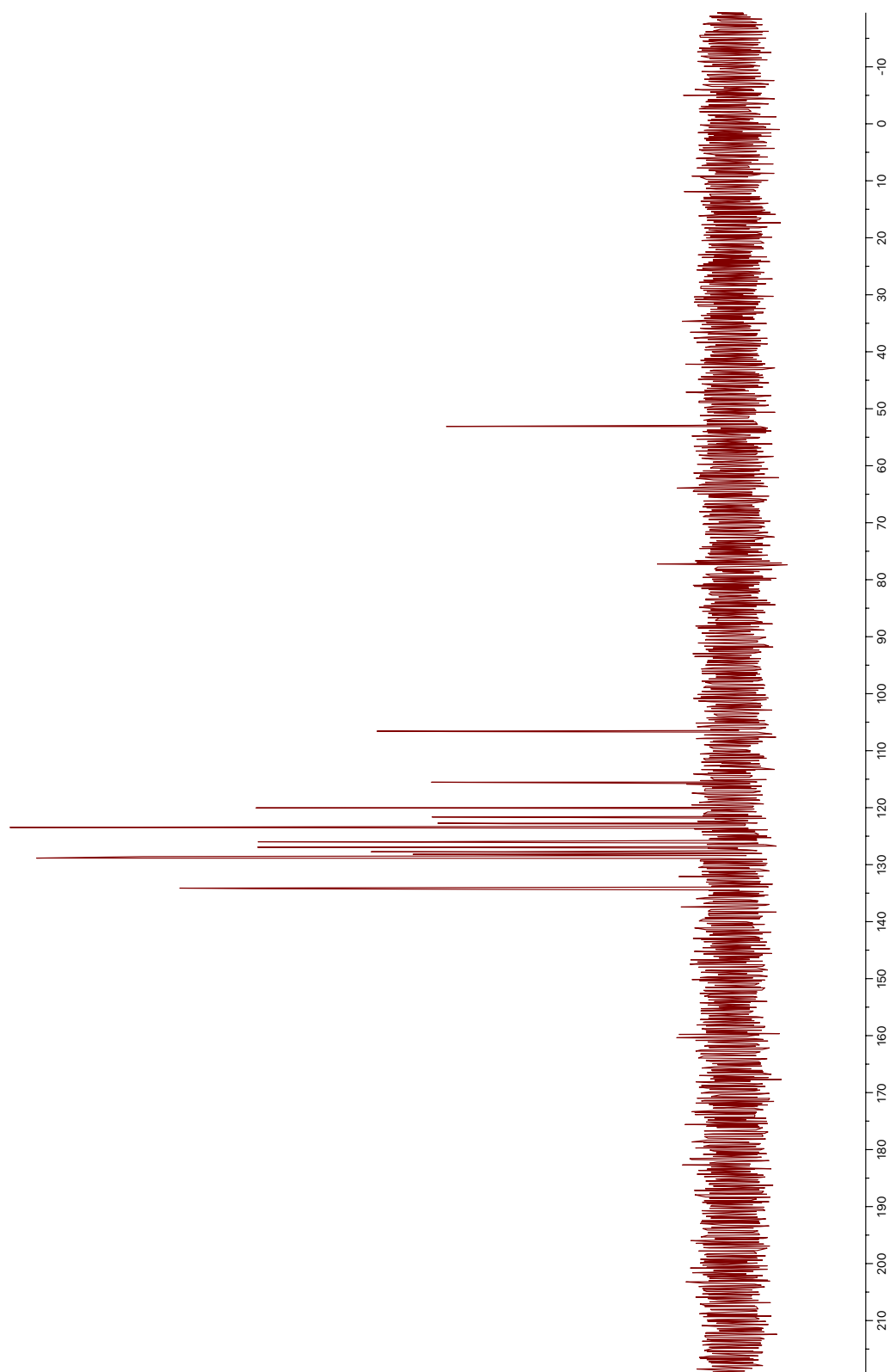


Figure 71. DEPT90 NMR spectrum of SPA-IV

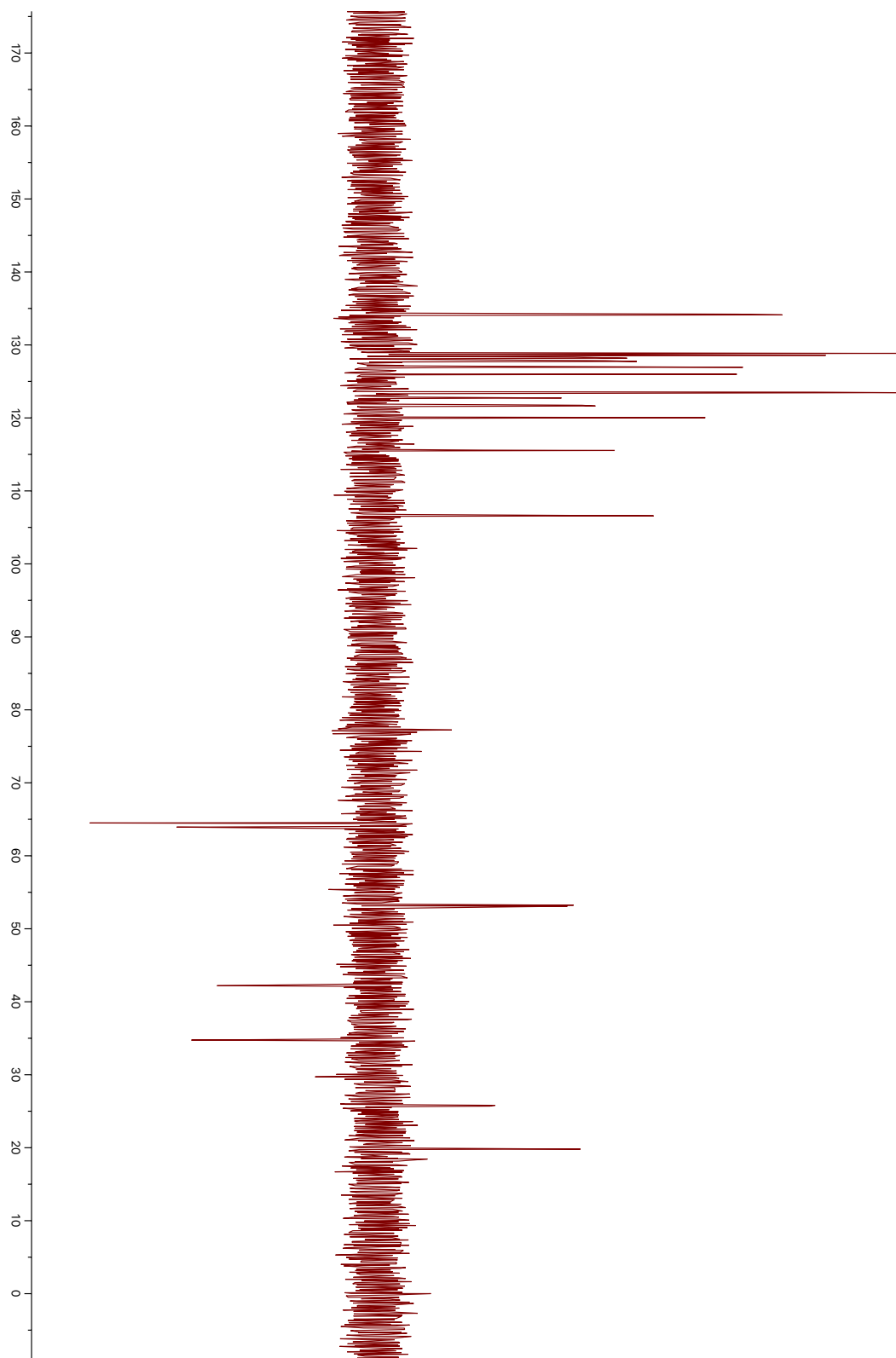


Figure 72. DEPT135 NMR spectrum of SPA-IV

B. IR Spectra

IR spectra were recorded at Thermo Scientific Nicolet iS10 ATR-IR spectrometer.

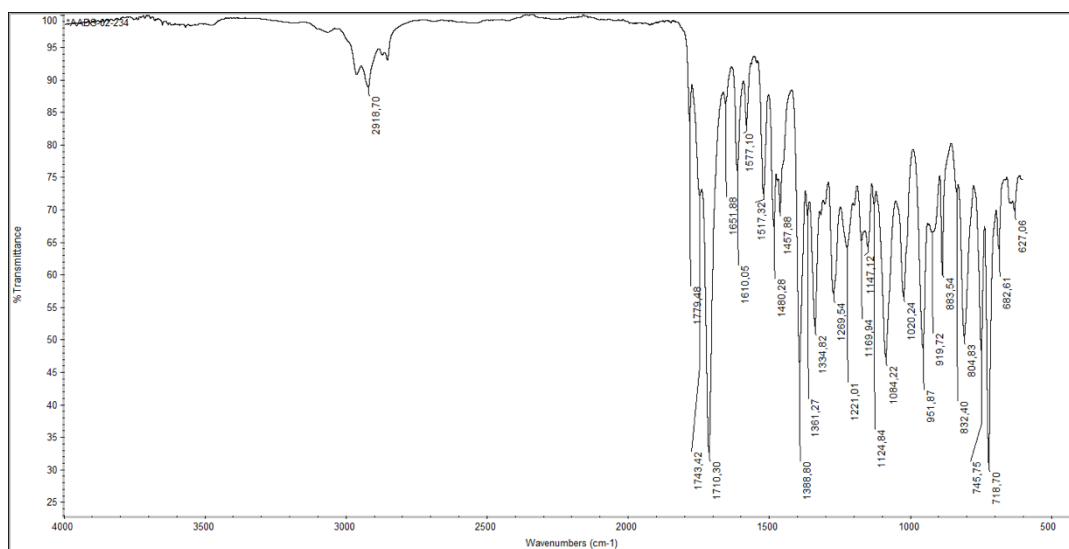


Figure 73. IR spectrum of SPA-I

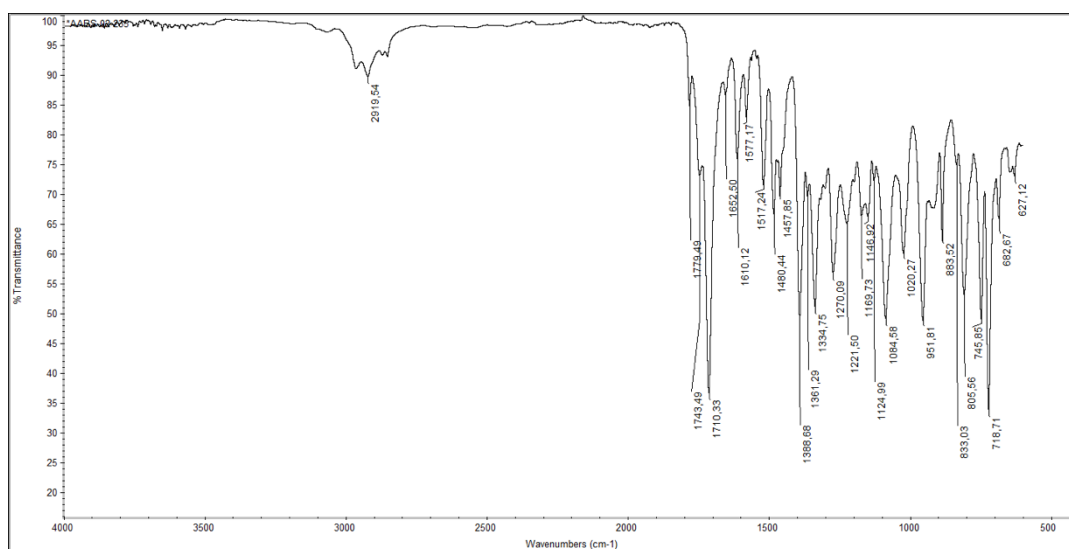


Figure 74. IR spectrum of SPA-II

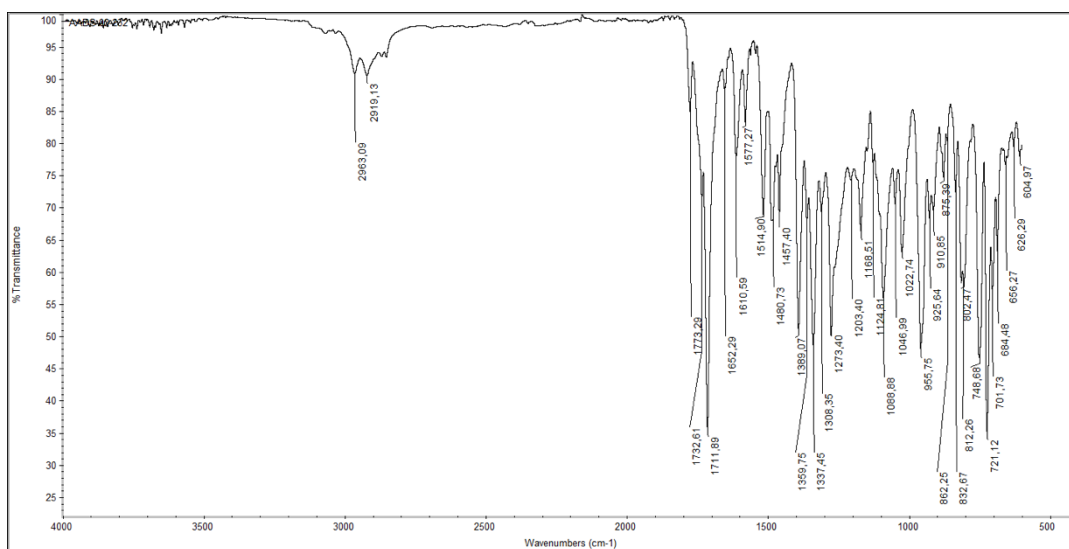


Figure 75. IR spectrum of SPA-III

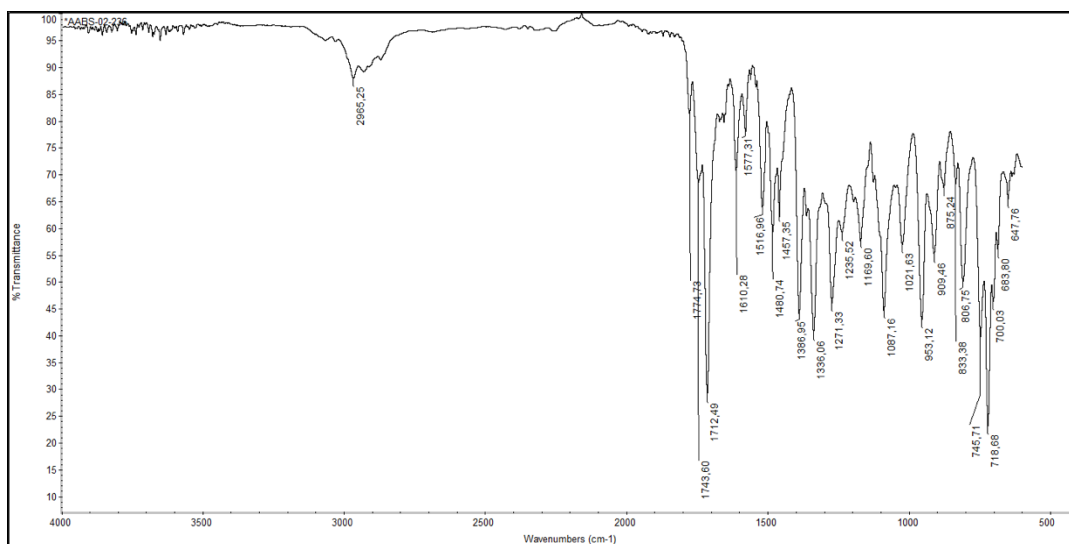


Figure 76. IR spectrum of SPA-IV

C. HRMS Spectra

High Resolution Mass Spectra (HRMS) Spectra were processed in positive mode on (ES+) using Time of Flight mass analyzer.

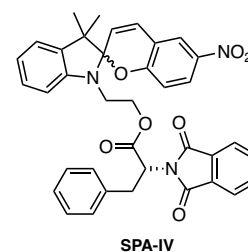
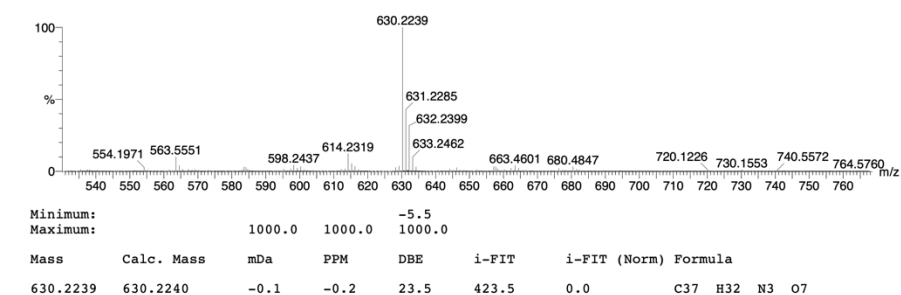
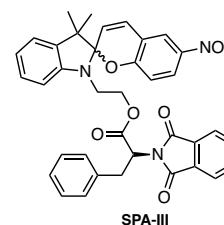
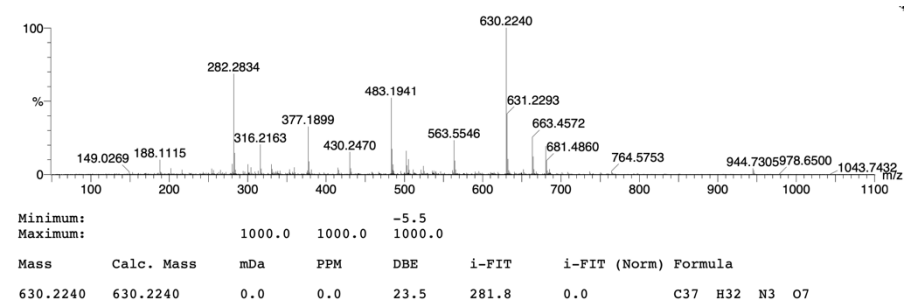
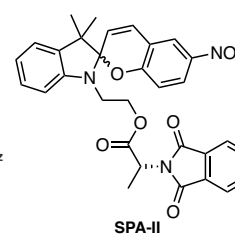
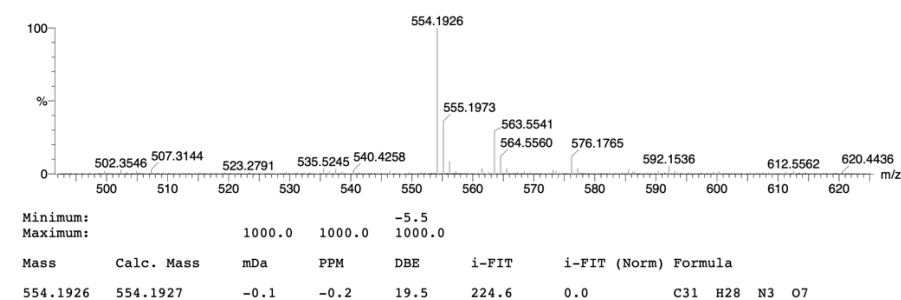
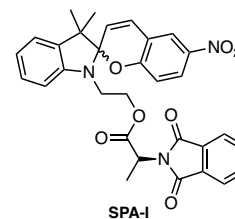
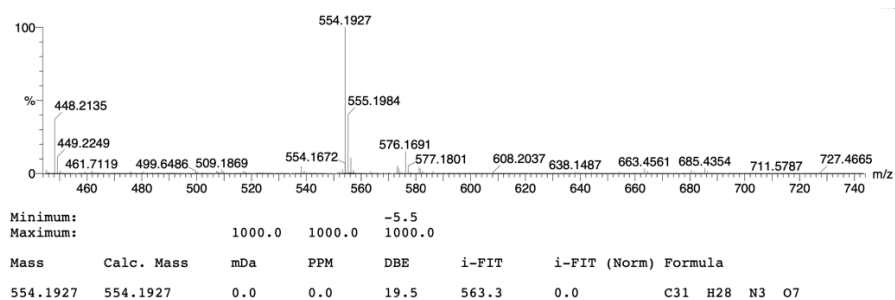


Figure 77. HRMS spectra of SPA-I, SPA-II, SPA-III, and SPA-IV

D. FLUORESCENCE Spectra

Fluorescence spectra were recorded at Perkin Elmer LS55 spectrofluorometer.

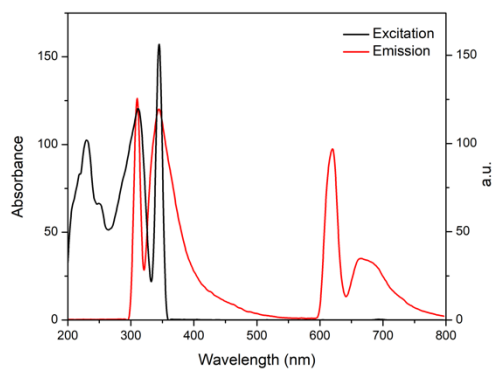


Figure 78. Fluorescence absorption and emission spectra of SPA-I in isopropanol

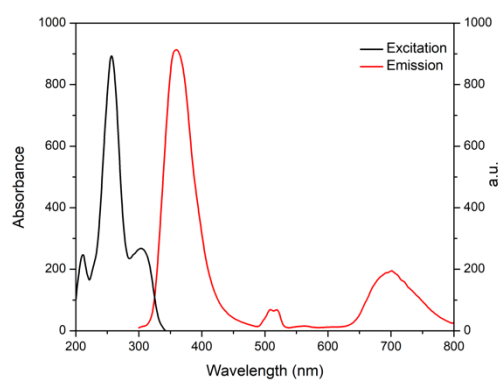


Figure 79. Fluorescence absorption and emission spectra SPA-II in isopropanol

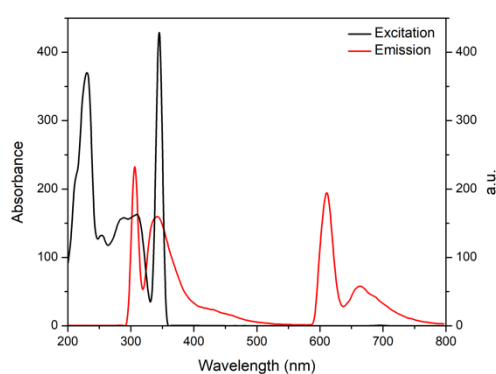


Figure 80. Fluorescence absorption and emission spectra of SPA-III in isopropanol

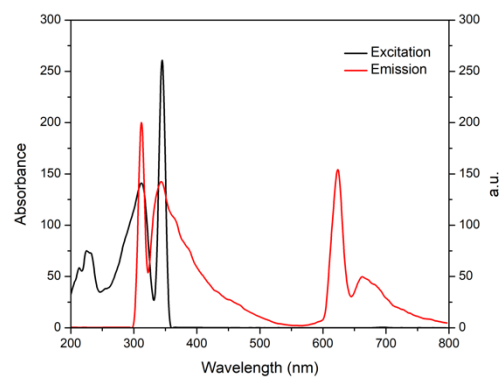


Figure 81. Fluorescence absorption and emission spectra of SPA-IV in isopropanol

E. UV-Vis Spectra

UV-Vis measurements were recorded with Shimadzu UV-2450 spectrophotometer.

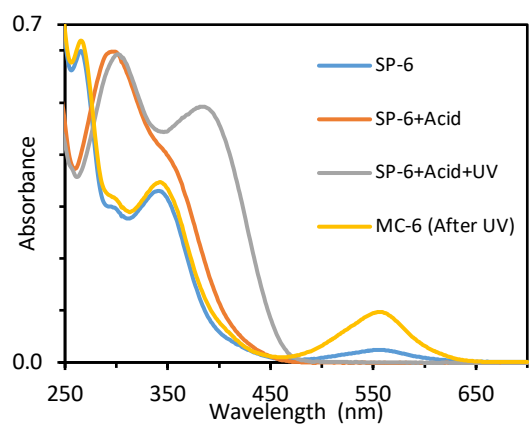


Figure 82. Acidochromism of Compound 6